

SCIENTIFIC PUBLICATIONS OF THE AMERICAN MUSEUM OF NATURAL HISTORY

AMERICAN MUSEUM NOVITATES

BULLETIN OF THE AMERICAN MUSEUM OF NATURAL HISTORY

ANTHROPOLOGICAL PAPERS OF THE AMERICAN MUSEUM OF NATURAL HISTORY

PUBLICATIONS COMMITTEE

ROBERT S. VOSS, CHAIR

BOARD OF EDITORS

JIN MENG, PALEONTOLOGY

LORENZO PRENDINI, INVERTEBRATE ZOOLOGY

ROBERT S. VOSS, VERTEBRATE ZOOLOGY

PETER M. WHITELEY, ANTHROPOLOGY

MANAGING EDITOR

MARY KNIGHT

Submission procedures can be found at <http://research.amnh.org/scipubs>

All issues of *Novitates* and *Bulletin* are available on the web from
<http://digitallibrary.amnh.org/dspace>

Order printed copies from <http://www.amnhshop.com> or via standard mail from:
American Museum of Natural History—Scientific Publications
Central Park West at 79th Street
New York, NY 10024

© This paper meets the requirements of ANSI/NISO Z39.48-1992 (permanence of paper).

ON THE COVER: *GOBIDERMA PULCHRUM* RESTORED BASED ON
AVAILABLE SPECIMENS.

CONRAD ET AL.: *GOBIDERMA PULCHRUM*

AMNH BULLETIN 362

2011

OSTEOLOGY OF *GOBIDERMA PULCHRUM*
(MONSTERSAURIA, LEPIDOSAURIA, REPTILIA)

JACK L. CONRAD, OLIVIER RIEPPEL,
JACQUES A. GAUTHIER,
AND MARK A. NORELL



BULLETIN OF THE AMERICAN MUSEUM OF NATURAL HISTORY

OSTEOLOGY OF *GOBIDERMA PULCHRUM* (MONSTERSAURIA, LEPIDOSAURIA, REPTILIA)

JACK L. CONRAD

*Department of Vertebrate Paleontology,
American Museum of Natural History,
Central Park West at 79th Street,
New York City, NY 10024;
Anatomy Department, New York College of
Osteopathic Medicine, New York Institute of
Technology, Old Westbury, NY 11568*

OLIVIER RIEPPEL

*Department of Geology, the Field Museum,
1400 South Lake Shore Drive, Chicago, IL 60605*

JACQUES A. GAUTHIER

*Yale Peabody Museum, Yale University,
170 Whitney Avenue, New Haven, CT 06511*

MARK A. NORELL

*Department of Vertebrate Paleontology,
American Museum of Natural History,
Central Park West at 79th Street,
New York City, NY 10024*

BULLETIN OF THE AMERICAN MUSEUM OF NATURAL HISTORY

Number 362, 88 pp., 56 figures, 1 table

Issued December 30, 2011

CONTENTS

Abstract	3
Introduction	3
Materials and Methods.	4
Materials	4
Methods	5
Systematics	6
Description	6
Skull and Mandible.	6
Axial Skeleton	55
Pectoral Girdle and Forelimb.	59
Pelvic Girdle and Hind Limb.	60
Phylogenetic Analyses.	64
Recent Phylogenetic Studies of Monstersauria.	64
Present Analysis	67
Discussion	70
Phylogenetic Implications	70
Maturity of Described Specimens.	71
Basal Monstersaurian Morphology.	71
A Revised Diagnosis of <i>Gobiderma pulchrum</i>	72
A Diversity of Carnivorous Cretaceous Gobi Lizards.	73
Conclusions	74
Acknowledgments	75
References	75
Appendix 1: Anatomical Abbreviations from Figures	80
Appendix 2: Morphological Phylogenetic Data Matrix	81

ABSTRACT

Joint expeditions by the American Museum of Natural History and Mongolian Academy of Sciences have recovered significant new remains of the basal monstersaur *Gobiderma pulchrum*. We describe these new specimens in detail and also revisit the originally described material in order to more fully understand this pivotal anguimorph taxon. The newly discovered specimens include skull and postcranial materials that add dramatically to the understanding of the osteology of *Gobiderma pulchrum*. We revise the diagnosis of this species, adding to the previously published diagnosis the following character states: premaxillary nasal process is narrowest mediolaterally; postfrontal and postorbital remain unfused; postorbital extends posteriorly for almost the entire length of the supratemporal fenestra; the Vidian canal is posteriorly enclosed by the parabasisphenoid; an anterior coracoid emargination is present; the pelvis is completely fused; and the lateral plantar tubercle is distally placed. A phylogenetic analysis confirms the placement of *Gobiderma pulchrum* as a non-helodermatid monstersaur. As such, the fact that it is known from reasonably complete remains makes it pivotal for understanding character evolution within Monstersauria. The Djadokhta Formation includes several carnivorous/insectivorous lizards and theropod dinosaurs—more than is usual for extant communities, but perhaps analogous in some ways to parts of modern Australia.

INTRODUCTION

Monstersauria is an ancient clade of anguimorph lizards that has been distinct at least since the earliest Late Cretaceous (Nydham, 2000; Conrad, 2008; Conrad et al., 2011). Today, monstersaurs are represented only by two species of *Heloderma*, known from the southwest of the United States and from western Central America. However, the clade was previously much more speciose (Estes, 1983; Gao and Norell, 2000; Nydam, 2000; Bhullar and Smith, 2008; Conrad, 2008; Conrad et al., 2011). Unfortunately, nearly all fossil monstersaurs are known from very incomplete material, often associated based on size and general similarity of nonoverlapping parts (e.g., *Eurheloderma gallicum*, *Paraderma bogerti*, and *Primerma nessovi* among others) (Hoffstetter, 1957; Estes, 1964, 1983; Nydam, 2000). By contrast, some taxa are known from complete or nearly complete skulls (e.g., *Estesia mongoliensis* and *Gobiderma pulchrum*) (Norell et al., 1992; Norell and Gao, 1997; Gao and Norell, 2000).

Monstersaurian holophyly and the monstersaurian status of *Estesia mongoliensis* was recently questioned based on data provided by a new specimen (Yi and Norell, 2010). However, Monstersauria is a stable clade and *Estesia mongoliensis* is a very *Heloderma*-like animal based on our observations, a recent combined-evidence analysis of anguimorphs (which included data from the new specimen)

(Conrad et al., 2011), and the analysis of the current paper (see below).

Gobiderma pulchrum is a relatively large (estimated at 310 mm precaudal length based on IGM 3/905; see below) squamate from the Late Cretaceous of Mongolia and China. It belongs to a clade of anguimorph squamates known as Monstersauria (Norell and Gao, 1997; Gao and Norell, 1998, 2000; Conrad, 2008; Conrad et al., 2011). Monstersaurs are best known by the two extant species of *Heloderma* (*Heloderma horridum* and *Heloderma suspectum*), the only extant lizards with potent venom (but see Fry, 2005; Fry et al., 2009) and a sophisticated venom-delivery system. By contrast, *Gobiderma pulchrum* lacks the grooved teeth present in *Heloderma* and in some fossil monstersaurs (e.g., *Estesia mongoliensis*, *Eurheloderma gallicum*). Indeed, *Gobiderma pulchrum* is a relatively basal monstersaur (see Norell and Gao, 1997; Gao and Norell, 1998, 2000; Nydam, 2000; Conrad, 2008; Conrad et al., 2011), and lacks synapomorphies of Helodermatidae (as defined by Conrad, 2008) such as a prefrontal-postfrontal contact, anteriorly expanded frontals, and absence (loss) of the pineal foramen, among others. In many ways, *Gobiderma pulchrum* is an important transitional form between monstersaurs and other anguimorphs.

Borsuk-Białynicka (1984) originally named and described *Gobiderma pulchrum* based on one complete and two partial skulls.

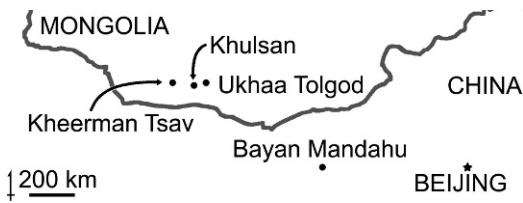


Fig. 1. Map showing the localities from which *Gobiderma pulchrum* has been collected (dots) and Beijing, China (star).

Gobiderma pulchrum was originally described as a necrosaurian grade platynotan (Borsuk-Białynicka, 1984). Lee (1997) suggested that *Parviderma inexacta* and *Gobiderma pulchrum* form a clade he termed Gobidermatidae (but see Norell and Gao, 1997). Cladistic analyses have identified *Gobiderma pulchrum* as a member of the *Heloderma* radiation with no special relationship to *Parviderma inexacta* (Norell and Gao, 1997; Gao and Norell, 1998; Nydam, 2000; Conrad, 2008).

The original *Gobiderma pulchrum* material comes from the Barun Goyot localities of Khulsan and Khermeen Tsav II (the “Red Beds”) (Borsuk-Białynicka, 1984; Gao and Norell, 2000). Subsequently discovered specimens are known from those localities and from the Djadokhta Formation (Bayan Mandahu, Tugrikin Shire, and Ukhaa Tolgod), all Campanian localities in the Gobi Desert of southern Mongolia and northern China (fig. 1).

Joint expeditions to the Gobi Desert of Mongolia by the Mongolian Academy of Sciences–American Museum of Natural History continue to produce new fossil reptiles of phylogenetic, paleobiogeographic, and paleoecological importance (see, for example, Conrad and Norell, 2006a; Turner et al., 2007b; and Norell et al., 2008). Recent expeditions to the Gobi Desert by the Mongolian Academy of Sciences–American Museum of Natural History have recovered literally hundreds of squamate fossils. Among these remains is new skeletal material of *Gobiderma pulchrum*, including skulls and the first significant postcranial remains of this species (Table 1).

Here, we offer new data on the morphology of *Gobiderma pulchrum* and a revised diagnosis of the species based on the originally described specimens and four newly recovered ones.

MATERIALS AND METHODS

MATERIALS

Institutional abbreviations: **AMNH**, American Museum of Natural History, New York City, USA; **FMNH**, Field Museum, Chicago, USA; **GM**, Geiseltal Museum, Martin-Luther University, Halle/Saale, Germany; **IGM**, Institute of Geology, Mongolian Academy of Sciences, Ulaan Bataar, Mongolia; **MAE**,

TABLE 1
Gobiderma pulchrum specimens studied for this paper along with locality data and the known parts of each specimen

Spec. #	Locality	Material
ZPAL MgR III/64	Hirmiin Tsav II	incomplete skull lacking left supratemporal arch, right jugal bar, and right mandibular ramus (holotype)
ZPAL MgR III/65	Hirmiin Tsav II	posterodorsal skull roof and braincase and incomplete mandible lacking anterior end of the dentary
ZPAL MgR III/66	Hirmiin Tsav II	incomplete skull lacking snout tip, right maxilla, right jugal, and right supratemporal arch; incomplete right mandible lacking dentary tip
ZPAL MgR I/54	Khulsan	partial antorbital snout
IGM 3/55	Üüden Sair	complete skull with mandibles, first two and a half vertebrae, osteoderms in place
IGM 3/57	Ukhaa Tolgod	partial articulated skull and lower jaws with dorsal part of the skull and ventral part of the mandibles
IGM 3/59	Hirmiin Tsav	partial skull with braincase and lower jaw, and several presacral vertebrae
IGM 3/905	Tögrökgiin Shiree	incomplete skull and skeleton including a nearly complete skull, 22 dorsal vertebrae, both sacral vertebrae, the first two caudal vertebrae, the right scapulocoracoid, the left manus, the pelvic girdle, the left hind limb including pes, a partial right pes, and a osteoderms associated the skull

Mongolian Academy of Sciences–American Museum of Natural History Expeditions, field numbers; **NHM**, the Natural History Museum, London, England; **UF**, Florida State Museum (University of Florida), Gainesville, Florida; **ZPAL**, Zakład Paleobiologii, Polska Akademia Nauk (Paleobiological Institute, Polish Academy of Sciences), Warsaw, Poland.

Following any of the above abbreviations, **FR** (most collections) or **PR** (**Field Museum**) signifies a fossil and **R** signifies a specimen of an extant species; these do not apply to IGM, MAE, or ZPAL specimens, all of which are fossils.

Comparative specimens:

Anguidae – *Abronia deppii* FMNH R 38523; *Anguis fragilis* AMNH R 56193; *Anniella nigra* FMNH R 213666; *Barisia imbricatus* FMNH R 6526, FMNH R 6528; *Celestes costatus* FMNH R 13254; *Diploglossus millepunctatus* FMNH R 19248; *Dopasia harti* FMNH R 24298; *Elgaria* sp. FMNH R 23235, FMNH R 213397; *Gerrhonotus liocephalus* FMNH R 22452; *Helodermoides tuberculatus* AMNH FR 5902, AMNH FR 6800, AMNH FR 8706; *Melanosaurus maximus* AMNH FR 5168, AMNH FR 5175; *Ophisaurus attenuatus* FMNH R 98466, FMNH R 98467, FMNH R 207671; *Ophiodes* sp. FMNH R 9270; *Paraglyptosaurus princeps* AMNH FR 6055; *Parophisaurus pawneensis* AMNH FR 8711; *Peltosaurus granulatus* AMNH FR 42913, AMNH FR 1710, AMNH FR 8138, FMNH PR 27072, FMNH UC391, FMNH UC1720; *Pseudopus apodus* FMNH R 216745, FMNH R 22088, FMNH R 22359.

Carusoidea – *Carusia intermedia* IGM 3/18, IGM 3/22, IGM 3/23, IGM 3/26; *Xenosaurus grandis* FMNH R 211833; *Xenosaurus platyceps* UF R 43396, UF R 43397, UF R 45590, UF R 53691, UF R 56122.

Goannasauria – *Adriosaurus suessi* NHM FR 2867; *Aiolosaurus oriens* IGM 3/171; *Cherminotus longifrons* ZPAL MgR III/59, ZPAL MgR III/67; *Coniasaurus crassidens* NHM FR 62, NHM FR 1937, NHM FR 23421, NHM FR 25790; *Coniasaurus gracilodens* NHM FR 44141; *Dolichosaurus longicollis* NHM FR 32268, NHM FR 49002, NHM FR 49907, NHM FR 49908; *Lanthanotus borneensis* FMNH R 130981, FMNH R 134711; *Ovoa gurvel* IGM 3/767; *Proplatynotia longirostrata* ZPAL MgR I/68; *Saniwa ensidens* FMNH PR 2378, FMNH PR 2380; *Telmasaurus grangeri* AMNH FR 6643; *Varanus acanthurus* FMNH R 218083, FMNH R 98935; *Varanus albigularis* AMNH R 47726, FMNH 17142, FMNH R 22354; *Varanus bengalensis* FMNH R 22495; *Varanus dumerilii* FMNH R 223194, FMNH R 22f8151; *Varanus exanthematicus* FMNH R 212985; *Varanus gouldii* FMNH R

250434; *Varanus griseus* FMNH R 31380; *Varanus komodoensis* AMNH R 37908, FMNH R 22199, FMNH R 22200; *Varanus niloticus* AMNH R 10524, AMNH R 74603, FMNH R 12300, FMNH R 17144, FMNH R 17145, FMNH R 17146, FMNH R 22084, FMNH R 22496, FMNH R 45807; *Varanus oliveaceus* FMNH R 223181; *Varanus rudicollis* AMNH R 141071; *Varanus prasinus* FMNH R 229907; *Varanus priscus* AMNH FR 1968, AMNH FR 6302, AMNH FR 6303, AMNH FR 6304, NHM FR 12007 (cast); *Varanus salvadorii* AMNH R 59873; *Varanus salvator* AMNH R 142471; FMNH 22204, FMNH 31320.

Monstersauria – *Estesia mongoliensis* AMNH FR 29072 (cast); IGM 3/196; *Eurheloderma galli-cum* NHM FR 3487; *Gobiderma pulchrum* IGM 3/55, IGM 3/57, IGM 3/59, IGM 3/905, ZPAL MgR III/64, ZPAL MgR III/65, ZPAL MgR III/66; *Heloderma horridum* AMNH R 57863, AMNH R 64128, FMNH R 22038, FMNH R 250611, FMNH R 31366, FMNH R 98468, FMNH R 98776; *Heloderma suspectum* AMNH R 72646, AMNH R 74778, AMNH R 142627, FMNH R 218077, FMNH R 22232, FMNH R 22249, FMNH R 98774; *Paraderma bogerti* AMNH FR 5804.

Other Anguimorpha – *Eosaniwa koehni* GM FR XXXVIII/57; *Dorsetisaurus purbeckensis* NHM FR 8061, NHM R 8064, NHM FR 8129, NHM FR 8110, NHM FR 8244, NHM FR 8247, NHM FR 8248; *Necrosaurus cayluxi* NHM FR 3486; *Necrosaurus* sp. NHM FR 6823; *Parasaniwa wyomingensis* AMNH FR 22012; *Paravaranus angustifrons* ZPAL MgR I/67.

Shinisauria – *Bahndwivici ammoskius* FMNH PR 2260; *Shinisaurus crocodilurus* FMNH R 233130, FMNH R 234242; UF R 57112, UF R 61149, UF R 61685, UF R 62315, UF R 62316, UF R 62497, UF R 62536, UF R 62578, UF R 68203.

METHODS

Cranial anatomical terminology used herein follows that of Oelrich (1956) and some more recent papers that offer modifications to that terminology (Maisano, 2001c; Conrad, 2004; Bever et al., 2005a). Postcranial anatomical terminology primarily follows the usages of Romer (1956), Rieppel (1980b), Estes et al. (1988), and Maisano (2001c). We have attempted to list alternate names and usages of anatomical features anywhere confusion seems possible.

In contrast to some recent work, especially by contributors to the open-access morphological library Digital Morphology (<http://digimorph.org/index.phtml>), we use the standard, nonmammal-based terminology when referring to the major axes of the vertebrate body; that is, we implement the terms transverse plane instead of coronal plane and frontal plane rather than horizontal plane. The term “sagittal plane” is universal.

Specimens were examined through direct observation, through the use of dissecting microscopes, and via high-resolution X-ray computed tomography (HRXCT) scanning at the HRXCT Facility at the University of Texas at Austin.

Because recent studies have demonstrated that *Gobiderma pulchrum* is a monstersaur (Gao and Norell, 1998; Conrad, 2008; Conrad et al., 2011) and because many other fossil monstersaurs are known from very incomplete remains (see Estes, 1964, 1983; Pregill et al., 1986; Norell et al., 1992; Norell and Gao, 1997; Gao and Norell, 2000), many comparisons made below are between *Gobiderma pulchrum* and extant *Heloderma*. Other comparisons are made where necessary and informative. Varanoidea and Platynota are used following Conrad (2008), but note that there are data suggesting that Monstersauria (Gila monsters, beaded lizards) and Goannasauria (mosasaurs, monitor lizards, earless monitors) may not form a clade exclusive of other extant anguimorph groups (Ast, 2002; Townsend et al., 2004; Vidal and Hedges, 2005; Conrad et al., 2011).

One specimen (IGM 3/55) was scanned using a FeinFocus microfocal X-ray source operating at 180 kV and 0.133 mA. Slice thickness corresponded to two lines in a CCD image intensifier imaging system, with a source-to-object distance of 39 mm. For each slice, 1800 views were taken with two samples per view. The field of image reconstruction offset of 5700 was employed with a reconstruction scale of 775.

The dataset consists of 695 HRXCT slices taken along the transverse (transverse) axis of the skull. Each slice image was gathered at 1024×1024 pixels resolution, resulting in an in-plane resolution of $12.2 \mu\text{m}$. The dataset was resliced along the other two orthological axes (frontal and sagittal) and three-dimensional visualizations were produced us-

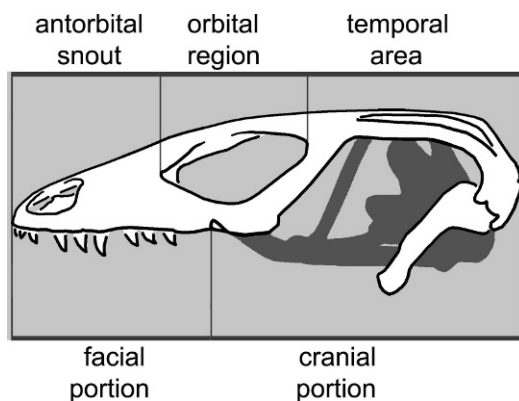


Fig. 2. The divisions of the skull as laid out in the manuscript. The antorbital region includes the part of the skull anterior to the anteriormost margin of the external orbital rim. The temporal area includes the skull posterior to the posteriormost margin of the orbit. The orbital area lies between those two areas. The facial part of the skull extends from the anterior margin of the ectopterygoid-maxillary contact forward. The cranial portion includes the part of the skull posterior to that point. Modified from Montero and Gans (1999) and as described by Conrad (2004).

ing VGStudio Max® 1.2 (Volumer Graphics, Heidelberg, Germany). Density and contrast between bone and matrix was sufficient to permit digital “preparation” of the specimen—rendering the matrix transparent.

An interactive, web-deliverable version of the HRXCT dataset, as well as slice-by-slice animations and three-dimensional reconstructions can be viewed on the Internet (http://digimorph.org/specimens/Gobiderma_pulchrum/) and the original full-resolution HRXCT data are available from the authors.

SYSTEMATICS

SQUAMATA OPPEL, 1811

ANGUIMORPHA FÜRBRINGER, 1900

MONSTERSAURIA NORELL AND GAO, 1997

GOBIDERMA PULCHRUM BORSUK-BIAŁYNICKA, 1984

DESCRIPTION

SKULL AND MANDIBLE

SKULL FORM: Skulls may be usefully divided into two different sets of anatomical

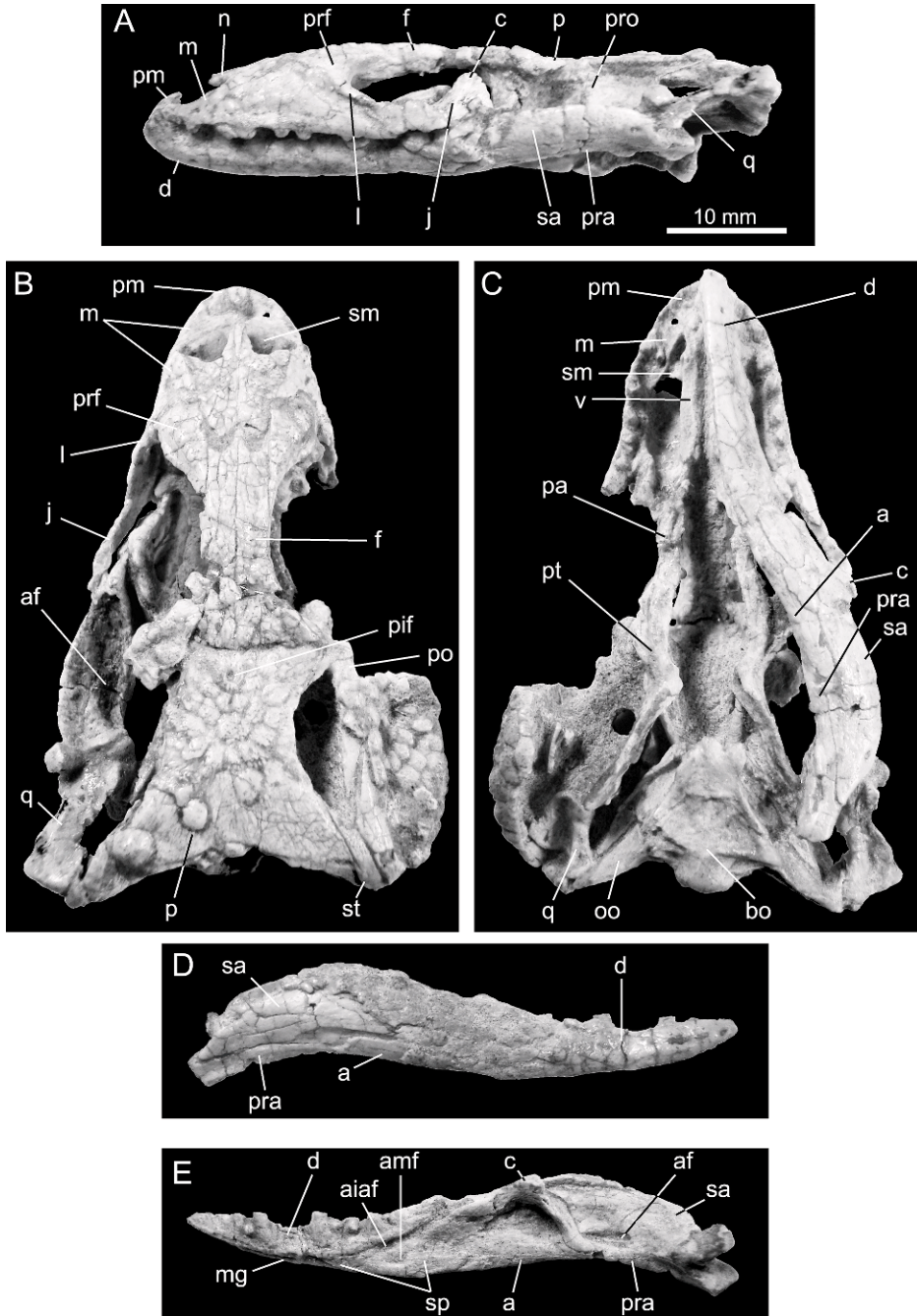


Fig. 3. *Gobiderma pulchrum*, holotype skull with lower jaws (ZPAL MgR III/64). Skull and left mandible in **A**, left lateral, **B**, dorsal, and **C**, ventral views. Right mandible in **D**, lateral and **E**, medial views.

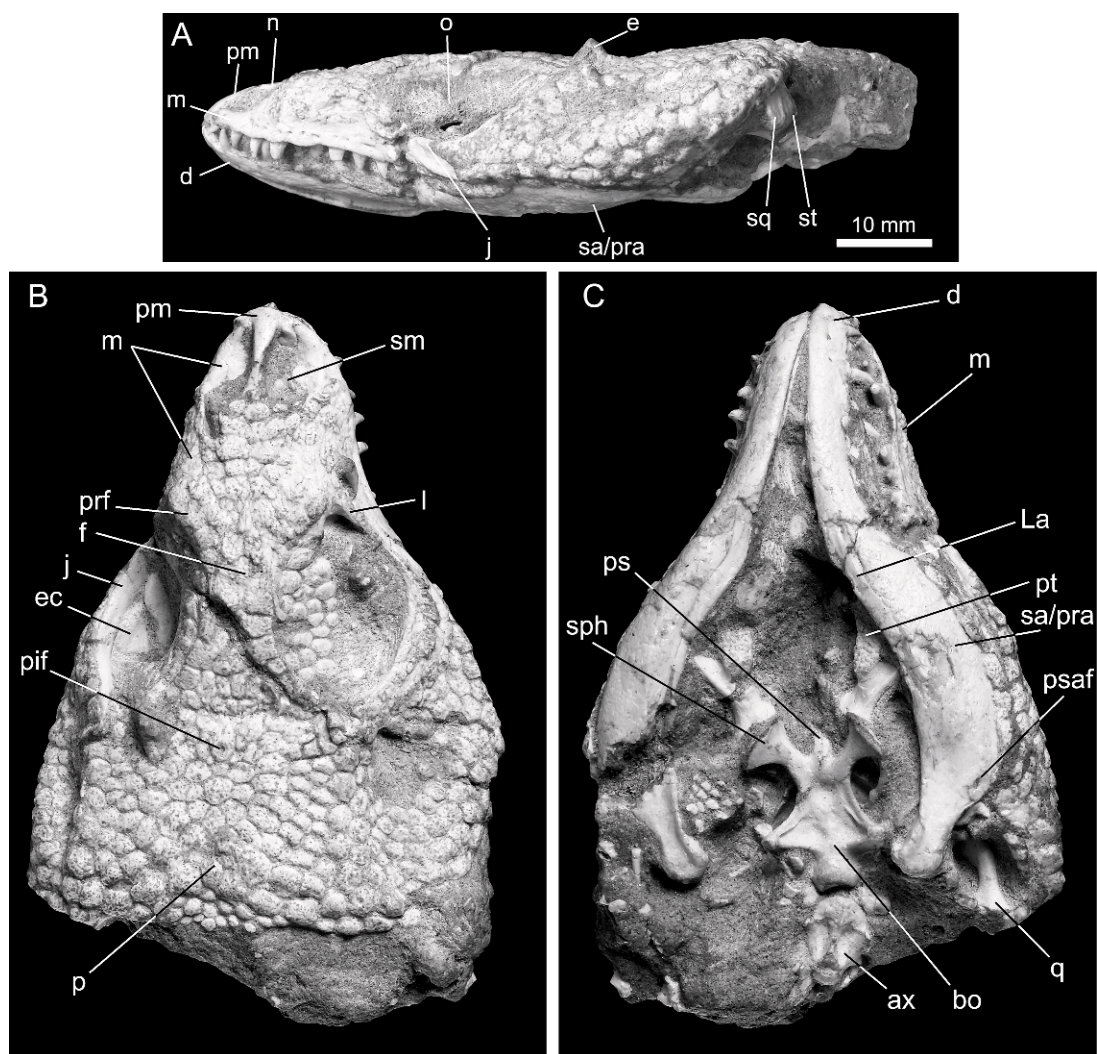


Fig. 4. *Gobiderma pulchrum* (IGM 3/55) skull with lower jaws in **A**, left lateral, **B**, dorsal, and **C**, ventral views.

regions. The skull may be separated into facial and cranial portions (at the maxilla-ectopterygoid contact) or into an antorbital snout, an orbital region, and a temporal area (including the skull table) (fig. 2). Both sets of terminology will be used below as they become relevant and informative.

Both the holotype (ZPAL MgR III/64) (fig. 3) and IGM 3/55 (figs. 4, 5) are relatively complete and largely preserve the overall shape of the skull. The holotype is more dorsoventrally compressed than IGM 3/55, especially posteriorly, as indicated by the position and

state of preservation of the epipterygoid in IGM 3/55. Dorsoventral compression in the holotype implies that the skull is somewhat wider than it was in life. IGM 3/55 preserves the shape of the skull very well. This skull is also somewhat dorsoventrally flattened and the dorsal part of the skull has moved slightly to the left. Even so, this extremely well-preserved skull retains the osteoderms in their original position and clearly shows the outline of the skull and snout. The skull of IGM 3/905 (fig. 6) shows no deformation at all and shows the appropriate depth of the snout to about the

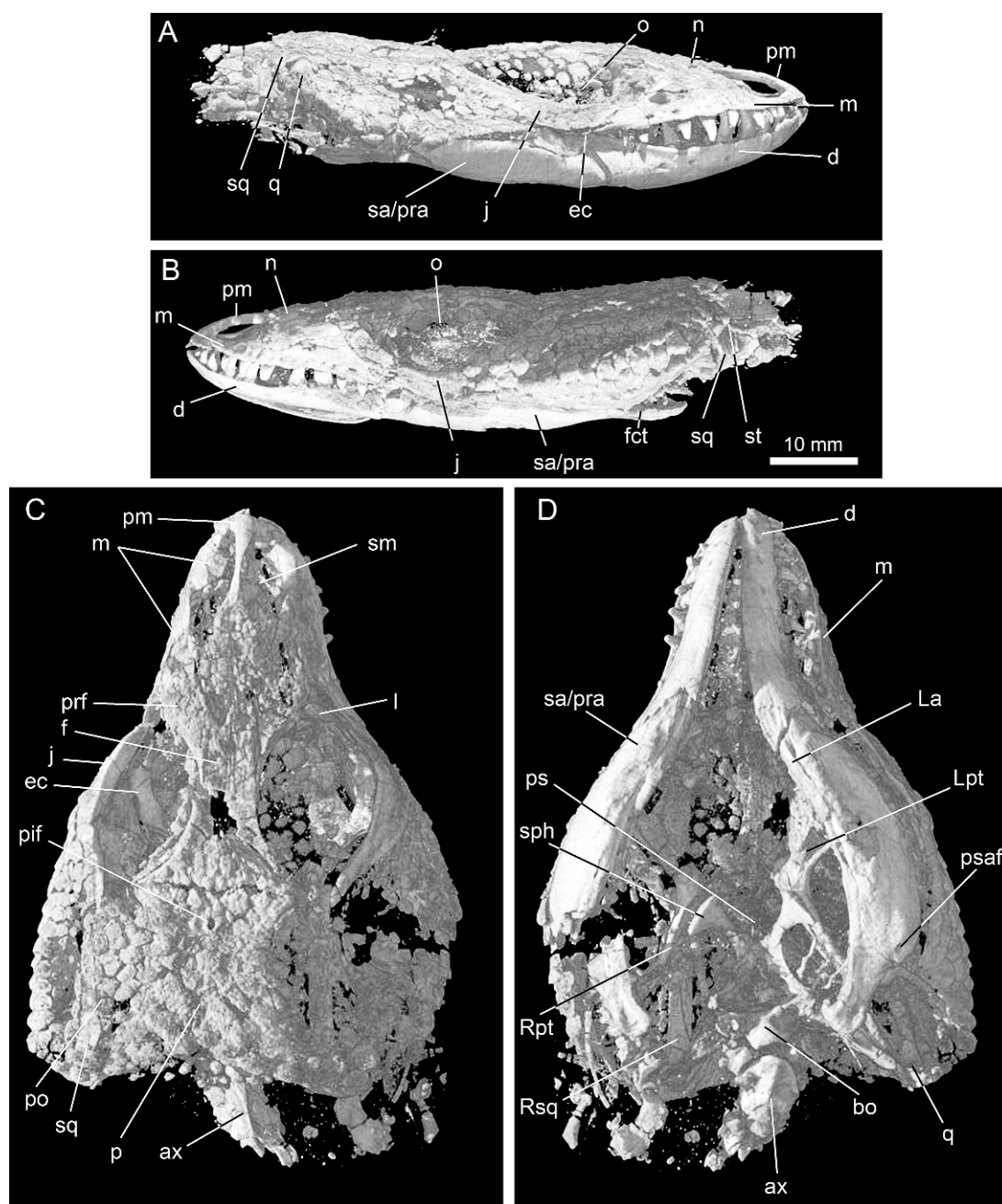


Fig. 5. High-resolution X-ray computed tomography scans of *Gobiderma pulchrum* (IGM 3/55) with matrix rendered invisible in **A**, right lateral, **B**, left lateral, **C**, dorsal, and **D**, ventral views.

midorbit. Thus, the all of the skull and mandibular elements are known with the only remaining ambiguity being in the postero-ventral splenial morphology at the angular contact, allowing us to confidently reconstruct

the skull (fig. 7). Overall, the skull of *Gobiderma* is deeper than previously illustrated (Borsuk-Białynicka, 1984).

The skull is broadest at the middle part of the orbit where the jugals arch laterally in a gentle

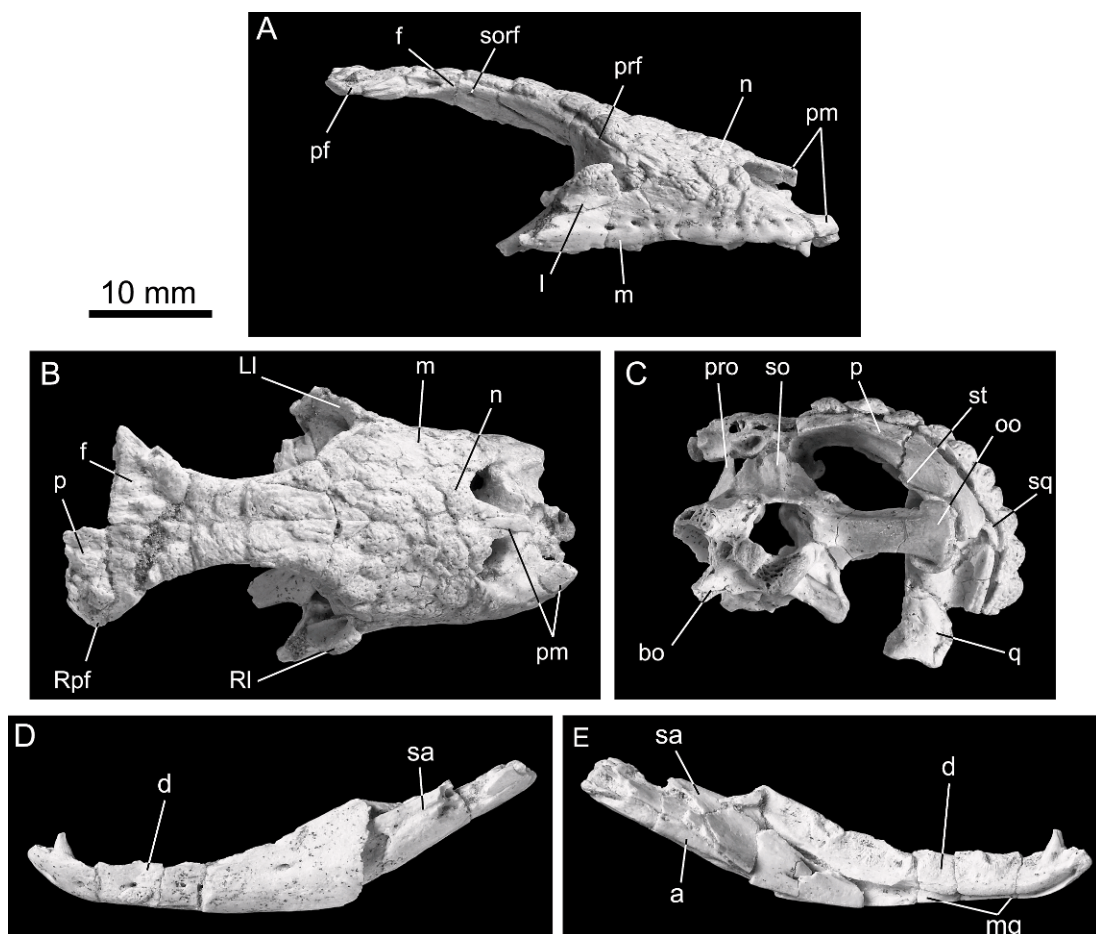


Fig. 6. *Gobiderma pulchrum*, (IGM 3/905) skull with lower jaws. **A**. Snout and orbital portions in right lateral and **B**, dorsal views. **C**. Braincase and right jaw suspensorium in posterior view. Partial right mandible in **D**, lateral and **E**, medial views.

curve. The left jugal of IGM 3/55 is preserved in near-life position with respect to the temporal area, so when viewed dorsally the approximate shape of the lateral margin of the skull (figs. 4A, 5A, B) can be observed. The snout tapers anteriorly to a narrow tip. The facial region is slightly more mediolaterally constricted at the anterior level of the anterior margin of the orbit than was evident in the previously described specimens (fig. 2) (Borsuk-Białynicka, 1984). This condition is evident in all the new specimens. Lateral exposure of the ectopterygoid in its natural articulation with the maxilla (figs. 4A, 5A, 7A, C; see below) demonstrates that the facial portion of the skull is slightly longer than the snout (figs. 2, 7).

The temporal area is roughly square in dorsal view (figs. 3B, 4C, 7B). The robust, complete, supratemporal arches delimit the temporal area laterally in dorsal view. Differentiation of the dorsolateral osteoderms mark where the dorsal surface of the skull table gives way to the lateral surface. The supratemporal arch lies primarily in the same dorsoventral plane as the parietal table for most of its length, but curves sharply posteroventrally, so that it is somewhat ventral to the level of the parietal skull table near the jaw suspensorium. Consequently, the posterior part of the dorsolateral margin of the skull is somewhat rounded in sagittal view at the level of the supratemporal process. The snout

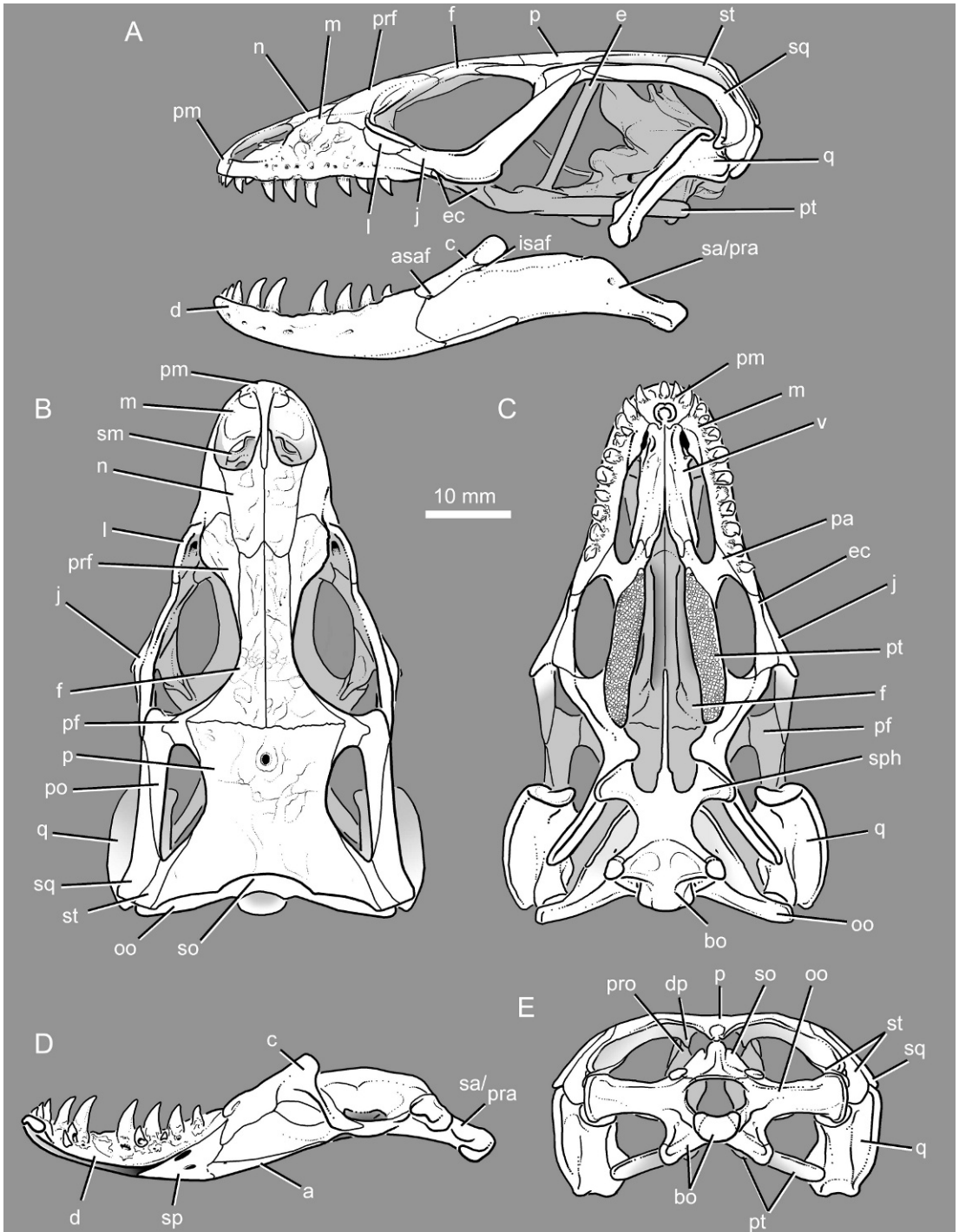


Fig. 7. Reconstructed skull and mandibles of *Gobiderma pulchrum* based on all available specimens. **A.** Skull and mandible in left lateral view. Skull in **B**, dorsal and **C**, ventral views. **D.** Mandible in medial view. **E.** Skull in posterior views. Note that the entire skull and mandible are known through comparison of available material.

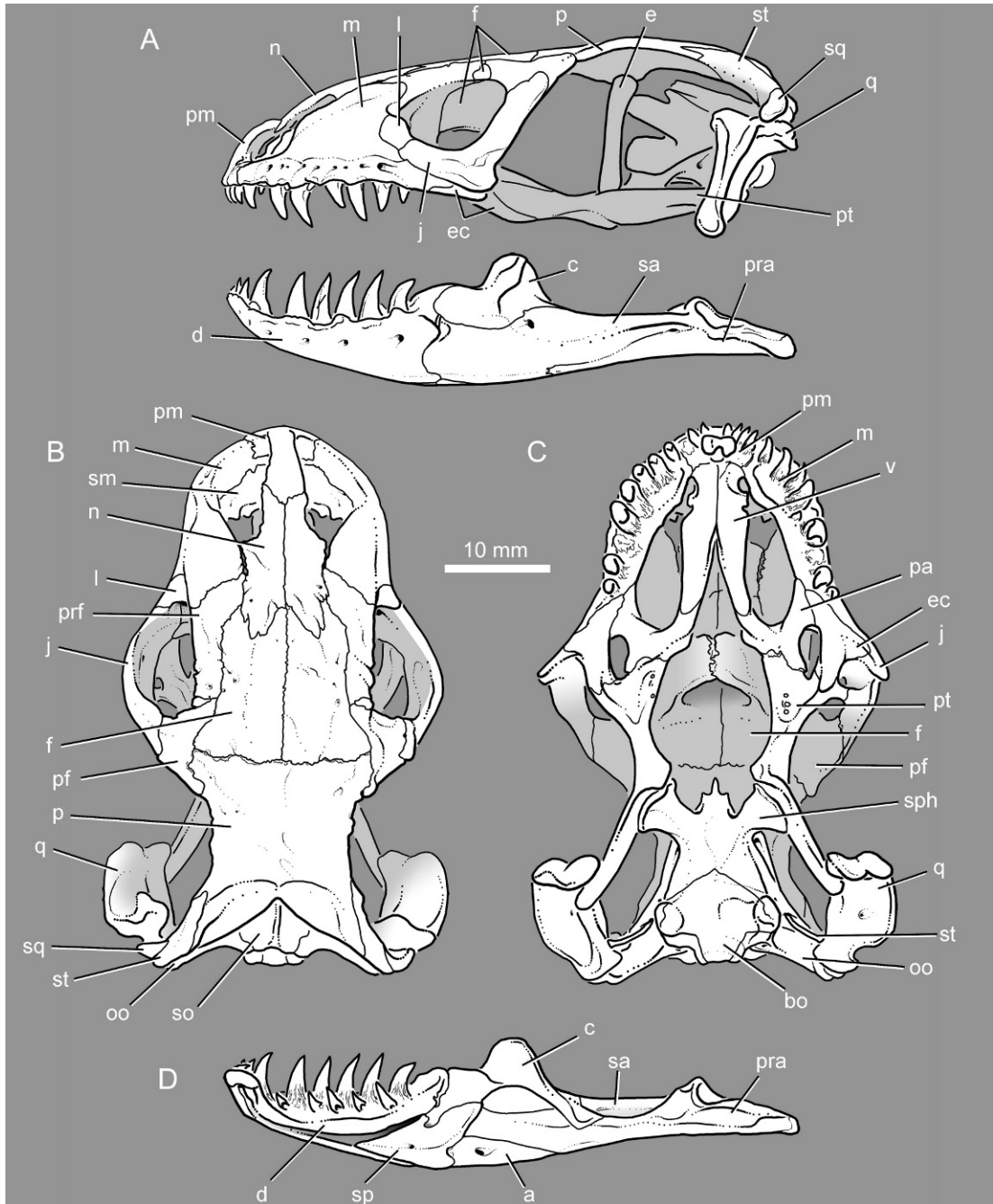


Fig. 8. Skull and mandible of *Heloderma suspectum* (AMNH R72646). A. Skull and mandible in left lateral view. Skull in B, dorsal and C, ventral views. D. Mandible in medial view.

of *Heloderma* is short and rounded in both dorsal and lateral views (fig. 8A, B). *Heloderma* lacks a complete supratemporal arch and the sagittal view of the skull through the level

of the supratemporal emargination is a dorsolaterally convex arch of osteoderms that overlie the adductor musculature. In contrast, the skull of *Gobiderma* is more angular.

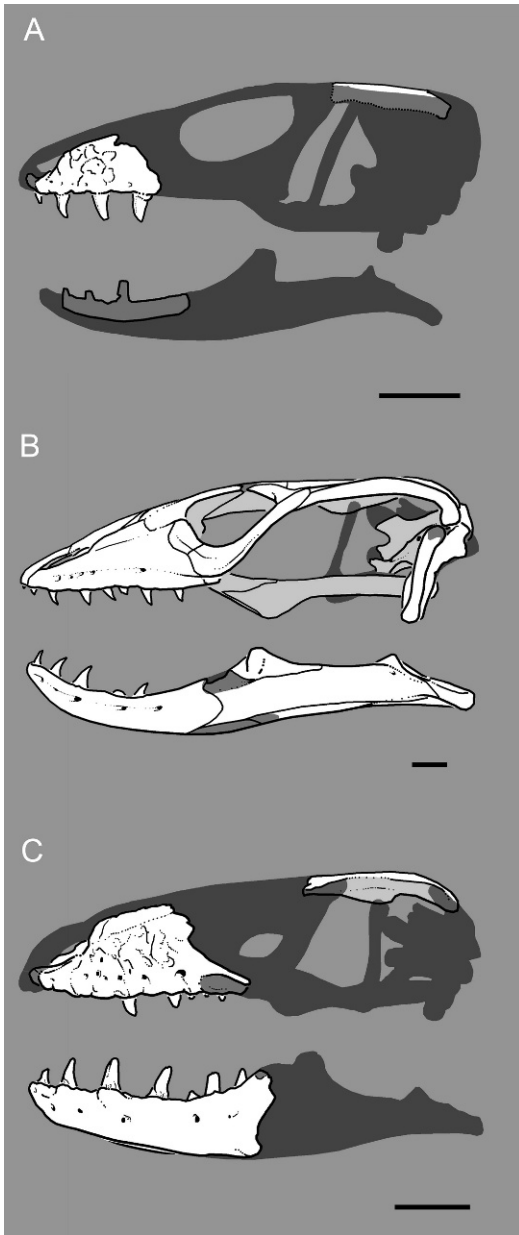


Fig. 9. Reconstructions of three monstersaurs in left lateral view. **A.** *Primaderma nessovi* (modified after Cifelli and Nydam, 1995, and Nydam, 2000); **B.** *Estesia mongoliensis* (modified after Norell et al., 1992, and Norell and Gao, 1997); **C.** *Eurheloderma gallicum* (Hoffstetter, 1957). Scale bars = 10 mm.

Primaderma nessovi probably also had the plesiomorphic angular skulls (based on the shape of the nasal process of the maxilla) (Nydam, 2000) (fig. 9A). The Cretaceous monstersaur *Estesia mongoliensis* had a rounded snout in dorsal view, but still had a somewhat pointed snout in lateral view (fig. 9B), similar to that of goannasaurs (sensu Conrad, 2008) such as some mosasaurs, *Varanus* and *Ovoo gurvel* (fig. 10A). *Eurheloderma gallicum* possessed a dorsally tall nasal process of the maxilla (Hoffstetter, 1957), possibly indicating a more *Heloderma*-like profile (fig. 9C).

The occipital condyle is a single posterior convexity composed of the basioccipital and the otooccipitals (figs. 4C, 5D, 7). The two otooccipital portions constitute slightly more than one half of the condyle. The holotype (ZPAL MgR III/64) (fig. 3), IGM 3/55 (figs. 4, 5), and ZPAL MgR III/65 (fig. 11) each has a completely preserved occipital condyle that is gently concave anteriorly such that the otooccipital parts extend posteriorly just beyond the level of the basioccipital midline portion. Extant *Heloderma* lack any anterior concavity of the occipital condyle (fig. 8B, C).

Gobiderma possesses external nares that are somewhat enlarged and project dorsally and somewhat anteriorly (figs. 3–7, 12), although not as much even as in extant *Heloderma* (fig. 8; the nares are not preserved in *Heloderma texana*; see Maisano, 2001a) or many goannasaurs (e.g., *Ovoo gurvel*; fig. 10A, B). The orbital region is equivalent to slightly more than one-quarter of the skull length. The supratemporal fenestra is a half-oval (D-shaped) in dorsal view; the lateral margin, formed by the supratemporal arch, is straight and the medial margin, formed by the lateral margin of the parietal table, is medially concave (figs. 3B, 7B). The infratemporal vacuity is rhomboid shaped and ventrally open as in most lepidosaurs. The suborbital fenestra is approximately two-thirds the length of the orbit and is medio-laterally much narrower than the orbit (figs. 3B, 4B, 5B, 7B). The suborbital fenestra is similar in shape and size to the supratemporal fenestra, but the rounded margin is oriented anterolaterally. The pyriform recess is broad posteriorly in the cranial portion of

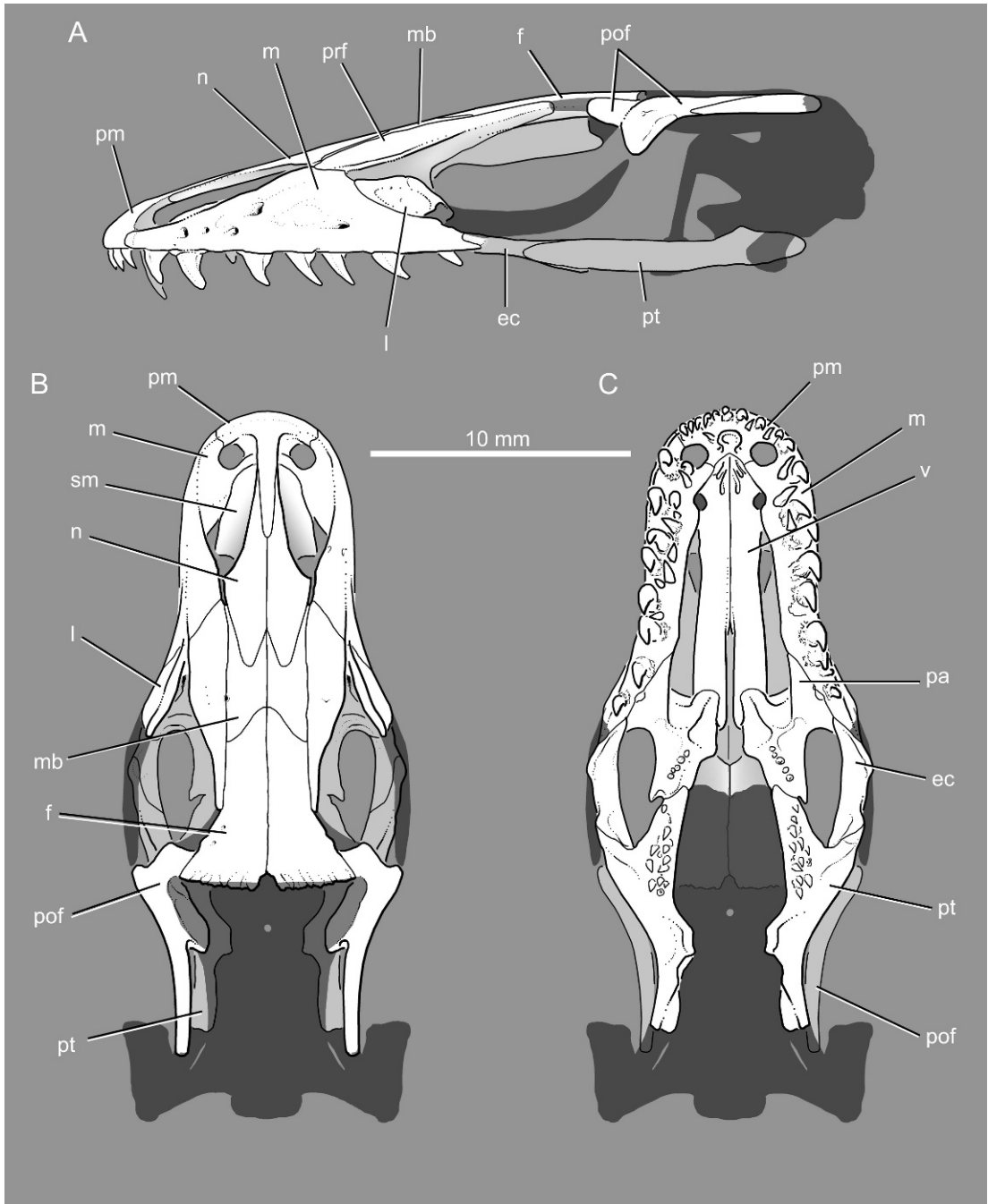


Fig. 10. Reconstructed skull of *Ovoo gurvel* based on the holotype (IGM 3/767), in **A**, left lateral view, **B**, dorsal view, and **C**, ventral view. Missing areas represented as semiopaque shadows. Scale bar = 10 mm.

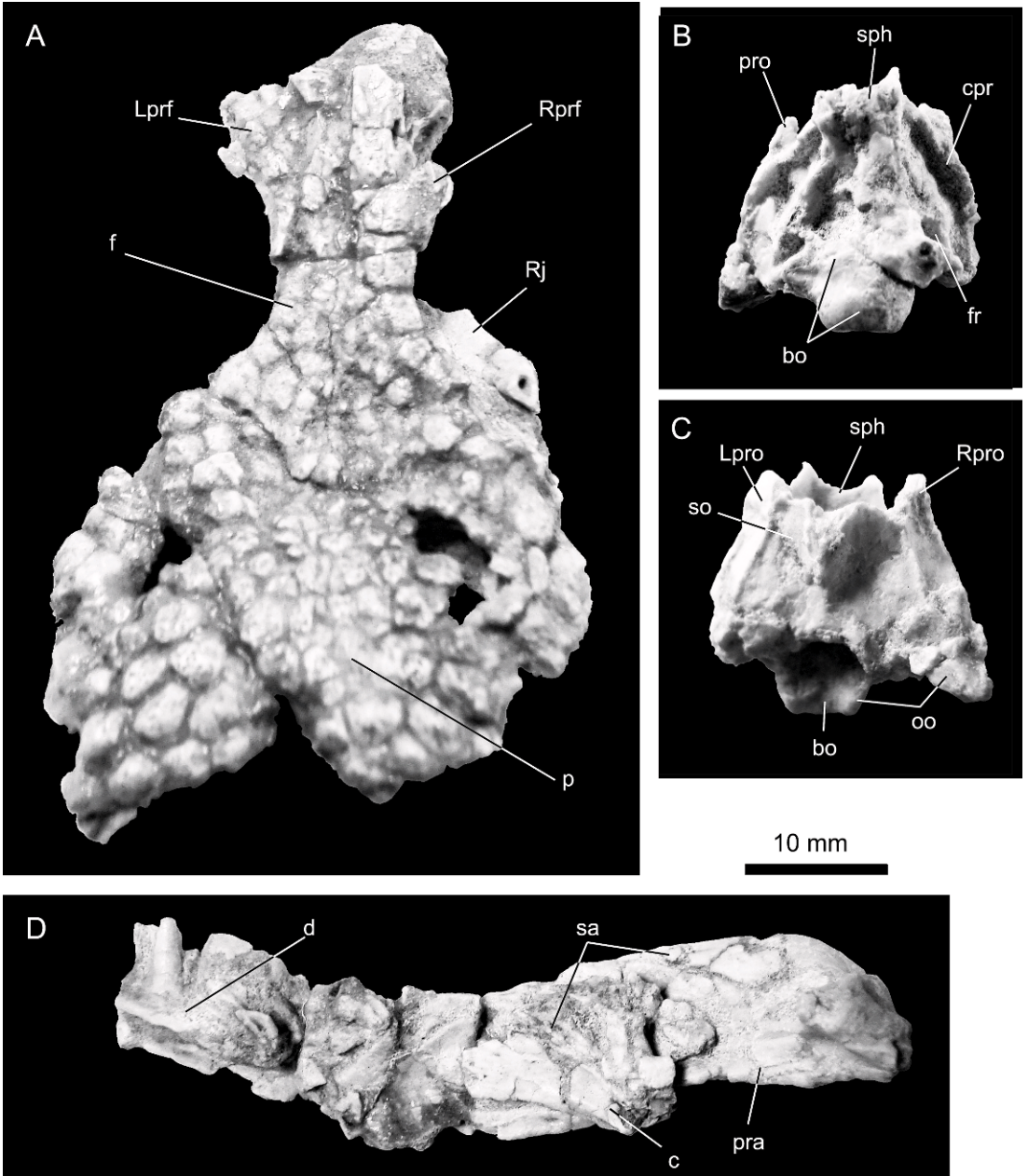


Fig. 11. *Gobiderma pulchrum* (ZPAL MgR III-65), partial skull and lower jaws. **A.** Orbital and temporal areas in dorsal view. Braincase in **B**, ventral and **C**, dorsal views. **D.** Posterior mandible lacking the anterior part of the dentary and the splenial in medial view.

the skull and its posterior margin is round and formed by the braincase. Its anterior margin is formed by the anterior palatal bones and is acuminate.

The posttemporal fenestra is a narrow, ovate-acuminate opening facing posteromedially at the posterior margin of the skull (fig. 6C). Its margins are formed dorsally by

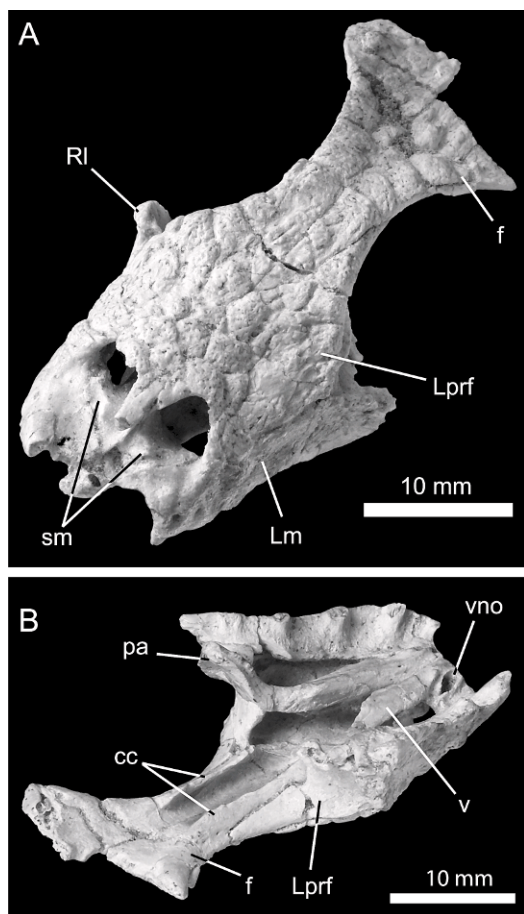


Fig. 12. Snout and orbital region of *Gobiderma pulchrum* (IGM 3/905). Skull in **A**, anterodorsolateral view, and **B**, posteroventrolateral view, illustrating the narial region, some skull sutures, the palate, and subolfactory processes.

the parietal and ventrally by the supratemporal and otooccipital. The foramen magnum is roughly circular, but its greatest diameter occurs below the dorsoventral midpoint, at the dorsolateral margin of the occipital condyle. The dorsoventral diameter is nearly as great.

No contact exists between the vomer and maxilla posterior to the vomeronasal opening (figs. 3C, 7C) (confirming the observations of Borsuk-Białynicka, 1984). However, the septomaxilla bridges the gap between the vomer and maxilla ventrally, effectively dividing the vomeronasal chamber from the internal naris as in *Xenosaurus*, *Shinisaurus*, anguids, and observed extant varanids.

MANDIBULAR FORM: Elements of the lower jaw are preserved in all the known specimens (table 1), but are best preserved in ZPAL MgR III/64 (fig. 3), IGM 3/55 (figs. 4A, C, 5A, B, D), and IGM 3/905 (fig. 6D, E). The robust lower jaw of *Gobiderma* is somewhat recurved; it forms a ventrally arched anterior curve and a dorsally arched posterior curve. Preserved portions of the mandible in IGM 3/905 are slightly out of articulation with one another and demonstrate overlap of the dentary-splénial unit with respect to the postdentary bones (fig. 6D, E) and, thus, the absence of a clear intramandibular joint like that of mosasaurs. A surface for a syndesmostic joint is also present at the anterior tip of the dentary. The dentary constitutes less than one-half of the length of the mandible and extends to about the level of the orbit midpoint when the upper and lower jaws are extended to the same anterior level (figs. 3–5, 7). IGM 3/55 preserves a complete splénial. The splénial extends anteriorly to about the midpoint of the dentary tooth row. Meckel's canal is open medially for its entire length. Both IGM 3/55 and ZPAL MgR III/64 are preserved with at least one complete lower mandibular ramus and demonstrate that the retroarticular process is strongly medially deflected (figs. 3B, 4C, 5D; also, see below).

PREMAXILLA: The premaxilla is well preserved and visible in IGM 3/55 (figs. 4A, B, 5A–C), IGM 3/905 (fig. 6A, B), and ZPAL MgR III/64 (fig. 3A, B). In IGM 3/55, the premaxilla is preserved in natural articulation with the rest of the skull, but the palatal contacts and posterior views are not available. The main premaxillary body has come loose from the rest of the skull in IGM 3/905, but the tip of the nasal process and most of the alveolar plate (= basal plate of Montero and Gans, 1999; and Conrad, 2004) remain in their natural positions (figs. 6B, 12). Part of the palatal view is visible in ZPAL MgR III/64, but the mandibular ramus and supporting matrix obscure the ventromedial part of the premaxilla (fig. 3C). The middle part of the nasal process is missing in IGM 3/905 and in ZPAL MgR III/64.

The premaxilla is a fused, single element contacting the nasals, maxillae, septomaxillae, and vomers. The main body of the

premaxilla forms the anteroventral margin of the bony external naris and the nasal process provides the anteromedial margin.

No remnant of a midline suture remains in the fused premaxilla. As with *Heloderma*, shinisaurs, and some anguids, the main body of the premaxilla is small and only narrowly visible in lateral view (figs. 3A, 4A, 5A, B, 7A). This differs from the condition in *Xenosaurus* and most *Varanus*, but see *Varanus acanthurus* (Mertens, 1942). A single ethmoidal groove is present just lateral to each side of the base of the premaxillary nasal process in IGM 3/55 and in ZPAL MgR III/64. IGM 3/905 does not possess these grooves. There are two small foramina ventrolateral to the base of the nasal process on the left side and one on the right, but these do not pass all the way through the premaxilla.

The elongate nasal process is broadest anteroventrally where it arises from the main premaxillary body. Near its base, the nasal process is approximately four tooth positions wide. The nasal process tapers posterodorsally to about the midlevel of the external naris where the lateral margins become more or less parallel for a short distance before tapering again. The nasals overlap the nasal process beginning at a point just behind that level. The nasal process is triangular in cross section with a flat external (anterodorsal) face and posteroventral ridge. The posteroventral ridge originates from the alveolar plate and extends along the underside of the nasal process for nearly the entire length of the premaxillary nasal process. Ventromedial flanges of the nasals underlie this ridge for the last two millimeters or so (fig. 13A). The posterodorsal terminus of the premaxillary nasal process lies at about the level of the posterodorsal narial margin or slightly behind that point. This contrasts with the condition in most goannasaurs, wherein the premaxillary nasal process does not approach the level of the posterior narial margin (e.g., *Ovoo gurvel*; fig. 10B), but is similar to the condition in others, such as the shinisaurs *Dalinghosaurus longidigitus* and *Bahndwivici ammoskius* (fig. 14A, B). This is influenced by the retraction of the nostrils in some taxa wherein the premaxillary nasal process is long (e.g., *Varanus*, *Saniwides mongoliensis*,

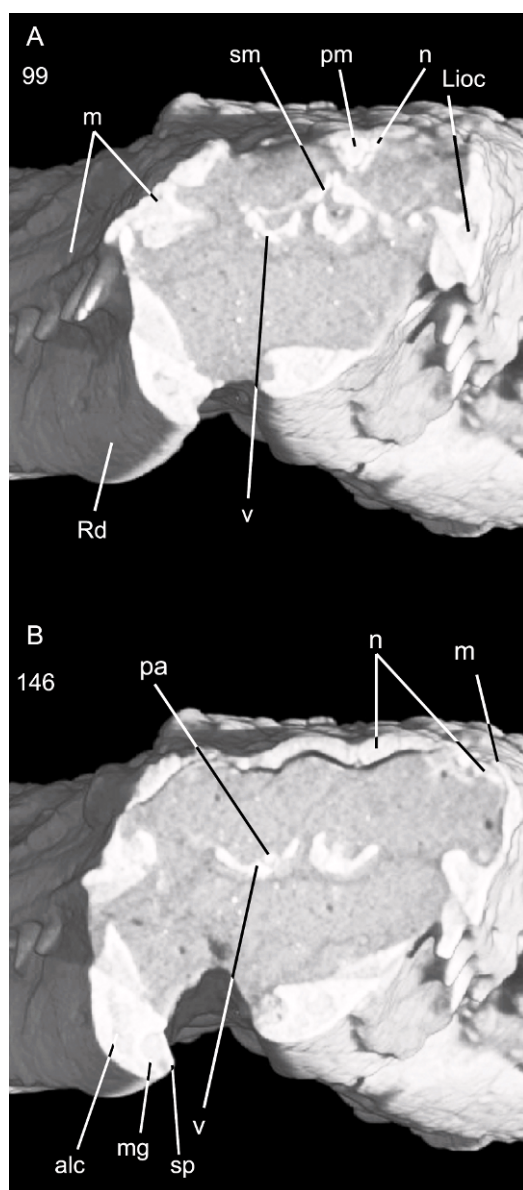


Fig. 13. Selected transverse HRXCT slices through the snout of *Gobiderma pulchrum*, (IGM 3/55). **A.** Transverse slice 99 (top) is through the anterior part of the snout near the posterior margin of the nares. **B.** Transverse slice 146 is through the midpart of the snout, near the posterior part of the vomer-palatine overlap.

Estesia mongoliensis [fig. 9B], *Ovoo gurvel* [fig. 10B]). In contrast, *Shinisaurus crocodilurus* possesses a very short premaxillary nasal process (Conrad, 2004) that terminates

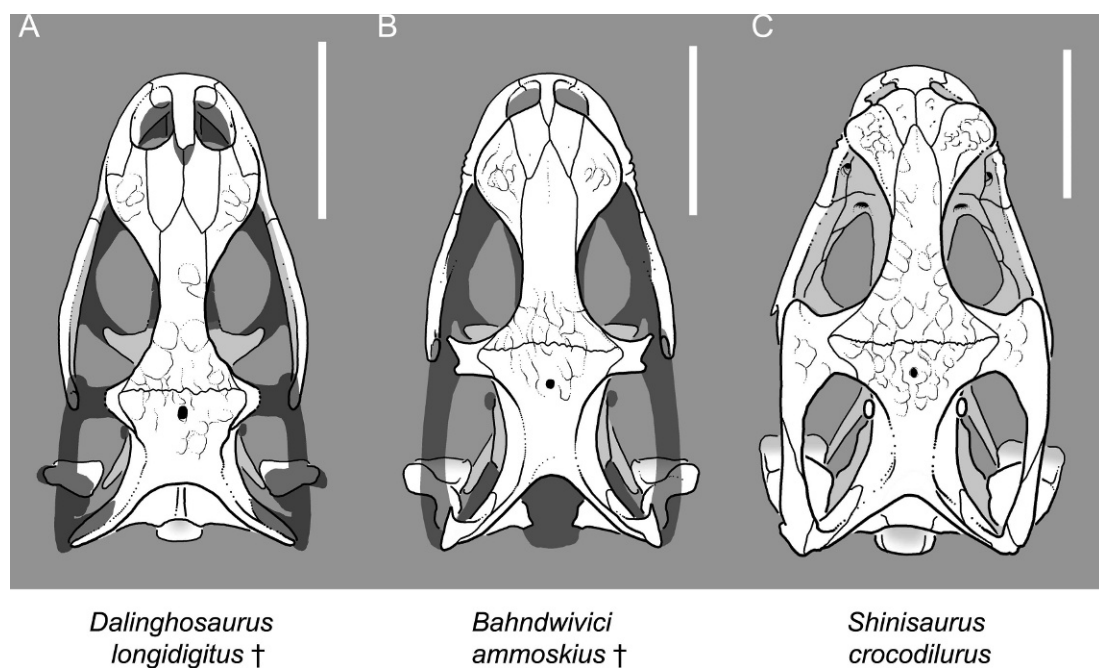


Fig. 14. Skulls of representative shinisaurs (sensu Conrad, 2008) in dorsal view. **A.** *Dalinghosaurus longidigitus* from Cretaceous of China (modified from Evans and Wang, 2005). **B.** *Bahndwivici ammoskius* from the Eocene of North America (FMNH PR2260). **C.** *Shinisaurus crocodilurus*, extant, from China (UF 11639). Missing areas represented as semiopaque shadows. Scale bars = 10 mm.

at about the midpoint of the relatively short external naris (fig. 14C). Extant *Heloderma* also possess relatively short premaxillary nasal processes as compared to goannasaurs and as compared with the breadth of the alveolar margin (see, for example, Bogert and Del Campo, 1956; Rieppel, 1980a; Bonine, 2005a; fig. 8B). *Bahndwivici ammoskius*, like *Gobiderma pulchrum*, shows a relatively longer nasal process that probably at least approached the level of the posterodorsal margin of the external naris (Conrad, 2006a; fig. 14B).

The width of the main body of the premaxilla, including the alveolar margin, is about equal to the length of the premaxillary nasal process. The anterior surface is very gently arched; there is little anteroposterior depth to the main body exclusive of the alveolar plate. The alveolar plate extends posteriorly nearly to the level of the anterior margin of the septomaxilla and it extends posteriorly beyond the ventral ridge of the nasal process and forms a short overlapping

joint (scarf joint) in which it ventrally overlaps the vomer. Anterolateral to this, the premaxilla is sutured to the maxilla in a mostly anteroposteriorly oriented contact. There is no premaxilla-maxilla aperture sensu Gao and Norell (1998).

A robust, bilobate, incisive process lies just anterior to the premaxilla-vomer suture. It is divided (fig. 7C), and is similar to the condition seen in extant *Heloderma* (fig. 8C), which is more extreme than in many other anguimorphs (e.g., *Carusia intermedia*; see fig. 15). The ventral surface of each lobe is a crescent that arches laterally, forming a small median depression between the two lobes. The total width of the incisive process is slightly less than the width of the vomers at their premaxillary contact.

MAXILLA: Coossification of osteoderms and their fusion to the maxilla makes the identification of sutures on any given specimen somewhat more difficult, but comparisons of specimens ZPAL MgR III/64, IGM 3/55, IGM 3/57, IGM 3/905, and HRXCT

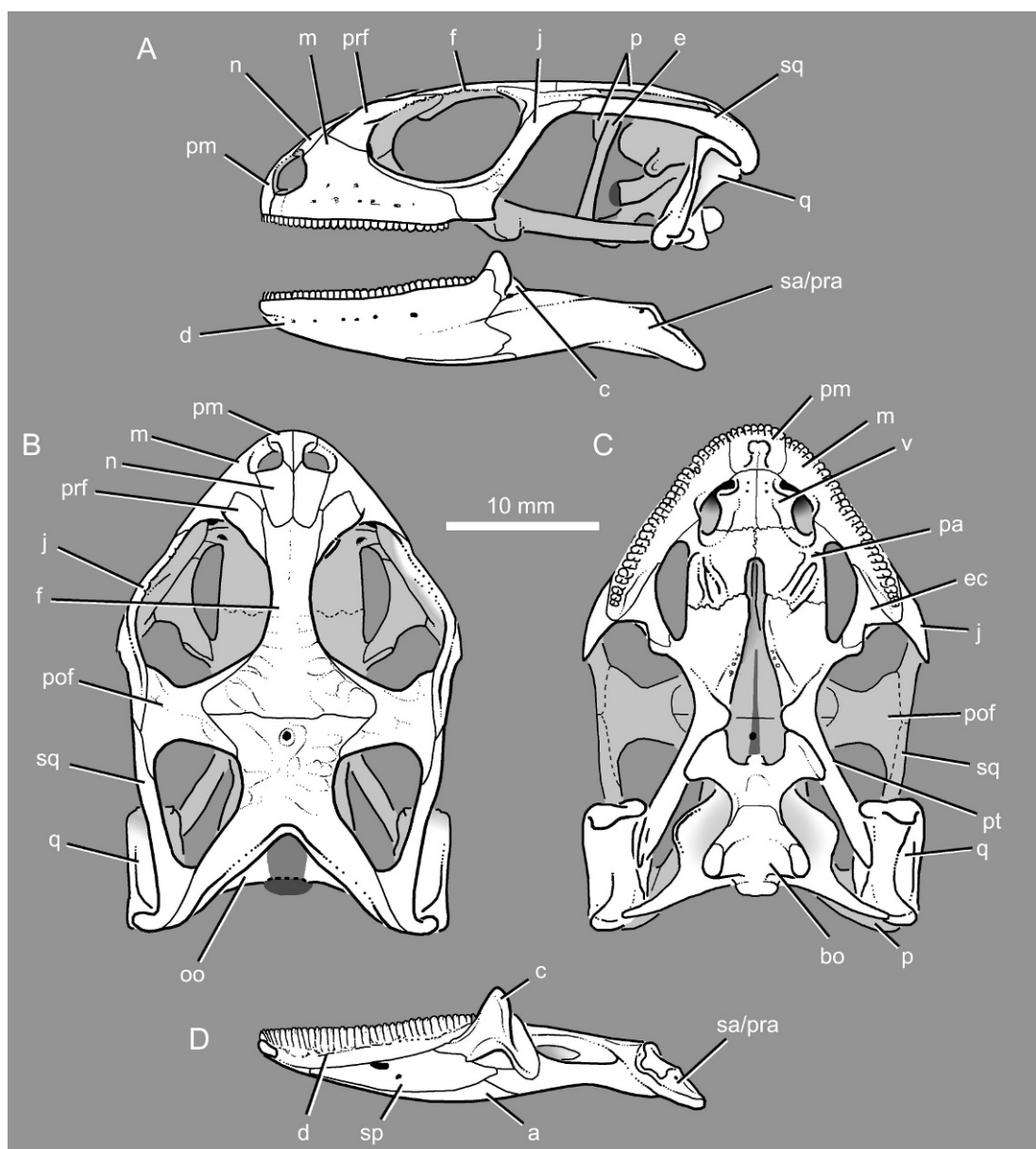


Fig. 15. Reconstructed skull of *Carusia intermedia* based on observations of specimens (IGM 3/18, IGM 3/22, IGM 3/23, IGM 3/26) and published photos, illustrations, and descriptions (Borsuk-Bialynicka, 1985; Gao and Norell, 1998; Alifanov, 2000). **A.** Skull and lower jaw in left lateral view. **B.** Skull, with jaw omitted, dorsal view, and **C.** ventral view. **D.** Right lower jaw in medial view. Missing areas represented as semiopaque shadows. Scale bar = 10 mm.

scans of IGM 3/55 render the details clearly. Removal of some of the osteoderms from the maxilla (through diagenetic forces and through preparation) reveals pitted sculpturing on the maxilla. This sculpturing is present

over most of the maxilla, but is absent ventral to the level of the labial foramina (figs. 3A, 4A, 5A, B, 6A).

The maxilla contacts the premaxilla, septomaxilla, nasal, prefrontal, lacrimal, jugal,

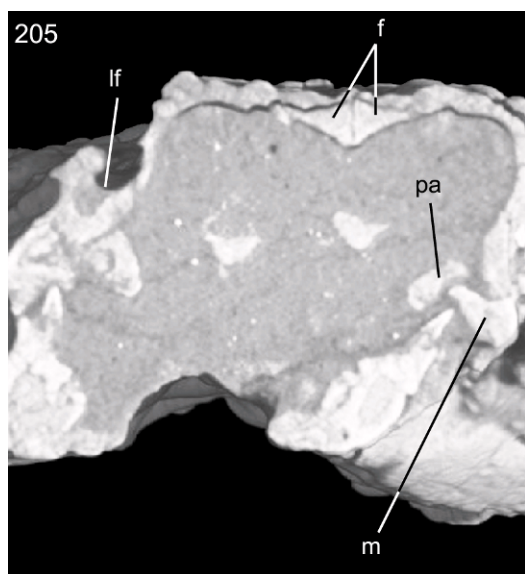


Fig. 16. Selected transverse HRXCT slice through the snout of *Gobiderma pulchrum* (IGM 3/55; transverse slice 205) just anterior to the level of the anterior margin of the orbit. Note the maxillopalatine contact, the paired frontals, and the posterodorsally expansive lacrimal foramen.

vomer, palatine, and ectopterygoid (figs. 3–7, 12, 16). The maxilla forms the ventrolateral and posterior margins of the external naris and the anterolateral margin of the vomeronasal fenestra (fenestra vomeronasalis externa of Oelrich, 1956; the opening to the Jacobson's organ chamber). The maxilla is subtriangular in lateral view with the apex of the nasal process forming an obtuse angle. The ventral portion, including the dental margin, is straight when viewed laterally and gently curved in ventral view (figs. 3–5). Laterally near the contact with the ectopterygoid, the dental margin is somewhat flared. The nasal process lies anterior to the midpoint of the tooth row and is dorsoventrally oriented in the parasagittal plane except near the dorsal one-quarter of its height where it is dorsomedially deflected. The maxilla extends anteriorly to underlie most of the ventrolateral part of the external naris and extends posteriorly nearly to the midpoint of the orbit.

The anterior part of the maxilla forks into a medial septomaxillary ramus and an external ramus (figs. 3B, 4B, 5C, 6B, 7B).

The external ramus extends nearly to the anterior margin of the skull, and is anteromedially curved. The external ramus tapers at its anterior end, but the terminus of the septomaxillary ramus is blunt. The anteromedial processes approach at midline, but do not contact one another (figs. 5C, 12A). Ventrally, the anteromedial process is contiguous with the palatal shelf. A weakly defined narial fossa is present anterior to and anterolateral to the septomaxilla (figs. 4B, 5C, 6B, 12A). It extends onto both the septomaxillary and external rami of the premaxillary process of the maxilla and onto the premaxilla.

Ventrally, the palatal shelf possesses a narrow contact with the vomer anterior to the vomeronasal fenestra (figs. 7C, 12B). A ridge extends from the common premaxilla-vomer-maxilla contact posteriorly along the lateral margin of the vomeronasal fenestra to the level where the septomaxilla connects the vomer and maxilla. A weak, shallow, fossa lies lateral to this ridge on the palatal shelf. A similar fossa for anterior maxillary replacement teeth, which also receives some of the crowns of functional dentary teeth, is present in extant taxa such as *Heloderma suspectum* (fig. 8C), *Ovoo gurvel* (fig. 10C), and *Varanus gouldii* (visible in Bonine, 2005a; and Maisano, 2001d, respectively). The palatal shelf tapers posterolaterally, forming the anterolateral margin of the internal naris. Posterior to the posterior part of this palatal shelf, the maxilla is mediolaterally narrow, only about as broad as the bases of the teeth plus the parapet.

A palatine flange is absent on the maxilla and the palatine forms a tongue-in-groove joint with the maxilla (fig. 16) where the palatine medially caps the maxilla and slightly overlaps it dorsally and ventrally. The palatine-maxilla contact begins in the posterior one-third of the internal naris and extends to near the posterior tip of the maxilla. The maxilla is mediolaterally tapered starting about one-third of the way into the palatine-maxilla contact and extends posteriorly. The posteroventral tip of the maxilla is a posterolaterally oriented point that is dorsally overlain by the jugal. The palatine-maxilla contact extends posteriorly to the level of the ultimate maxillary tooth (figs. 7C,

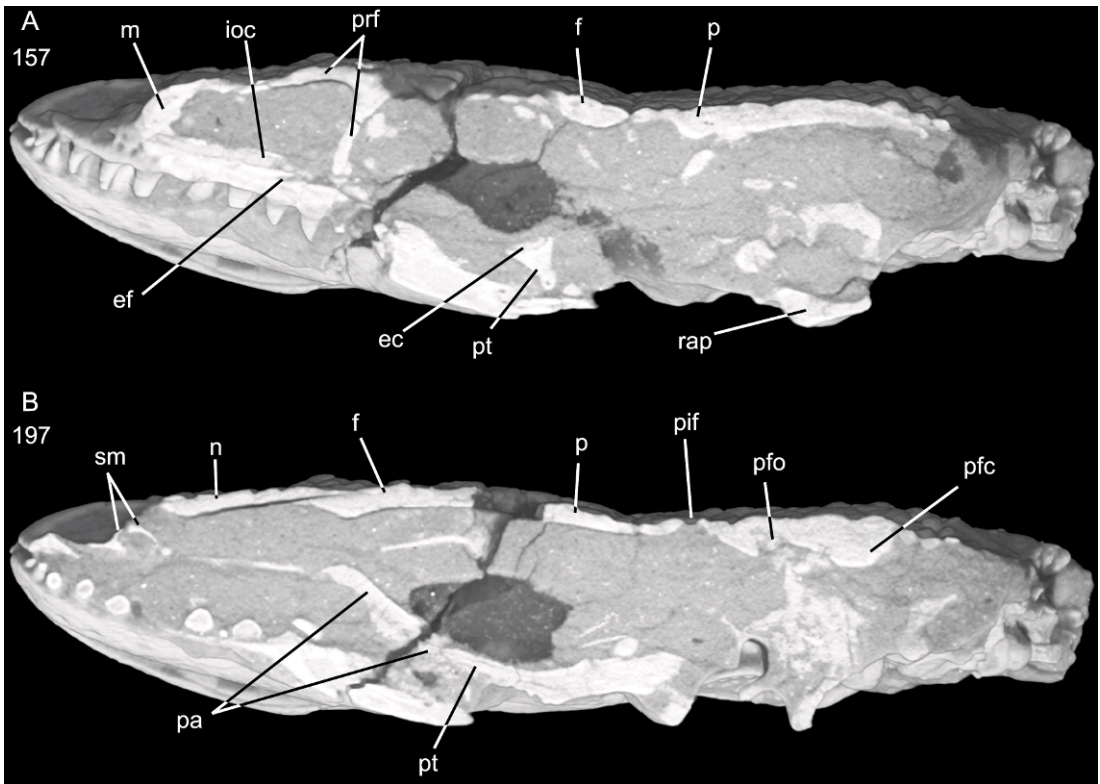


Fig. 17. Selected parasagittal HRXCT slices through the skull and mandible of *Gobiderma pulchrum*, (IGM 3/55). **A.** Parasagittal slice 157 is through the left side of the specimen. **B.** Parasagittal slice 197 is very near the midline.

12B, 16). Posterior to that level, the maxilla is medially overlain by the ectopterygoid. The maxilla-jugal contact is narrow, occurring mostly on the lateral skull surface and lying between the lacrimal, palatine, and ectopterygoid. The jugal lies mostly dorsal to the maxilla as in many goannasaurids, contrasting the condition in non-glyptosauroid anguils and carusioids.

The medial surface of the maxilla is hidden in most specimens, but can be seen through the palate and orbitonasal fenestra in IGM 3/905 and in the HRXCT scans of IGM 3/55. Posteriorly, the maxilla forms the anterolateral margin of the medially open bony lacrimal canal. There is a narrow gap, equal to about 1.5 tooth-position lengths, between the infraorbital foramen in the palatine (the anterior palatine foramen) and the posterior opening of the infraorbital canal of the maxilla (fig. 17A). The infraorbital canal

(figs. 13A, 17A) is relatively small when compared with extant platynotans (e.g., *Heloderma*, *Shinisaurus*, *Varanus*). In *Ctenosaura pectinata* (and presumably many other squamates), the maxillary infraorbital canal carries the superior alveolar artery, vein, and nerve forward into the maxilla where it branches and exits through a number of labial foramina on the maxilla and premaxilla (Oelrich, 1956). *Gobiderma pulchrum* specimens reveal nine (IGM 3/905, IGM 3/55 right side, ZPAL MgR III/64) or 11 (IGM 3/55 left side) labial foramina near the maxillary dental margin, often with additional foramina dorsally near the narial opening. The posteriormost maxillary labial foramen on each maxilla usually projects posterolaterally, and the anteriormost labial foramina are typically anteriorly oriented. The remaining labial foramina are usually directed mediolaterally.

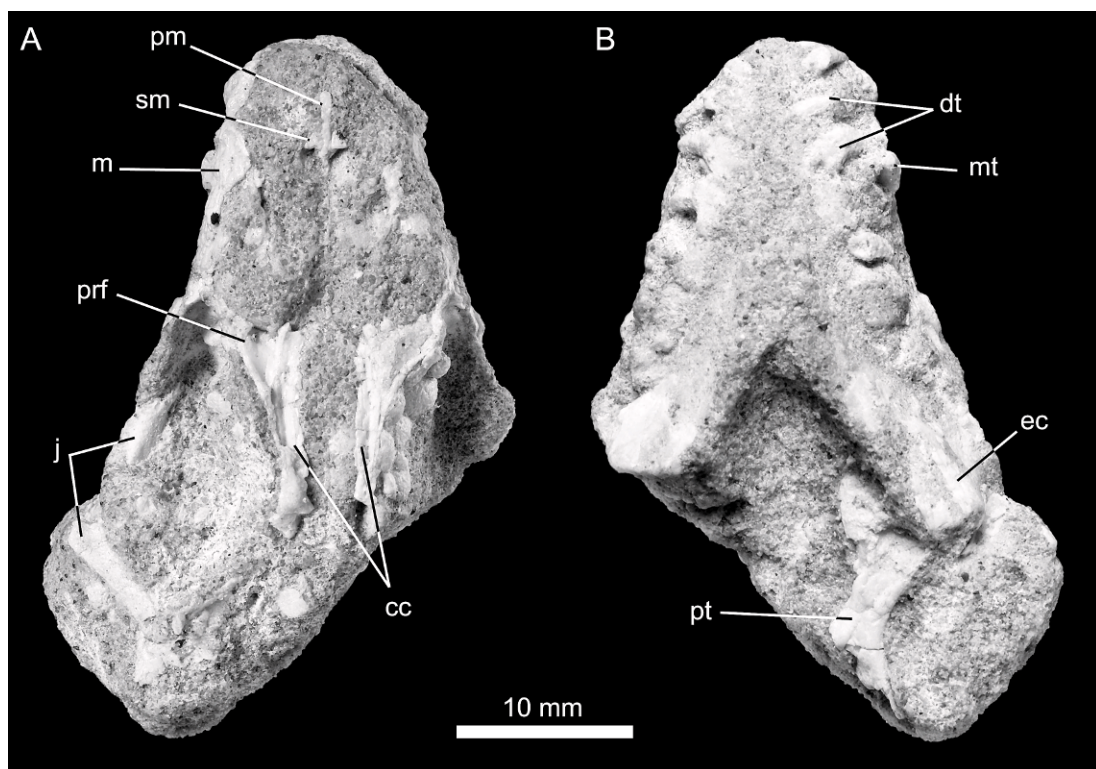


Fig. 18. *Gobiderma pulchrum* (IGM 3/57), partial anterior part of the skull with partial mandibles. The A, dorsal and B, ventral parts of the specimen have been eroded, thus allowing observation of bone articulations.

The nasal process (= dorsal process or facial process of some authors) is roughly triangular in lateral view. Its dorsal apex is located adjacent to and slightly anterior to the anteroposterior midpoint of the maxilla. The nasal process originates near the midpoint of the external naris and ascends gently posterodorsally and somewhat medially to form the posterolateral margin of the external naris (figs. 3A, 4A, 5A, B, 6A, 7A, 12A, 17A); the anterior margin of the nasal process is not sharply offset from the anteroventral part of the maxilla forming the ventrolateral margin of the external naris. The maxilla-nasal suture extends posteriorly and slightly medially where the dorsal margin of the nasal process extends onto the dorsal surface of the prefrontal. The posterodorsal apex of the nasal process terminates at the level of the anterior margin of the orbit. Lateral to the apex, the nasal process is posteriorly excavated so that the suture is an

anteriorly convex arch where the dorsolateral surface of the prefrontal communicates with the skull surface (figs. 4A, 5B, 7A). The maxillary suture extends posteriorly below this exposed portion of the prefrontal and the maxilla extensively overlaps the lateral face of the prefrontal, but without extending posterodorsally to the orbit. The lacrimal contact with the maxilla is an anteroventrally convex arch where the lacrimal invades the nasal process. Posteroventrally, the shape of the suture straightens and is a nearly uninterrupted line extending to the jugal contact and then to the posteroventral margin of the maxilla. The posteroventral tip of the maxilla is notched where the ectopterygoid communicates with the external surface of the skull (figs. 5A, 7A, C, 18B).

The orientation of the anterior margin of the nasal process is variable within anguimorphs, ranging from a distinctly offset nasal process (e.g., *Carusia intermedia*; fig. 15A) to

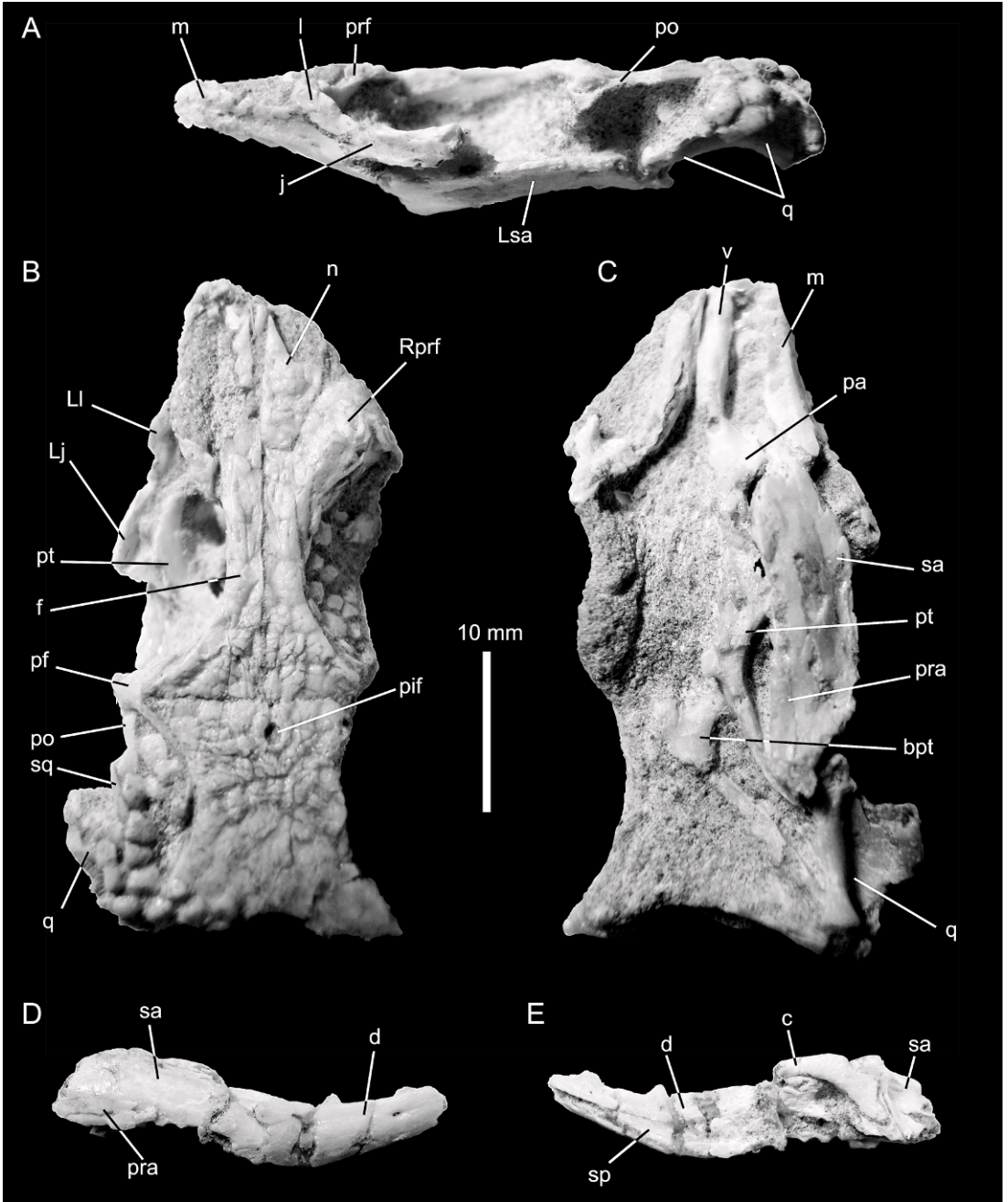


Fig. 19. Nearly complete skull and left mandible of *Gobiderma pulchrum* (ZPAL MgR III/66) in **A**, left lateral view, **B**, dorsal view, and **C**, ventral view. The right mandible is shown in **D**, lateral and **E**, medial views.

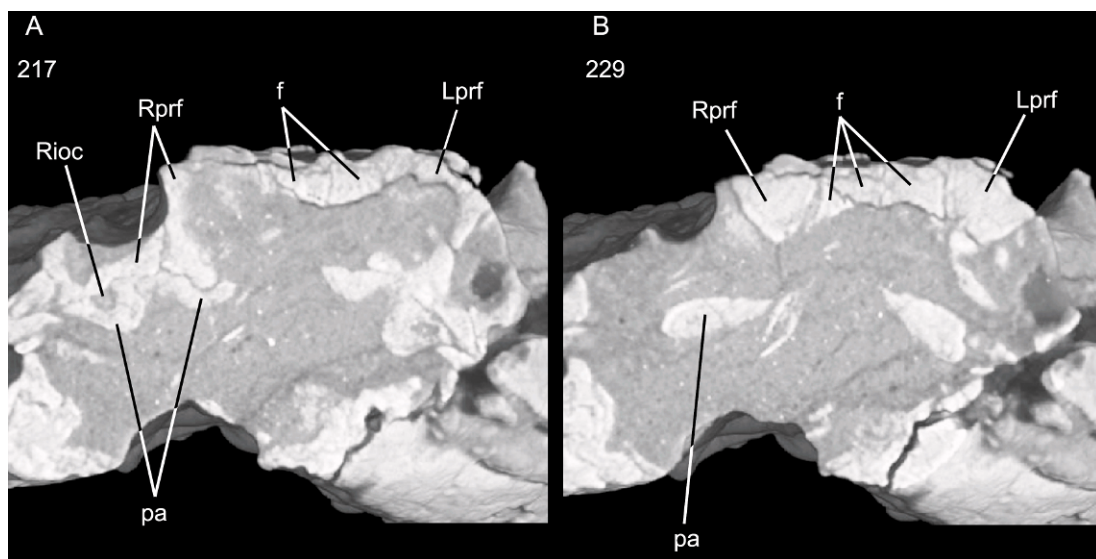


Fig. 20. Selected transverse HRXCT slices through the facial portion of the skull in *Gobiderma pulchrum* (IGM 3/55). **A.** Slice 217 is at the level of the anterior margin of the orbit. **B.** Slice 229 is posterior to that point, but in the anterior one-third of the orbit.

essentially absent in most monstersaurs and many goannasaurs as well (figs. 7–10). Many anguimorphs also possess the ectopterygoid notch on the posteroventral margin of the maxilla (figs. 8A, C, 9B, C, 10A, C), but it is notably absent in others (e.g., *Carusia intermedia*; fig. 15). Among the taxa lacking the ectopterygoid notch are *Heloderma texana* (see Maisano, 2001a), *Paravaranus angustifrons*, *Saniwides mongoliensis*, *Telmasaurus grangeri*, most anguids (but not *Anniella pulchra*, *Dopasia harti*, *Peltosaurus granulatus*, or *Pseudopus apodus*), and mosasaurs.

NASAL: Osteoderms overlies the nasals and often fuse with them. However, preparation and diagenetic forces have made visible the sutures in ZPAL MgR III/64 (fig. 3B), IGM 3/905 (fig. 6B), and ZPAL MgR III/66 (fig. 19B). The HRXCT scans of IGM 3/55 offer further details (figs. 5C, 13, 17). The paired nasals contact the premaxilla, septomaxillae, maxillae, prefrontals, frontals, and one another for approximately 2/3 of their length. About the anterior three-tenths of the suture is interrupted by the nasal process of the premaxilla, and the posterior one-sixth is interrupted by the anteromedial wedge of the frontals. Each nasal is gently mediolaterally

convex, more so anteriorly, with its rounded apex occurring near the midline suture.

The exposed part of the articulated nasal is irregularly shaped in dorsal view (fig. 3B, 5C, 7B). The posterior end describes a posterior arch. Whereas the narial and frontal margins of the nasal are nearly parallel, the maxilla-prefrontal and internasal (midline) margins are subparallel. Because it dorsally overlaps the frontal, the posterior part of the nasal is hidden in ventral view; thus the nasal appears nearly triangular when viewed through the palate. The anterior edge of the nasal is anteriorly concave. It has an elongate premaxillary process and a short anterolateral process, and forms a uniformly arching posterodorsal margin to the external naris. Because the premaxilla slightly overlies the nasals, invasion of the internasal suture by the premaxilla is more extensive dorsally than ventrally. The nasals form a dorsal groove with thin ventral laminae underlying the posterodorsal part of the premaxillary nasal process (fig. 13A). Similarly, the maxilla narrowly overlaps the lateral surface of the nasal for most of the length of the nasal posterior to the narial margin (fig. 13B).

PREFRONTAL: Prefrontals are preserved and were studied in IGM 3/55 (figs. 3A, B,

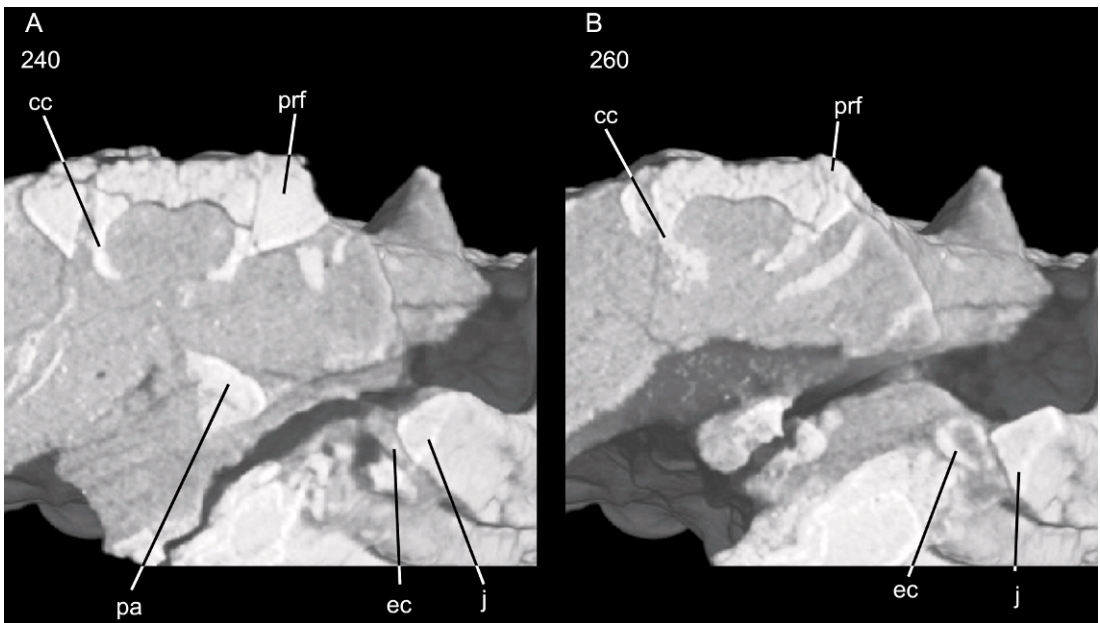


Fig. 21. Selected transverse HRXCT slices through the skull and mandible of *Gobiderma pulchrum* (IGM 3/55). Note the presence of and development of the subolfactory processes of the frontal (cc, cristae cranialia, of some authors; see text).

4A, B, 17, 20, 21), IGM 3/59 (fig. 22), IGM 3/905 (figs. 6, 12), ZPAL MgR III/64 (fig. 3), and ZPAL MgR III/66 (fig. 19). Prefrontals are also preserved in IGM 3/57 (fig. 18) and ZPAL MgR III/65 (fig. 11A), but they are too incomplete to add meaningful data or any details not discernible from the specimens listed above.

The robust prefrontal contacts the maxilla, nasal, lacrimal, and palatine. It forms much of the anterior and anterodorsal borders of the orbit, the lateral border of the orbitonasal fenestra, and the posterior wall to the nasal chamber (figs. 18A, 20, 23). The prefrontal is triradiate in lateral view, possessing an orbital process, a palatine process, and a nasal process. The nasal process extends anteriorly to about the midpoint of the maxilla (figs. 3B, 5C, 7A, B, 19B). However, the maxilla overlaps most of the lateral face of the prefrontal (figs. 3B, 7A, B, 12A). In dorsal view, the visible part of the articulated prefrontal is elongate, posteriorly tapered, and anteriorly rounded (teardrop shaped).

No palpebral is preserved in any specimen of *Gobiderma*. There is an apparent articular surface at the anterolateral corner of the

orbit. It occurs on the posterolateral margin of the prefrontal, and is most pronounced just dorsal to the dorsal terminus of the orbital ridge of the lacrimal (visible in figs. 3A, 6A). This subtriangular articular surface faces laterally/posterolaterally and extends posteromedially onto the orbital process. The apparent articular surface would be suitable for supporting a *Shinisaurus*- or *Varanus*-style palpebral with a broad proximal face. A robust ridge is present dorsal to the “articular surface,” oriented with the main plain of the frontal process and extending to about the same level as the posterior margin of orbital process. This ridge might be a brace for the palpebral if one was present. There is no subpalpebral fossa like that of shinisaurids (Conrad, 2004, 2006a).

Heloderma lacks a palpebral and possesses no antorbital emargination such as the one described above as an apparent articular surface (see data in Maisano, 2001a; Bonine, 2005a, 2005b; the Deep Scaly Project, 2007). Importantly, the *Lanthanotus borneensis* palpebral was unrecognized until recently (Maisano et al., 2002), but that very small palpebral occurs in the absence of a clearly

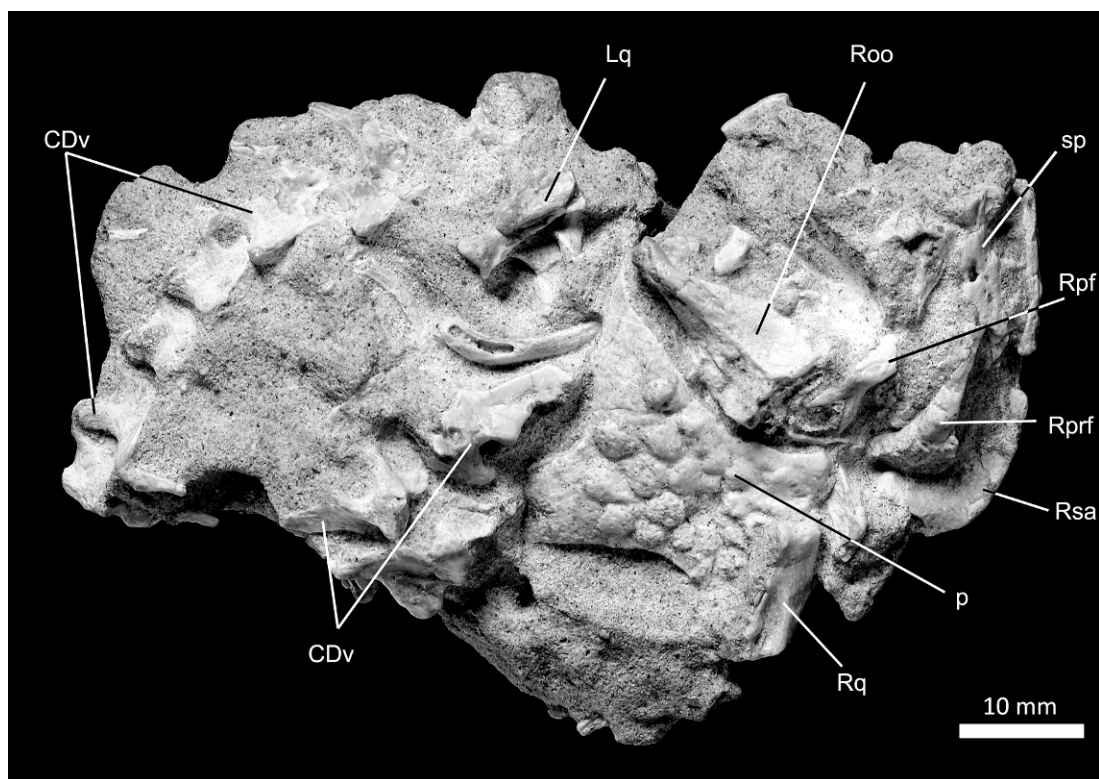


Fig. 22. Partially articulated incomplete skeleton of *Gobiderma pulchrum* (IGM 3/59), including a partial skull, mandibles, osteoderms, and axial column.

defined facet on the prefrontal (see Rieppel, 1980b, 1983; Maisano, 2001b; Maisano et al., 2002).

Importantly, there is no direct evidence of a palpebral in *Gobiderma pulchrum*, even

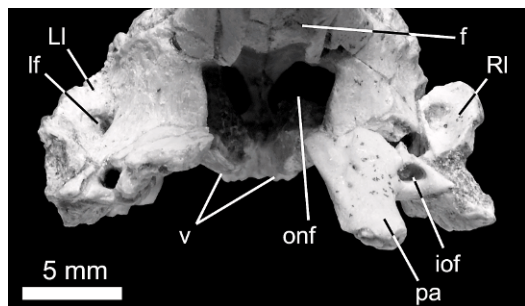


Fig. 23. *Gobiderma pulchrum* (IGM 3/905), posterior view of facial part of the skull illustrating the orbitonasal fenestra and lacrimal foramina, among other morphological characteristics.

from the HRXCT scans of the very well-preserved specimens IGM 3/55.

Ventral to the possible palpebral facet, the prefrontal has a dorsoventrally oriented contact with the lacrimal that approaches, but does not contribute to, the posterior lacrimal foramen (figs. 16, 23). Its medial margin forms the lateral side of the orbitonasal fenestra with almost no contribution from the frontal (figs. 21, 23). The prefrontal-palatine contact is dorsally arched in orbital and rostral views (fig. 23). The posterolateral part of the orbital process is longer than the medial part and extends lateral to the level of the palatine infraorbital canal. Its tapered tip contacts the jugal and palatine (fig. 23). The prefrontal forms the anteromedial margin of the lacrimal canal within the nasal chamber.

The frontal process of the prefrontal is an elongate, tapered projection that extends along the lateral/ventrolateral surface of the

frontal for about 2/5 of the orbit. Its blunt posterior tip terminates near the narrowest point of the interorbital region (figs. 3B, 4B, 5C, 7B, 11A, 12, 18A, 19B). Its dorsal margin bears osteoderms above the level of the presumed palpebral ridge. These osteoderms are present anteriorly to the point of contact with the maxilla.

Pregill et al. (1986) describe a condition for extant *Heloderma* where extensive connective tissue joins the nasal with the maxilla and prefrontal. They suggest that the bony naris is not so posteriorly extensive in *Heloderma* as sometimes thought; the apparent separation of the nasal from the maxilla and/or prefrontal might instead result from desiccation of dried skeletal specimens (Pregill et al., 1986). High-resolution X-ray tomography (HRXCT) scans of juvenile *Heloderma suspectum* are consistent with that hypothesis (Bonine, 2005b). However, HRXCT scans of adult *Heloderma suspectum* skulls show that an osteoderm invades the space between the maxilla, prefrontal, and nasal posteriorly (visible in Bonine, 2005a: transverse slice 107), suggesting that the posterior extension of the narial opening is genuine, not an artifact of desiccation (see also Nydam, 2000). Regardless, the condition of a vacuity between the nasal and the prefrontal and maxilla is not present in *Gobiderma pulchrum*. Instead, the maxilla and nasal share a strong contact anterior to the anterolateral processes of the frontal as in many other anguimorphs, including shinisaurs (fig. 14) and *Carusia intermedia* (fig. 15B).

LACRIMAL: Both lacrimals are preserved in IGM 3/55, IGM 3/905, ZPAL MgR III/64. The right lacrimal is slightly out of articulation in IGM 3/905 and has a small amount of damage dorsally, but also clearly reveals most of the contacts (fig. 6A, B). The left lacrimal is preserved in natural articulation in ZPAL III/66 (fig. 19A, B). The left lacrimal on IGM 3/905 and both lacrimals in IGM 3/55 are in articulation and partly hidden by overlying osteoderms.

The lacrimal contacts the maxilla, prefrontal, jugal, and palatine. It forms the anteroventral margin of the orbit. The orbital ridge extends onto the lacrimal from the jugal (figs. 3A, 4A, 5A, B, 7A), and some dermal rugosities are present. The posterior lacrimal

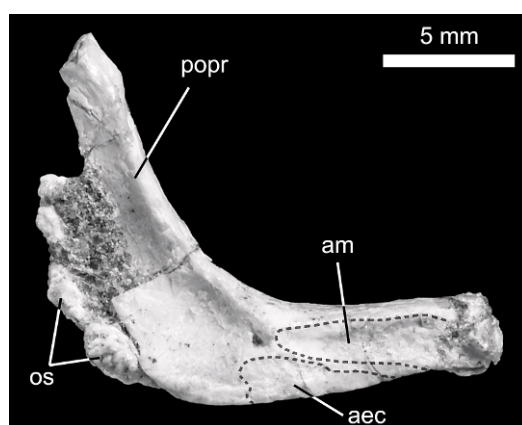


Fig. 24. Right jugal of IGM 3/905 in medial view. Note the posteroventral process and the articular facets for the maxilla and ectopterygoid, among other anatomy.

foramen (the posterior opening of the lacrimal canal) lies completely within the lacrimal rather than between the lacrimal and prefrontal (fig. 23). It is an oval opening with a fossa extending posteroventrally from its posterior opening.

In lateral view, the ventral and anteroventral margins of the lacrimal form a broad arc. It contacts the prefrontal at its anterior extremity, then arches ventrally to partly invade the posterior part of the maxillary nasal process, then forms a relatively straight, posterodorsally oriented contact with the anterior tip of the jugal.

JUGAL: Both jugals are completely preserved in IGM 3/55 (figs. 4A, 5A, B). Most of the left jugals are preserved in ZPAL MgR III/66 (fig. 19A, B) and IGM 3/905 (fig. 24). A small part of the medial surface of the left jugal is visible in IGM 3/59, and the anterior parts of the jugals are preserved in the holotype (ZPAL MgR III/64) (fig. 3A). All the jugals from the newly discovered material retain some osteoderms on their lateral surface, yet comparisons among these specimens reveal most of the jugal morphology (reconstructed in fig. 7A–C).

The L-shaped jugal contacts the maxilla, lacrimal, postorbital, palatine, and ectopterygoid. It forms the ventral border and most of the posterior border of the orbit and bears much of the orbital ridge. The jugal part of the orbital ridge is distinct anteriorly, but

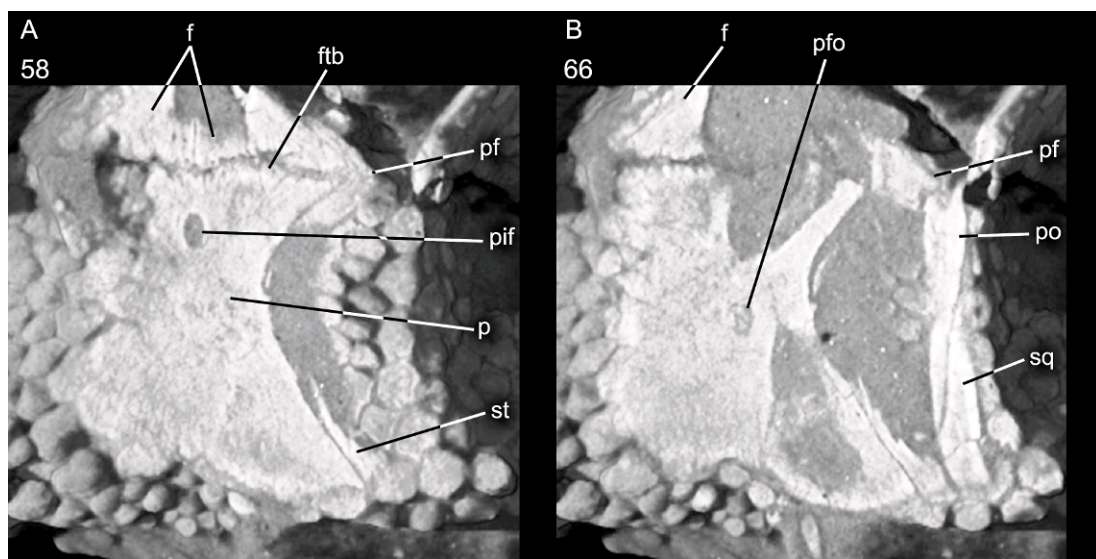


Fig. 25. Selected frontal HRXCT slices through the dorsal part of the cranial portion of the skull in *Gobiderma pulchrum* (IGM 3/55), illustrating details of the parietal and the supratemporal arch. **A.** Frontal slice 58 shows the contacts between the postfrontal and parietal, between the suprafrontal and parietal, the frontoparietal suture, and the pineal foramen. **B.** Frontal slice 66 illustrates the contacts between postfrontal, postorbital, and squamosal, and the pineal fossa.

flattens into the main part of the jugal posterior to the angle of the orbital margin. The jugal does not reach the anterior margin of the orbit, instead terminating just anterior to the posteriormost margin of the lacrimal. Dermal sculpturing is present on the suborbital process and extends a short distance up the postorbital process.

Presence of the orbital ridge laterally and a short medial suborbital ridge gives the anterior part of the suborbital process a subtriangular cross section anteriorly (fig. 21A, B), but the orbital ridge becomes less developed posteriorly. An ascending ridge is present on the medial surface of the postorbital process. The medial suborbital ridge and the postorbital ridge intersect at a small, but distinct, tubercle near the posteroventral margin of the orbit (fig. 24). An ectopterygoid facet lies ventral to the medial suborbital ridge. The medial suborbital ridge and associated posterior tubercle may be braces or buttresses to help support the ectopterygoid contact.

The jugal primarily lies dorsal to the maxilla where they overlap, in contrast to the condition in some anguroids (such as

Carusia intermedia; fig. 15A). A tongue-in-groove joint is present between the ventral jugal surface and the dorsal surface of the maxilla. The right side of IGM 3/905 shows that the maxilla has a weak dorsal trough receiving the jugal and buttressing it.

The jugal is broadest at the posteroventral angle. A small, but distinct, posteroventral process is present and mostly posteriorly directed (figs. 7A, 24). The postorbital process tapers posteriorly. Dilation of the postorbital process is absent, contrasting the condition of *Xenosaurus*, *Exostinus*, *Melanosaurus maximus*, and some mosasaurids. Posteriorly, the tip of the jugal approaches the anterior tip of the squamosal, apparently without contacting it (see fig. 5A; reconstructed in fig. 7A–C).

POSTFRONTAL: Among the new specimens, the postfrontal is well preserved and exposed in only IGM 3/59 (fig. 22), and therein only the left postfrontal is preserved. Part of the frontal process of the left postfrontal is preserved in IGM 3/905 (fig. 6A, B). The right postfrontal is well preserved and exposed in the holotype specimen (fig. 3A, B). The left postfrontal is visible in ventral

view in ZPAL MgR III/65; the left postfrontal is visible in dorsal view in ZPAL MgR III/66 (fig. 19A, B). Further details may be gleaned from the HXRCT scans of IGM 3/55 (figs. 5A–C, 25).

The postfrontal and postorbital remain distinct (unfused) elements in *Gobiderma pulchrum* (figs. 7A, B, 25). The postfrontal contacts the postorbital, frontal, and parietal. It forms the posterodorsal margin of the orbit and narrowly contributes to the anterior margin of the supratemporal fenestra (figs. 5C, 7, 11A, 25). The postfrontal is V-shaped in dorsal view (figs. 5C, 6B, 7B, 22, 25). Its divided medial surface spans the frontoparietal suture. Anteriorly, the frontal process extends along the posterodorsal and posteromedial margins of the orbit, but does not approach the frontal process of the prefrontal. The parietal process is similar in length and robustness to the frontal process and is dorsally overlapped by a dorsolateral lip of the parietal table. The posterior and lateral margins of the postfrontal bear an extensive articular surface that receives the anterior ramus of the postorbital (fig. 25). This articular surface extends onto the dorsolateral surface of the lateral process of the postfrontal (fig. 25A). It tapers medially and does not reach the level of the mesial division between the frontal and parietal processes. There is no contact between the jugal and postfrontal.

The postfrontal of *Gobiderma pulchrum* and *Heloderma* differ markedly. Because of the flat lateral margin formed by the posterior part of the frontal and the anterior part of the parietal, *Heloderma* lacks a postorbital and medial division (forking) of the postfrontal, contrasting the condition found in *Gobiderma pulchrum* and many other anguimorphs (e.g., figs. 10B, 14C, 15B, C). The jugal broadly contacts the postfrontal laterally and somewhat dorsally in *Heloderma* (fig. 8A–C), but there is little or no contact between these elements in *Gobiderma pulchrum*. Importantly, although the varanid *Lanthanotus borneensis* also lacks a postorbital, its postfrontal retains more of the presumed plesiomorphic morphology in retaining the medial forking.

POSTORBITAL: Postorbitals are preserved in IGM 3/55, IGM 3/57, IGM 3/59, IGM 3/

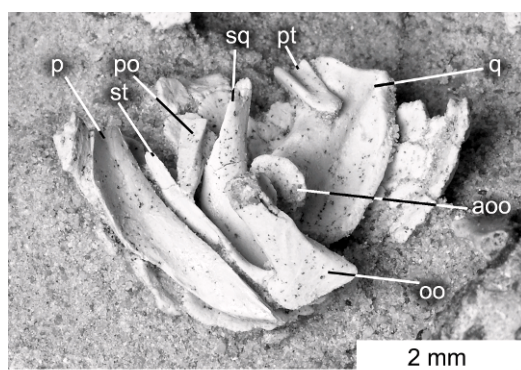


Fig. 26. *Gobiderma pulchrum* (IGM 3/905), ventral view of the left jaw suspensorium and surrounding structures.

905, ZPAL MgR III/64, and ZPAL MgR III/66, but well preserved and exposed only in IGM 3/905 (fig. 26) and ZPAL MgR III/64 (fig. 3B). Only the anterior part of the left postorbital contacting the postfrontal is preserved in IGM 3/57, IGM 3/59, ZPAL MgR III/66. Most of both postorbitals (although not the anterior portion contacting the postfrontal) are well preserved in IGM 3/905 and the right postorbital is preserved in articulation with the postfrontal and the squamosal in ZPAL MgR III/64. The HRXCT scans of IGM 3/55 clearly show the relationship of the postorbital with the surrounding bones (fig. 25).

The elongate postorbital contacts the postfrontal, jugal, and squamosal. It is relatively straight, with an expanded anterior end and a tapering posterior end. It laterally overlies the postfrontal, and is overlain by the jugal anterolaterally and the squamosal posterolaterally. The expanded anterior end of the postorbital possesses a broad, triangular, facet for articulation with the postfrontal on its dorsal surface. The postorbital possesses a deep posterior notch that accepts a process of the postfrontal (fig. 25B). Ventrally, the postorbital has a very short ventral (orbital) process that is extensively overlain by the jugal (reconstructed in fig. 7A). The squamosal process is elongate and triangular in cross section. Its lateral surface forms an elongate tongue-in-groove joint with the squamosal. The squamosal facet extends farther anteriorly than was reconstructed

previously (compare figs. 7, 25B and Borsuk-Białynicka, 1984: fig. 4d), extending nearly to the jugal overlap. The squamosal process extends posteriorly well beyond the midpoint of the supratemporal fenestra and well beyond the level of the anteromedial terminus of the supratemporal, and nearly contacts the supratemporal at the posterior margin of the supratemporal fenestra. This contrasts the condition seen in many anguioids (e.g., *Carusia intermedia*; fig. 15B) and the shini-saur *Shinisaurus crocodilurus* (fig. 14C), but is more similar to the elongate postorbital of many varanids (see *Ovoogurvel*; fig. 10B).

SQUAMOSAL: The squamosals are well represented by the available material. They are visible only in IGM 3/905 (fig. 26) and in the HRXCT scans of IGM 3/55 (figs. 5B, 25C, 26) among the new material. The holotype (ZPAL MgR III/64) (fig. 3B) possesses a nearly complete right squamosal and ZPAL MgR III/65 possesses only the anterior part of the left squamosal. Both squamosals are preserved in contact with, but slightly out of articulation with, the postorbitals in IGM 3/905. Both are missing their anterior tips, but are otherwise beautifully preserved. The specimen IGM 3/55 retains the squamosals in articulation (figs. 5C, 25). The right squamosal of ZPAL MgR III/64 further demonstrates the nature of the postorbital-squamosal contact (fig. 3B).

The squamosal contacts the postorbital, supratemporal, and quadrate. It forms the dorsolateral margin of the skull posteriorly, contributes narrowly to the posterolateral margin of the supratemporal fenestra, and forms most of the dorsal margin of the infratemporal emargination (figs. 7B, 25).

The postorbital part of the squamosal tapers to a point. The squamosal extends further anteriorly than previously suspected and probably approached the jugal on the lateral surface of the postorbital (note that the anterior extension of the squamosal is visible in Borsuk-Białynicka, 1984: pl. 6.1). The squamosal has a gentle, lateral curve along its lateral border for about half its length, and approximately the posterior one-quarter of the bone is downturned toward the quadrate suspensorium (visible in fig. 26; shown in the reconstruction in fig. 7A). The postorbital dorsomedially overlaps the squa-

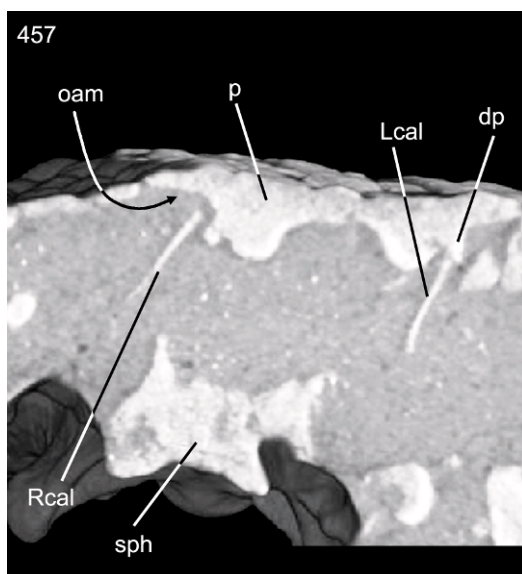


Fig. 27. Transverse HRXCT slice through the skull and mandible of *Gobiderma pulchrum* (IGM 3/55) at the anterior part of the cranial portion of the skull. Note the ventral jaw adductor shelf on the parietal, the descending processes of the parietal, and the crista alaris of the proötic.

mosal for about one-half the length of the squamosal (fig. 25). Posterior to the postorbital overlap, the squamosal narrowly contributes to the supratemporal fenestra, and then is posterolaterally angled along its extensive supratemporal contact (see figs. 7B, 25B). The supratemporal overlap of the squamosal extends for slightly less than one-half the length of the latter. Thus, the postorbital very nearly contacts the supratemporal.

The posteroventral head of the squamosal is rounded in lateral view and dorsolaterally overlies the quadrate (see below). An obtuse posteromedial angle is formed between the postorbital and supratemporal articular faces of the squamosal, but there is no distinct dorsal process like that seen in many iguanians, teiids, *Meyasaurus diazromerali* (Evans and Barbadillo, 1997), and carusioids (Borsuk-Białynicka, 1985; Gao and Hou, 1995; Gao and Norell, 1998; fig. 15B).

SUPRATEMPORAL: Supratemporals are well preserved and visible in IGM 3/905 (figs. 26, 27B), IGM 3/55 (and scans of the

latter; figs. 4A, 25), and ZPAL MgR III/64 (fig. 3B). Both supratemporals are well preserved and exposed in ZPAL MgR III/64. The posterior part of the left supratemporal is visible in articulation from the posterior view of IGM 3/55. Both supratemporals are visible in IGM 3/905; the right one is visible in ventral and posterior view and the left one is visible in ventral view. The latter is complete and demonstrates some of the details of the contact between the supratemporal and the parietal (fig. 27B).

The supratemporal contacts the squamosal, parietal, quadrate, and otooccipital. It forms approximately one-half the length of medial border of the supratemporal fenestra. It also contributes significantly to the suspension of the quadrate. The supratemporal is dorsoventrally broadest along its middle two-thirds; its anterior and posterior ends are tapered. For most of its length, the supratemporal is J-shaped in cross section and the short arm of this shape wraps around the ventral surface of supratemporal process of the parietal and narrowly separates the paroccipital process of the otooccipital from the parietal (figs. 7E, 26). The anterior margin of the supratemporal extends beyond the posterior margin of the parietal table (fig. 25).

The supratemporal of *Gobiderma pulchrum* is generally similar to that of extant *Heloderma* (compare figs. 7B, 8A, B) despite the differences in the morphology of the supratemporal arch. The condition in *Estesia mongoliensis* is somewhat less certain because the squamosal and the parietal are appressed and may obfuscate a significant portion of the supratemporal anteriorly. Shinisaurids possess a more strongly bifurcated supratemporal with a pronounced anterolateral ramus (fig. 14B, C). Many anguids possess a closer connection between the posterior part of the squamosal and the parietal, resulting in the mediolaterally compressed supratemporal morphology lacking significant bifurcation (but see the gerrhonotines illustrated by Criley, 1968). *Carusia intermedia* apparently lacks a supratemporal (Borsuk-Białynicka, 1985; Gao and Hou, 1995; Gao and Norell, 2000) (fig. 15). *Xenosaurus* possesses a mediolaterally narrow and anteroposteriorly short supratemporal lying mostly posterior

and posteromedial to the ascending process of the squamosal.

FRONTAL: Frontals are preserved in IGM 3/905, IGM 3/55, IGM 3/57, ZPAL MgR III/64, ZPAL MgR III/65, ZPAL MgR III/66. The specimen IGM 3/57 preserves only part of the subolfactory processes of the frontal and a small part of the left posterolateral margin (fig. 18A). The frontals in IGM 3/55 remain in natural articulation with all the surrounding bones, but their relationships with those bones are visible only through the HRXCT scans (figs. 5C, 16, 17, 20, 21, 25). The frontals are very well preserved and exposed in IGM 3/905 in which they are visible in dorsal, ventral, and lateral views, remaining articulated with the nasals and prefrontals (figs. 6, 12, 23). Both the dorsal and ventral surfaces of the frontals of ZPAL MgR III/64 are visible (fig. 3B, C), but only the dorsal surface has been prepared in ZPAL MgR III/65 (fig. 11A) and the dorsal and lateral parts in ZPAL MgR III/66 (fig. 19B). Osteoderms obscure most of the dorsal surface of ZPAL MgR III/65.

The frontals contact at midline for their entire length, and each also contacts the nasal, prefrontal, postfrontal, and the parietal. The frontal forms a narrow portion of the dorsal orbital margin dorsally, between the frontal processes of the prefrontal and postfrontal. The orbital margins of the two frontals are parallel (rather than constricted to form an hourglass shape), but each frontal expands laterally posterior to the level of the orbit (figs. 3B, 4B, 5C, 6B, 7B, 11A, 12, 19B). This posterior expansion begins at about the level of the anterior tip of the frontal process of the postfrontal and extends posteriorly to the frontoparietal suture. The dorsal surface of the frontal is covered with irregular ridges that contribute to the attachment of the osteoderms and were augmented through coossification.

Anterior to the level of the anterior margin of the orbit, the frontal tapers to a point. The angle between the two tapered anterior margins is close to 90° in ventral view. At the level where this anterior tapering begins, a very narrow flange of the prefrontal underlies the frontal. In dorsal view, the nasofrontal suture is W-shaped, with the nasals overlying the anterior part of the

tapering frontal (figs. 5C, 7B, 19B). The ventral surface of the frontal is somewhat ventrally expanded and gently bulbous just posterior to the level of the nasal overlap. Thus, the frontal is thickest just posterior to the level where the nasal overlies it and near the midline (figs. 16, 17B, 20). The ventral buttress from the prefrontal also occurs at this level (fig. 20A).

Posterior to the thickened region of the frontal, the bone is ventrally excavated to accommodate the olfactory tract (figs. 12B, 18A, 21). This dorsally concave area is partly housed laterally by strongly developed subolfactory processes, which possess a small ventromedial inflection, but which do not contact or approach one another at midline (fig. 21). The subolfactory processes are most pronounced anteriorly, but do not approach the palatines (figs. 12, 20B, 21). The subolfactory processes become smaller at the level of the frontal contribution to the orbital margin and are indistinct by the level of the anterior margin of the frontal process of the postfrontal. Elongate swellings, contiguous with the posterior part of the subolfactory processes, run along the lateral margins of the frontal and form narrow parietal flanges at the transverse frontoparietal suture (visible in fig. 12B).

Tiny supraorbital foramina are visible in the frontal orbital margins of IGM 3/905 and ZPAL MgR III/66. There is a single foramen on the right side (fig. 6A: sorf) and two small foramina on the left side of IGM 3/905 and one on each side in ZPAL MgR III/66.

PARIETAL: Parietals are well preserved in IGM 3/55 (figs. 4A, B, 5A–C), IGM 3/905 (figs. 6A–C, 27), IGM 3/59 (fig. 22), ZPAL MgR III/64 (fig. 3A, B), ZPAL MgR III/65 (fig. 11A), and ZPAL MgR III/66 (fig. 19A, B). A disarticulated parietal is preserved in IGM 3/59 and exposed in dorsal view. A small portion of the parietal is missing in IGM 3/905 and it is broken into three pieces, but most of the morphology (dorsal and ventral) is visible in this specimen. The parietal of ZPAL MgR III/65 is preserved with its ventral surface completely visible.

The parietals are confused into a single element. The parietal contacts the postfrontal, frontal, supratemporal, proötic, epipterygoid, and the processus ascendens tecti synotici (figs. 3B, 4B, 5C, 7B, 11A, 17, 19B,

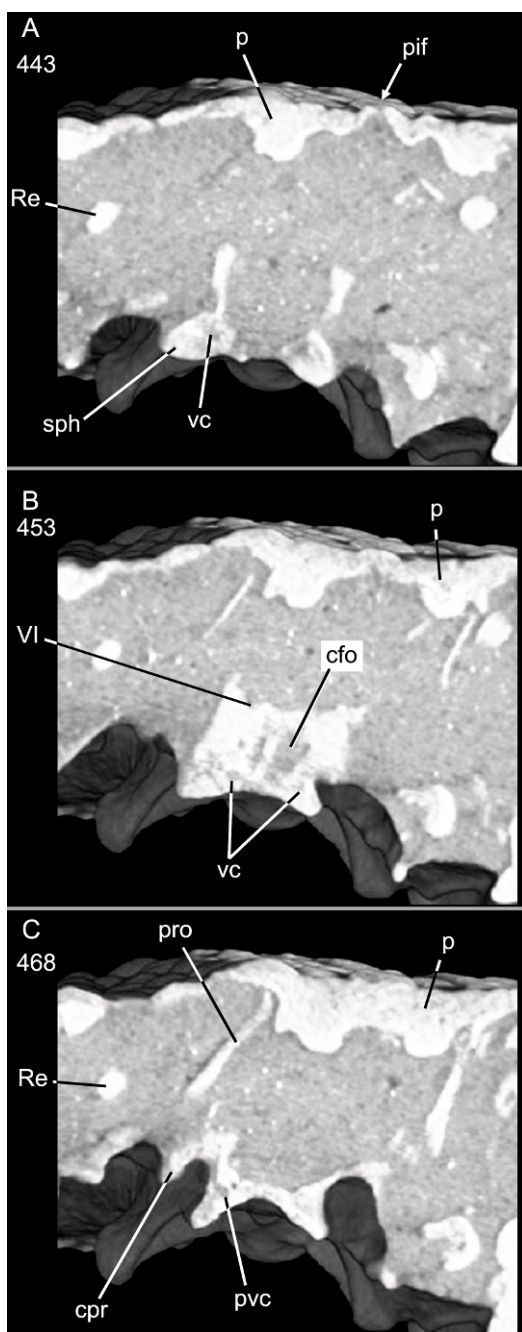


Fig. 28. Selected transverse HRXCT slices through the skull of *Gobiderma pulchrum* (IGM 3/55) at the level of the anterior part of the cranial portion. Sections **A.** near the base of the basiptyergoid processes; **B.** just posterior to the dorsum sella; **C.** at the level of the posterior opening of the Vidian canal.

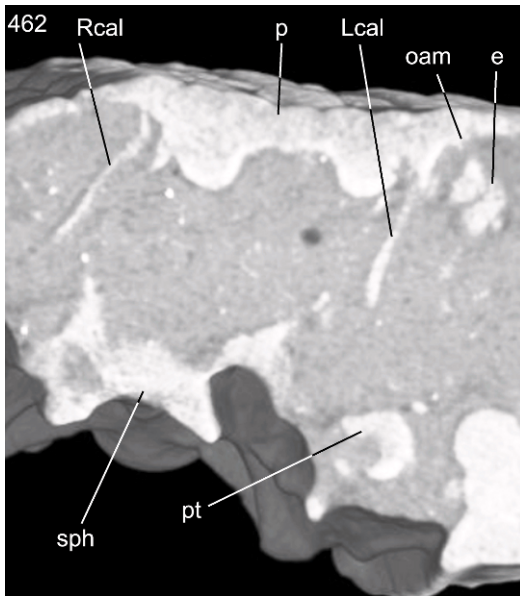


Fig. 29. Transverse HRXCT slice through the skull of *Gobiderma pulchrum* (IGM 3/55) posterior to the orbit, at the level of the anterior part of the braincase, just posterior to the basiptyergoid processes, illustrating the contact of the prootic and parietal.

22, 25, 27B, 28–30). The supratemporal narrowly separates the parietal from the otooccipital and the squamosal. The parietal encloses the pineal foramen whose external aperture is tiny (visible in IGM 3/55 and IGM 3/59) (figs. 3B, 4B, 5B, 7B, 17B, 19B, 22, 25, 28), but is much larger within the parietal and ventrally (fig. 25A). The parietal forms the anteromedial margin of the supratemporal fenestra and the dorsal margin of the posttemporal fenestra. The parietal table is rectangular, but has medially concave lateral margins in dorsal view (figs. 3B, 5B, 7B, 19, 22, 25). Posterolaterally, the supratemporal processes curve posteroventrally toward the quadrate's suspension.

The frontoparietal suture is transverse with only weak interdigitations. No distinct frontal flanges are present; thus, there are parietal flanges on the frontal, but no frontal flanges on the parietal (figs. 6B, 12B, 17, 19, 25). The lateral margins of the parietal are medially concave and the dorsal surface forms a thin lateral shelf and the adductor musculature

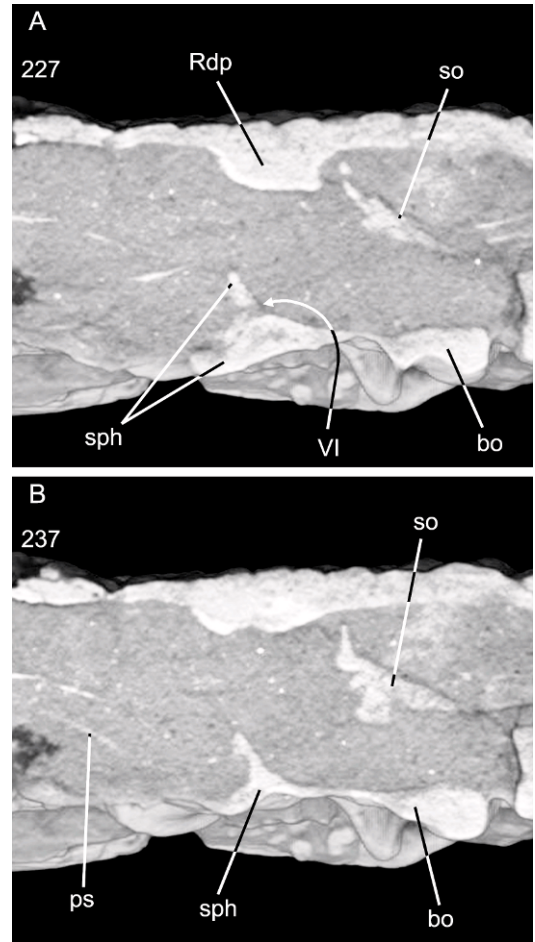


Fig. 30. Selected parasagittal HRXCT slices through the skull of *Gobiderma pulchrum* (IGM 3/55). **A.** Section 227 parasagittal section through the left abducens canal (VI) also illustrates the descending processes of the parietal and occipital condyle. **B.** Section 237 illustrates a nearly sagittal section through the braincase.

arises from the ventral surface of this shelf (figs. 28, 29). Therefore, the decensus parietalis is noncontiguous with the lateral margin of the parietal as it is in some anguimorphs (e.g., shinisaur, varanids). The decensus parietalis is an elongate crest rather than a fingerlike ventral projection like that of scincomorphs and basal anguimorphs such as *Carusia intermedia* (fig. 15A). Even so, the parietal descending process in *Gobiderma pulchrum* contacts the crista alaris proötica and the epiptyergoid (figs. 28B, C, 29).

A postfrontal facet extends along the anterolateral surface of the parietal to a point slightly posterior to the level of the pineal foramen. Posterior to the pineal foramen, the parietal forms the medial margin of the supratemporal fenestra dorsally. However, posteriorly, the lateral surface becomes somewhat medially concave. Within this lateral concavity is an anteroposteriorly extensive facet receiving the supratemporal such that the lateral surface of the parietal is excluded from the supratemporal fenestra posteriorly (figs. 7B, 25, 26).

The elongate supratemporal processes extend posterolaterally at an obtuse angle from each other. The dorsal surfaces of the supratemporal processes are broad (figs. 3B, 5C, 7B, 22, 25) like those of *Heloderma* (fig. 8B), contrasting the condition seen in many other anguimorphs and the monster-saur *Estesia mongoliensis* in which the dorsal surface of the supratemporal process is very narrow and bladelike (Norell et al., 1992) more similar to the condition present in several other anguimorph groups.

A cross section of the long axis of the supratemporal process is L-shaped. The leading edge, the edge adjacent to the posteromedial margin of the supratemporal fenestra and the supratemporal bone, is dorsoventrally broad. Its ventral margin is ventrally overlapped by the supratemporal for most of its length (see above; fig. 26). The posterior edge is expressed as a lamina that partly connects the bases of the two supratemporal processes and probably acted as a flange to which the nuchal musculature ventrally inserted. A similar lamina is present in extant *Heloderma*, but it is less extensive and is commonly limited to the anterior (proximal) parts of the supratemporal processes.

The parietal fossa is located just posterior to the level where the wide parts of the supratemporal processes approach each other and join the main body of the parietal (ventral to the parietal table; figs. 17B, 25). Its anterior margin is delimited by the inflated area at the union of the continuances of these dorsoventrally broadened parts (figs. 28, 29). The lateral and posterior margins of the parietal fossa are formed by the postfoveal crests (cristae postfovealis of

Klembara, 1979, 1981, 1986), which contact at midline posteriorly and extend onto the ventral surface of the supratemporal lamina.

A parietal referred to *Primaderma nessovi* possesses a broad parietal fossa delimited anteriorly by a midline crest. Its posterior margin, apparently, is open, but the specimen is too incomplete to be certain of its details (see Nydam, 2000: fig. 4).

In contrast to the parietals of *Gobiderma pulchrum* and *Heloderma*, the supratemporal processes of the *Estesia mongoliensis* and *Eurheloderma gallicum* are elongate. *Estesia mongoliensis* has supratemporal processes that are subequal in length to the main body of the parietal (Norell et al., 1992). *Eurheloderma gallicum* apparently possesses supratemporal processes anteroposteriorly slightly shorter than the main body of the parietal (Hoffstetter, 1957). It is noteworthy, though, that the holotype of *Eurheloderma gallicum* is a maxilla and that Hoffstetter referred parietals with two distinctly different patterns of osteodermal encrustation patterns on them to this species (Hoffstetter, 1957), leaving open the question of which might belong to *Eurheloderma gallicum*, if either.

The parietal of the intermediate monster-saur *Palaeosaniwa canadensis* is poorly known, but it does seem to lack a pineal foramen (Balsai, 2001), a condition present in Helodermatidae (sensu Conrad, 2008).

SEPTOMAXILLA: Septomaxillae are visible in IGM 3/905 (fig. 12), IGM 3/55 (figs. 4B, 5B, 13A, 17B), and ZPAL MgR III/64 (fig. 3B), but are mostly hidden in the external view of IGM 3/55. The specimen IGM 3/905 preserves the septomaxillae in situ and completely free of matrix. A small part of the posteromedial tip of septomaxilla is preserved in IGM 3/57 (fig. 18A).

Each septomaxilla is dorsally arched in parasagittal section (fig. 17B). It contacts the maxilla, vomer, and (via the internarial septum) the premaxilla. The septomaxilla forms the dorsal roof of the cavity for Jacobson's organ (which is also the floor of the narial chamber) and the posterior margin of the vomeronasal fenestra between the maxilla and vomer.

The septomaxilla is subtriangular. The anterior tip is located near the midline and forms a posterolateral suture with the maxilla

to near the posterolateral margin of the external naris (figs. 12, 13A). From there, the contact extends posteriorly to the posterior extent of the septomaxilla. The posterior margin of the septomaxilla is gently anteriorly arched. The medial margin is dorsally deflected and would have laterally overlain the cartilaginous internarial septum (fig. 13A). A distinct, fingerlike anterodorsal process is preserved in IGM 3/905. It originates about one-quarter of the distance from the antero-medial margin of the septomaxilla and lies near the anterolateral margin of the bone (fig. 12). Lateral to this process, the dorsal surface of the septomaxilla slopes anterolaterally. Posterior to the fingerlike process, the septomaxilla is excavated into a shallow, elongate trough that extends to the posterior margin where the septomaxilla bridges the gap between the vomer and maxilla (figs. 3C, 7C).

VOMER: Both vomers are preserved and exposed in IGM 3/905 (fig. 12B) and ZPAL MgR III/66 (fig. 19C). Although both vomers are preserved in ZPAL MgR III/64 (fig. 3C), only the right is exposed. In ZPAL MgR III/66, the anterior ends of both vomers are not preserved. In IGM 3/905, the right vomer is incomplete, but the left is complete and remains articulated (fig. 12B). Vomers are also well preserved in IGM 3/55 and visible in the HRXCT. Those of IGM 3/59 are hidden by surrounding bones and matrix.

The paired vomers are narrow, with reduced palatal shelving (fig. 12B). Each elongate vomer contacts the premaxilla, maxilla, septomaxilla, and palatine. The vomer forms the medial borders of the vomeronasal fenestra and internal choana, and the anterolateral margins of the so-called interpterygoid vacuity or pyriform recess. It is approximately twice the length of the palatine, extending from the level of the anterior margin of the septomaxilla to about the level of the lacrimal foramen. In cross section, each vomer is U-shaped with a relatively tall medial ascending process and a less pronounced lateral ascending process (fig. 13).

The vomers contact along the midline for more than one-half of their total length. Each vomer bears a small, anteriorly directed foramen at the anterior end, just lateral to the midline contact. A small ridge and shallow trough lie lateral to this foramen.

The trough is bounded posteriorly by a small tubercle that lies slightly anterior to the level of the posterior margin of the vomeronasal fenestra. This tubercle also forms the ventro-medial margin of a second elongate fossa that extends dorsally and somewhat posteriorly toward the anterior margin of the internal choana and extends onto the ventral surface of a short septomaxillary process. Between this level and the level of the palatine contact, the vomer is generally ventrally convex, although the medial surface is slightly offset from the ventral and ventrolateral surfaces (fig. 13). The right vomer has a pair of very small foramina posterior to the level of the anterior margin of the vomeronasal fenestra. Each vomer possesses a tiny foramen just medial to the ventral apex of the bone and slightly anterior to the level of the pair of foramina on the right vomer.

The posterior end of the vomer tapers posterodorsally and, to a lesser extent, mediolaterally with a ventral overlap of the palatine. The posteroventral margin is bifurcate where it overlies the anterior end of the palatine. Dorsally, the vomer approaches, but does not contact, the orbital pillar of the prefrontal. The palatine invades the open space formed between the two ascending processes of the vomer (fig. 13B).

PALATINE: Among the new specimens, only IGM 3/905 preserves palatines that are exposed (figs. 12, 23). The left palatine is incomplete, only the median part and the anterior part of the maxillary process are preserved. The right palatine is complete to near the posterior tip of the pterygoid process. Both palatines are well preserved in IGM 3/55 (figs. 5D, 13B, 16, 17B, 20, 21). Both palatines are well preserved and exposed in ZPAL MgR III/64 (fig. 3C). A partial left palatine and a very damaged and partial right palatine are preserved in ZPAL MgR III/66 (fig. 19).

The paired palatines do not contact at midline and each is triradiate with vomerine, maxillary, and pterygoid processes. The palatine contacts the prefrontal, lacrimal, maxilla, vomer, pterygoid, and ectopterygoid, and forms the anterior margins of the suborbital fenestra and the median part of the lateral margins of the pyriform recess (figs. 3C, 5D, 7C, 12).

Anteriorly, the vomerine process extends anterodorsally and the maxillary process extends almost directly laterally (figs. 3C, 7C, 16, 17B). Between these two processes is an elongate choanal groove extending to the level of the anterior margin of the suborbital fenestra (figs. 3C, 7C, 19C, 20A). The maxillary process is anteroposteriorly broad and relatively narrow dorsoventrally. Its posteromedial edge is overlain by the ectopterygoid. The vomerine process dorsally overlies the posterior end of the vomer and passes ventrally through the space created by the bifurcated posterior end of the vomer (fig. 13B). The dorsal surface of the vomerine process is relatively flat, but the ventral surface is convex in cross section, forming the medial border to the internal choana. This ventral convexity fades into the thickened main body of the palatine posterior to the choanal groove (figs. 19C, 20B).

The posterior palatine foramen (the posterior opening of the infraorbital canal within the palatine) pierces the maxillary process (fig. 23). Just anterior to the posterior palatine, the infraorbital canal is dorsally roofed by the palatine and prefrontal (fig. 20A). Anterior to that level, the maxilla contributes to the dorsolateral margin of the palatine infraorbital canal (fig. 17A).

The pterygoid process does not extend substantially past the level of the anterior orbital margin. Its pterygoid overlap is elongate and tapers posterolaterally (reconstructed in fig. 7C). The posteromedial surface of the palatine has a grooved articular surface for the anteromedial portion of the palatine process of the pterygoid. This groove is delimited dorsally by a small, overhanging lip (the dorsomedial extension of the dorsal surface of the palatine) and ventrally by a buttress for the palatine teeth.

Palatine teeth are present on the ventromedial edge of the palatine from about the level of the anterior margin of the suborbital fenestra to a level just posterior to the ectopterygoid-maxilla contact. These teeth are tiny and arranged in a single line that lay along the lateral surface of the large patch of pterygoid teeth (see below; fig. 17B).

PTERYGOID: Pterygoids are preserved with IGM 3/55, IGM 3/57, IGM 3/905, ZPAL MgR III/64, and ZPAL MgR III/66. The

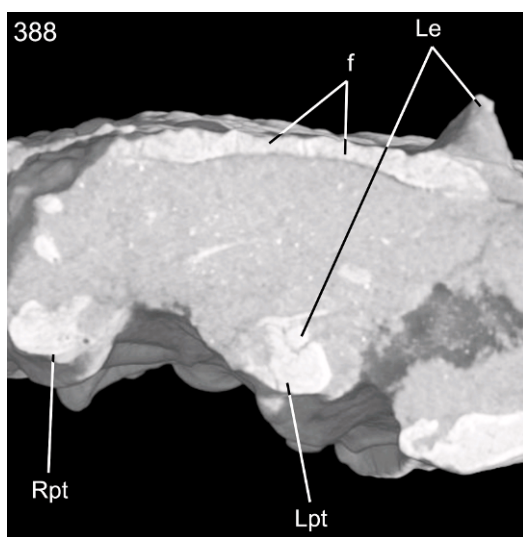


Fig. 31. Transverse HRXCT slice through the skull of *Gobiderma pulchrum* (IGM 3/55) illustrating the pterygoids and the left epipterygoid contact.

pterygoids of IGM 3/55 (figs. 4C, 5D, 17, 31) and ZPAL MgR III/64 (fig. 3C) are the best preserved. Most of the left pterygoid in the region of the epipterygoid is preserved in IGM 3/57 (fig. 18B). Most of the left pterygoid and parts of the right are preserved, but in pieces, in IGM 3/905 (not figured). These specimens, along with the HRXCT scans of IGM 3/55, allow a complete reconstruction of the pterygoid (fig. 7C).

The paired pterygoids are the longest bones in the skull, contacting the posteromedial margins of the quadrates and extending to a level near the anterior margin of the orbit. Anteriorly, the pterygoids converge to relative proximity, extending along the anteromedial borders of the palatine, but they do not approach or contact at the midline (figs. 3C, 5D, 7C). Together they define the broad posterior part of the pyriform recess. Each triradiate pterygoid contacts the parabasisphenoid, palatine, ectopterygoid, epipterygoid, and quadrate. The central portion (the body of the pterygoid) is robust. It gives rise anteriorly to the dentigerous palatine process and the ectopterygoid process, houses the columellar fossa, and leads to the posterior quadrate process. The pterygoid forms much of the medial and posterior margins of the suborbital fenestra.

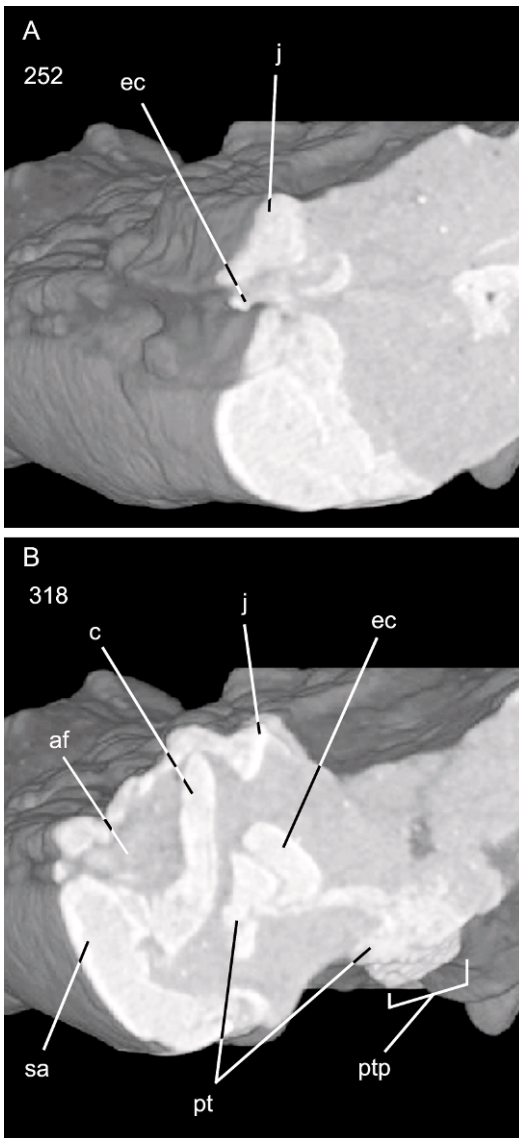


Fig. 32. Selected transverse HRXCT slices through the skull and right mandible of *Gobiderma pulchrum* (IGM 3/55) in the orbital region. **A.** Section 252 illustrates the anterolateral, postmaxillary part of the maxilla, among other structures. **B.** Section 318 through skull illustrates various palatal and mandibular contacts. Note the expansive dorsolaterally open adductor fossa, the complex pterygoid-ectopterygoid contact, and the large patches of pterygoid teeth.

The palatine process of the pterygoid is robust and bears a large patch of tiny pterygoid teeth (figs. 3C, 4C, 5D, 7C, 32B). These teeth lie on a ventrally flat pterygoid plate and are arranged into loose rows. At its widest point, this pterygoid plate is about seven tooth positions wide. It extends from a point near the level of the anterior margin of the suborbital fenestra posteriorly to a point close to the basiptyergoid processes. Its morphology is generally similar to the pterygoid tooth plates seen in many other Cretaceous Mongolian taxa, especially *Estesia mongoliensis* (Norell et al., 1992), *Parvi-derma inexacta* and *Saniwides mongoliensis* (Borsuk-Białynicka, 1984; Alifanov, 2000).

A robust, triangular, transverse process (ectopterygoid process) extends anterolaterally from near the posterior end of the pterygoid plate. Its lateralmost portion is thick and dorsoventrally expanded (figs. 17A, 32B). The medial surface extensively contacts the palatine process via a dorsoventrally thin, but mediolaterally expansive, suborbital lamina (sensu Conrad, 2004), similar to that present in extant *Xenosaurus* (see descriptions and figures in Barrows and Smith, 1947; McDowell and Bogert, 1954; Rieppel, 1980a; and Conrad, 2004).

Extant *Heloderma* possess an elongate anterolateral flange lying in a groove on the dorsolateral surface of the ectopterygoid, approaching the jugal-ectopterygoid contact (McDowell and Bogert, 1954; Gao and Norell, 1998). *Estesia mongoliensis* possesses a similar morphology, but with the anterolateral pterygoid process lying in a less recessed groove on the ectopterygoid. A similar morphology is present in *Gobiderma* wherein a large anterolateral process of the pterygoid dorsally and laterally overlies the ectopterygoid (fig. 32B). This process does not contact the jugal.

Posterior to the common origin of the palatine and transverse processes, the pterygoid is robust and nearly cylindrical in cross section. Its posterior section is swollen at the common level of the columellar fossa and basiptyergoid articulation, the point setting off the quadrate process from the main body of the pterygoid. The columellar fossa, which receives the epityergoid (fig. 31), is deep and most developed anteriorly, although the ectopterygoid facet notches its anterior mar-

gin. The posteromedial and posterior margins are more sloping than the sharp anterior margins and the fossa tapers posteriorly, so that that margin is somewhat acuminate. The large parabasisphenoid facet faces posteromedially and is slightly inclined dorsomedially. It is round and broad anteriorly and tapers somewhat posteriorly. Its ventral margin is somewhat flatter, giving the whole facet a somewhat D-shaped margin. A robust basiptyergoid buttress is present (figs. 3C, 4C, 5D, 7C, 19C). It is largest anteroventrally where it extends medially as a strong flange, but it also continues as a small lip anteriorly that wraps around the medial surface of the bone and contributes to the medial margin of columellar fossa.

The quadrate process of the pterygoid is elongate and robust. Its ventral surface is concave, in contrast to *Estesia mongoliensis* and extant *Heloderma*, which possess columnar quadrate processes. The quadrate process is subequal in length to the palatine process, but the former is somewhat less robust than the latter.

ECTOPTYERGOID: Partial ectopterygoids are preserved in IGM 3/57, IGM 3/905, and ZPAL MgR III/64. Complete, articulated ectopterygoids are preserved in IGM 3/55 and are visible using the HRXCT scans (figs. 17A, 21B, 32). The ectopterygoid morphology differs from the tentative reconstruction of Borsuk-Białynicka (1984).

Each ectopterygoid contacts the maxilla, jugal, and pterygoid (reconstructed in fig. 7C). The ectopterygoid laterally arches toward the jugal before extending anteriorly. Its broad anterior end forms an elongate contact with the maxilla and approaches the palatine without contacting it. A small posterolateral postmaxillary process wraps around the posterior end of the maxilla and is exposed on the lateral surface of the skull (figs. 5A, 7A, 18B, 32A). Posteromedially to the maxillary and jugal contacts, the body of the ectopterygoid is elliptical in cross section as it arches toward the pterygoid. The anterior part of the pterygoid-ectopterygoid contact is a tongue-in-groove articulation in which a lateral/ventrolateral groove on the ectopterygoid receives the dorsomedial part of the ectopterygoid process of the pterygoid (fig. 32B). More posteromedially, this contact becomes

a simpler, overlapping joint with a long posteromedial process of the ectopterygoid lying atop the pterygoid. The very elongate contact between the maxilla and ectopterygoid is similar to the condition seen in *Heloderma* (e.g., fig. 8C), but somewhat different from many goannasaurs wherein the ectopterygoid has a short maxillary overlap (e.g., fig. 10C).

EPIPTYERGOID: Epiptyergoids are preserved and visible in IGM 3/55 (fig. 4A) and IGM 3/905 (fig. 33C). The left epiptyergoid is externally visible in IGM 3/55 and it is partially hidden by matrix and surrounding bones as it pokes through the osteodermal coating on the dorsal skull roof (figs. 4A, B, 31). The right epiptyergoid has shifted such that it lies posterodorsally within the skull. The dorsal one-half of the right epiptyergoid is preserved slightly out of articulation, but still contacting the proötic, in IGM 3/905.

The epiptyergoid is typical of squamates in being elongate, dorsoventrally oriented, and columnar (see figs. 28, 31, 33C and the reconstruction in fig. 7A). It contacts the parietal (the descending flange), proötic, and pterygoid. Its ventral surface lies in the columellar fossa and its dorsal part lies adjacent to the crista alaris proötica and contacts the parietal. Near the middle of its length, the epiptyergoid is circular in cross section, but it becomes somewhat mediolaterally compressed dorsally.

QUADRATE: Both quadrates are preserved in articulation with the surrounding skull bones (but not the mandible) in IGM 3/905 (see figs. 26, 35) and only the ventral part of the right tympanic crest is damaged (fig. 35). Both quadrates are preserved in articulation in IGM 3/55 as shown by the HRXCT scans (figs. 5D, 34). In ZPAL MgR III/64, both quadrates remain in articulation (figs. 3A–C). The left quadrate is preserved in articulation, but is mostly hidden dorsally by overlying bones and osteoderms in ZPAL MgR III/66 (fig. 19A–C).

The quadrate forms a bridge between the dermal skull roof, palate, braincase, and lower jaw. It contacts the supratemporal, squamosal, pterygoid, otooccipital, articular, and prearticular (figs. 5C, 7A–C). The quadrate forms the posterior border of the infratemporal vacuity. It is broadest in both

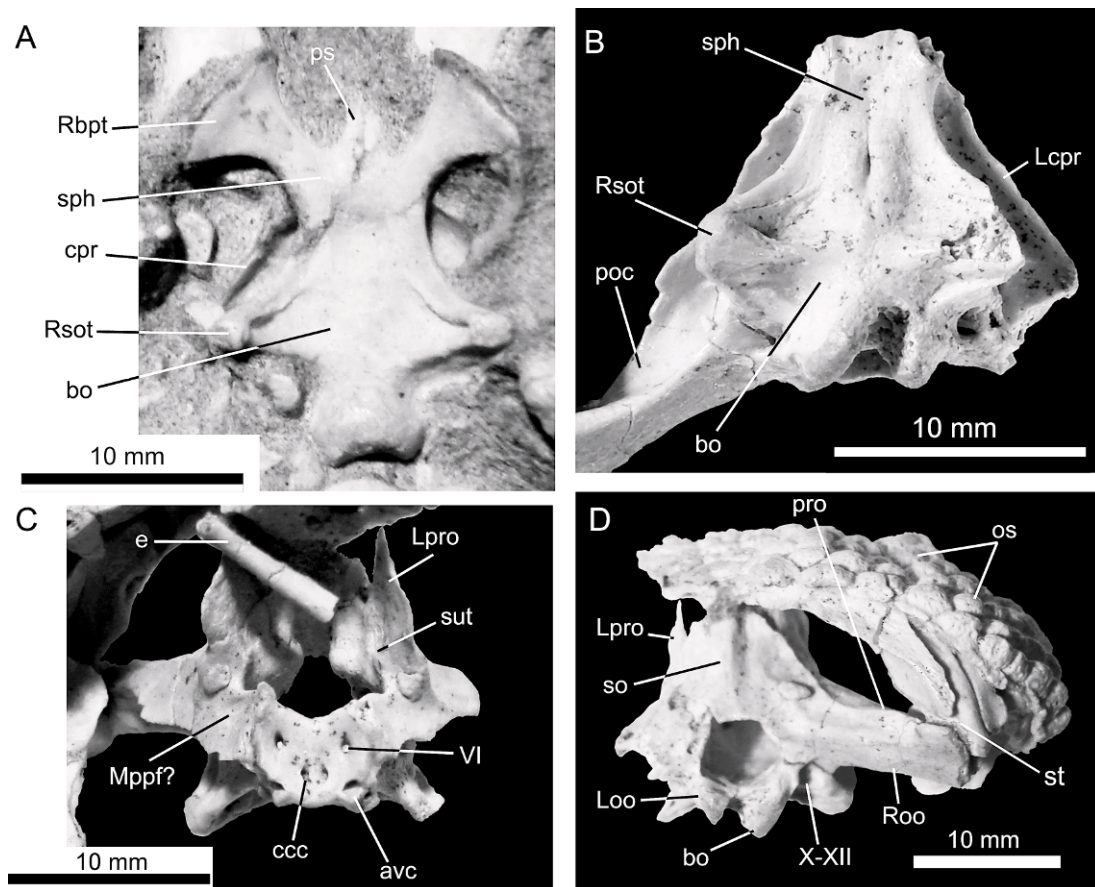


Fig. 33. Braincase of *Gobiderma pulchrum*. **A.** IGM 3/55 in ventral view and IGM 3/905 in **B.** ventral, **C.** anterior, and **D.** posterior/posterodorsal views.

anteroposterior and mediolateral planes at its cephalic condyle where it is Y-shaped. The quadrate foramen passes anteromedially through the tympanic crest of the quadrate.

Gobiderma pulchrum is streptostylic. The cephalic condyle of the quadrate is weakly divided into a broad posterior facet receiving the tip of the paroccipital process (figs. 26, 27B) and a dorsolateral notch with a small common facet for the squamosal and supra-temporal. The posterior crest curves strongly posteriorly starting at about the dorsal one-third (figs. 3A, 7A, 19A). The tympanic crest is mediolaterally oriented and constitutes about one-half the breadth of the quadrate (figs. 34, 35). A small and thin medial crest originates at about the middle of the quadrate and becomes more pronounced dorsally.

It is similar in size and robustness to the tympanic crest.

The ventromedial surface of the quadrate bears a pronounced pterygoid lappet (fig. 34). This lappet is anteromedially oriented and ventrally contiguous with the articular condyle of the quadrate.

PARABASIPHENOID: We refer to the compound structure formed by fusion of the dermal parasphenoid and the endochondral basisphenoid as the *parabasisphenoid*. This differs from some recent studies that have referred to this structure as the *sphenoid* (e.g., that of Bever et al., 2005a; and Conrad and Norell, 2006b). We use this terminology because it highlights the relationships of the braincase element in question and more accurately describes that element while also

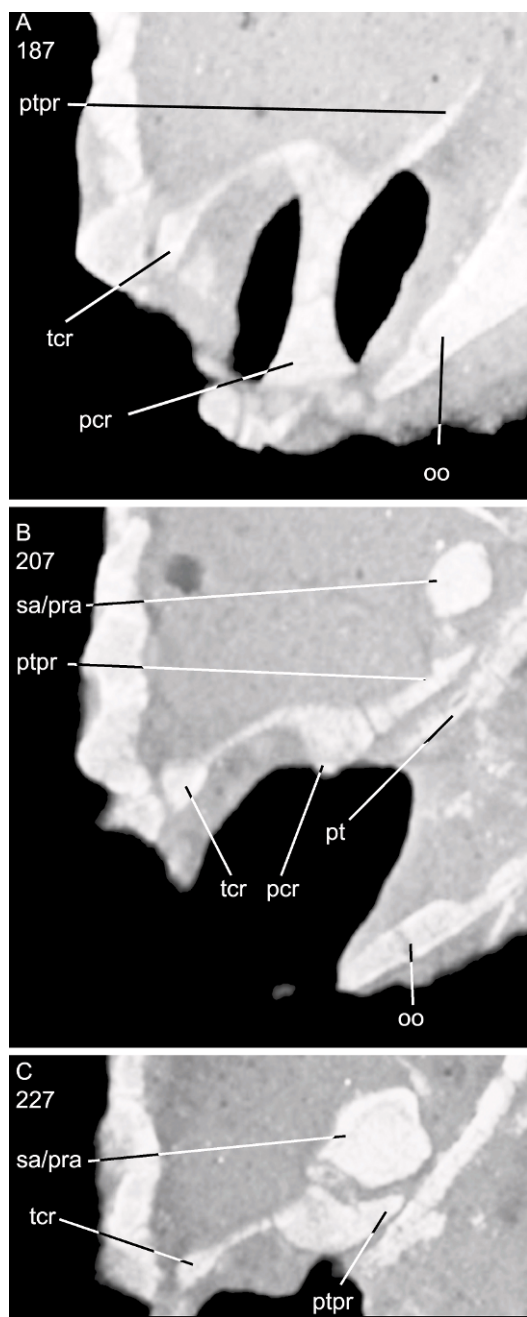


Fig. 34. Frontal HRXCT slice through quadrate and left paroccipital process in *Gobiderma pulchrum* (IGM 3/55). **A.** Section 187 near the dorsoventral midpoint of the quadrate illustrating the extensive pterygoid process of the quadrate. **B.** Section 207 approaching the mandibular condyle including the dorsally projecting part of the mandible (sa/ptra) that forms the anterior glenoid

separating it from the various sphenoid elements in other vertebrate groups (e.g., alisphenoid, orbitosphenoid, etc.).

The parabasisphenoid is preserved in IGM 3/55 (figs. 4C, 5D, 28–30, 33A), IGM 3/905 (figs. 27A, 33B, C, D), ZPAL MgR III/64 (fig. 3C), and ZPAL MgR III/65 (fig. 11B, C). The left basiptyergoid process is preserved in ZPAL MgR III/66 (fig. 19C). The braincase of the holotype has been slightly compressed and lacks most of both basiptyergoid processes, but is otherwise well preserved and lies in articulation (fig. 3A, C). ZPAL MgR III/65 includes a braincase that has been isolated from the rest of the skull through preparation and diagenetic forces with some damage to various areas. In IGM 3/905, the braincase is clear of matrix, undistorted, and completely articulated as a unit, but the basiptyergoid processes have been broken off the parabasisphenoid. It is complete and exposed in ventral view in IGM 3/55; this can be supplemented by the HRXCT scans.

The parabasisphenoid is pentaradiate in ventral view, possessing paired basiptyergoid processes, paired speno-occipital processes, and an anterior parasphenoid rostrum. The parabasisphenoid contacts the pterygoids, basioccipital, and proötics. It carries the abducens, Vidian, and cranial carotid canals, and forms the posterior margin of the pyriform recess. Slight compression of the braincase in IGM 3/55 has moved the individual elements just enough to make out the suture lines (fig. 33A).

The parasphenoid rostrum extends well anterior to the level of the posterior margin of the pterygoid facet on the basiptyergoid process (fig. 30B). The crista sellaris does not extend far anteriorly, but is well developed as a dorsoventral wall at the anterior part of the braincase floor. Posterior to the dorsum sella, the dorsal surface of the parabasisphenoid is concave such that the anterior part of cranial the cavity is very deep dorsoventrally. In anterior view, the crista sellaris arches

←

buttress, also with a considerable pterygoid process of the quadrate. **C.** Section 227 through the middle part of the mandibular condyle.

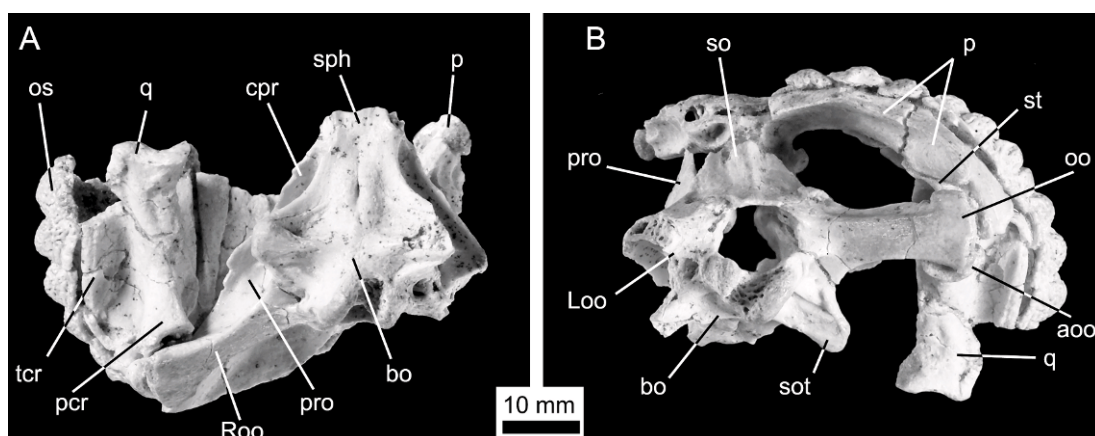


Fig. 35. Braincase and right suspensorium of *Gobiderma pulchrum* (IGM 3/905) in **A**, ventral and **B**, posterior view. Note that anterior is toward the top in **A**.

ventrally between the two robust basisphenoid alar processes (fig. 33C). The alar process is anterodorsally arched and transitions smoothly to the main body of the proötic (fig. 36A, B). The basisphenoid-proötic contact at the posterior part of the alar process is a narrow, but robust, abutting contact. The suture extends from the dorsal part of the dorsal surface of the alar process posteroventrally onto the crista proötica (proötic crest), then to the anterodorsal margin of the posterior opening of the Vidian canal (fig. 33A, B). The crista proötica extends onto the basisphenoid very narrowly, but terminates anteriorly near the base of the basiptyergoid processes. This is similar to the condition in many anguimorphs (e.g., *Carusia intermedia*; fig. 15C), although not in *Lanthanotus borneensis* and some *Varanus*. Posterior to the posterior Vidian canal opening, the parabasisphenoid-proötic suture continues posteroventrally to a point about midway between the posterior opening of the Vidian canal and the fenestra ovalis where it is interrupted by an anterior projection of the basioccipital. The parabasisphenoid-basioccipital suture extends onto the base of the spheno-occipital tubercle. Thus, the parabasisphenoid contributes most of the ventrolateral margin of the braincase via narrow, spheno-occipital processes overlying the anterolateral portions of the basioccipital (figs. 7C, 33A, B). The suture between these two bones extends anteromedially on the

ventral surface of the braincase to about the level of the posterior opening of the Vidian canal, where the suture becomes transverse to the midline.

The abducens canal is oriented almost directly anteroposteriorly (fig. 29A). It is posterodorsal to the anterior opening of the Vidian canal and dorsolateral to the anterior opening of the cranial carotid canal (fig. 28B). The cranial carotid canals typically lie in a deep retractor fossa in squamates, but this fossa is almost completely lacking in *Gobiderma pulchrum* (fig. 36A, B). The anterior opening of the Vidian canal is well separated from the cranial carotid canal, lying between the bases of the basiptyergoid process and the parasphenoid rostrum. The Vidian canal appears to lie mostly within the parabasisphenoid, but the proötic contributes to the dorsomedial margin of its posterior opening (at that point, the canal also carries the cranial carotid artery; fig. 36A, B).

Some specimens of modern *Heloderma* possess an extension of the crista proötica formed by ossification of surrounding connective tissue, which produces a common canal for the posterior opening of the Vidian canal and the hyomandibular branch of the facial nerve (Evans, 2008; fig. 36D). This condition is unknown in other squamates, including *Gobiderma pulchrum* and *Estesia mongoliensis*, the only fossil monstersaurs for which adequate braincases are known (fig. 36).

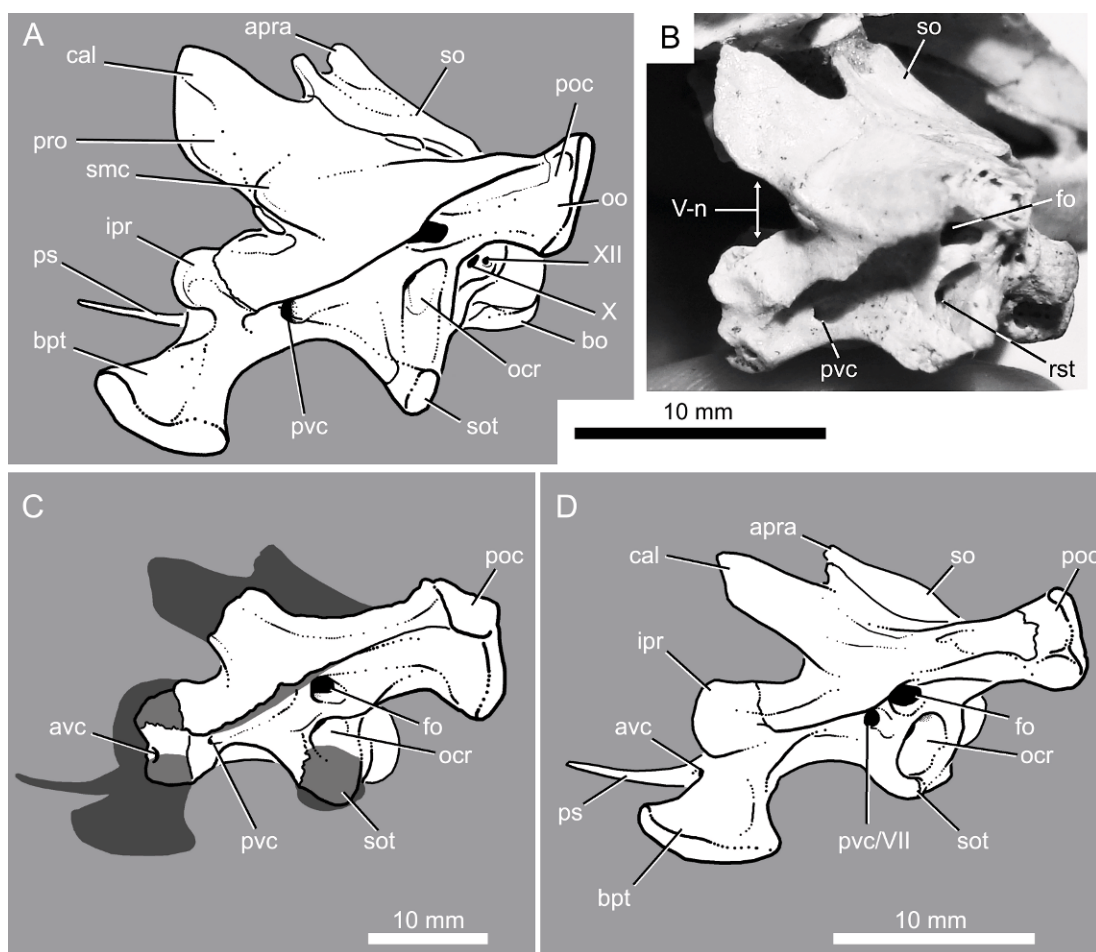


Fig. 36. The braincases of selected monstersaurs. **A.** Reconstructed braincase of *Gobiderma pulchrum* in left lateral view primarily based on ZPAL MgR III/64, ZPAL MgR III/65, IGM 3/905, and IGM 3/55. **B.** Braincase of IGM 3/905 in left lateral view. **C.** Reconstruction of the braincase of *Estesia mongoliensis* in left lateral view (modified after Norell et al., 1992, and Norell and Gao, 1997). **D.** Braincase of *Heloderma horridum* in left lateral view (based on comparisons among AMNH R 64128, Boulenger, 1891, the Deep Scaly Project, 2007, and Evans, 2008). Note that reconstructed areas are represented by semiopaque shadows.

There is a ventral concavity near the midline of the parabasisphenoid at the parabasisphenoid-basioccipital contact in IGM 3/55. The ventral surface of the parabasisphenoid is variable between IGM 3/55 and IGM 3/905 (compare figs. 3C, 4C, 5D, 11B, 33A, B). In the former, a dorsal concavity into the ventral surface of the braincase lies near the midline of the parabasisphenoid at the parabasisphenoid-basioccipital contact. In the latter, a pair of ventral convexities is present, divided by a

narrow sulcus. The holotype possesses neither of these features, instead possessing a smooth, flat ventral surface to the parabasisphenoid (fig. 3C). The condition in IGM 3/55 was originally probably like that of the type before it collapsed. Squamates typically have a thin point in the braincase floor near the parabasisphenoid-basioccipital contact and this area may be prone to plastic deformation or crushing during fossilization.

BASIOCCIPITAL: The basioccipital is preserved in IGM 3/55 (figs. 4C, 5D, 30, 33A,

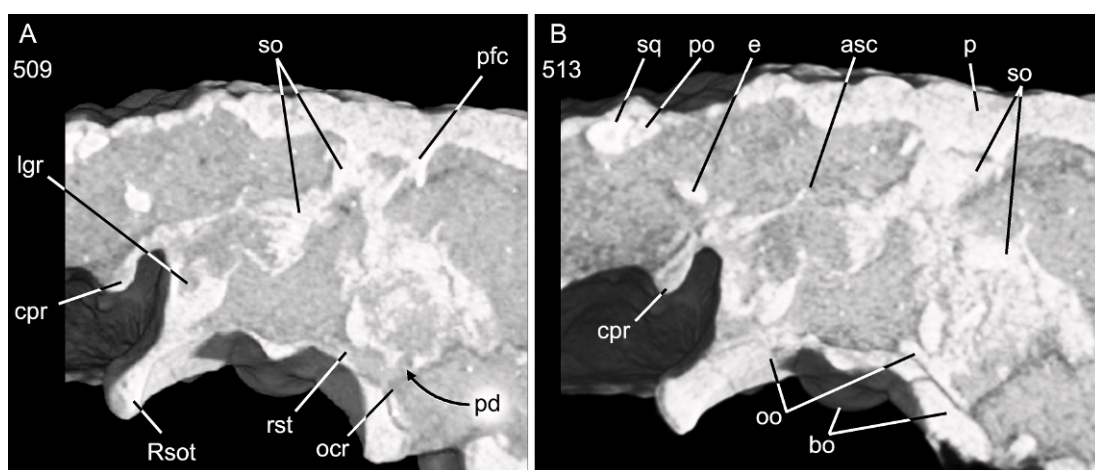


Fig. 37. Transverse HRXCT section through the braincase of *Gobiderma pulchrum* (IGM 3/55), highlighting inner ear morphology. **A.** Section 509, through the level of the occipital recess at the recessus scalae tympani at the anterior end of the sphenio-occipital tubercle. **B.** Section 513, through a level just posterior to the recessus scalae tympani, highlighting, among other things, the postorbital-squamosal contact and the suture between the otooccipital and the basioccipital.

37, 38), IGM 3/59, IGM 3/905 (figs. 33B, D, 35, 36B), ZPAL MgR III/64 (fig. 3C), and ZPAL MgR III/65 (fig. 11B, C). It is almost completely hidden by matrix in IGM 3/59 (basioccipital not labeled). In IGM 3/905, the basioccipital is completely exposed, but the occipital condyle is damaged such that about one-half of the basioccipital contribution has been lost. Also, the apex of the left sphenio-occipital tubercle has been eroded. Otherwise, this basioccipital is complete and very well preserved without distortion. The basioccipital is well preserved and visible in the HRXCT scans of IGM 3/55 (see figs. 37, 38). One exception is the anteromedial part of the basioccipital, where there is damage. However, this part of the braincase is well preserved in the holotype (fig. 3C).

The basioccipital is a median element contacting the parabasisphenoid, proötics, otooccipitals, atlas, and axis. It forms the medial portion of the occipital condyle and the posteroventral floor of the brain chamber. The dorsal surface of the basioccipital (the floor of the brain chamber) is ventrally concave both in sagittal (fig. 30) and transverse planes (figs. 28C, 37).

In ventral view, the basioccipital is trapezoidal. Its anterolateral margin, demarcated by the sphenio-occipital tubercles, is nearly

twice the width of the posterior end. The sphenio-occipital tubercles are robust and directed ventrolaterally (figs. 33, 35, 36A, B, 37, 39). An anteroposteriorly broad, but medially tapering, lamina (the basituberal lamina) extends medially from each sphenio-occipital tubercle for the length of about one-third the greatest basioccipital width. Medial to this point, the basituberal lamina joins the main body of the ventral floor of the basioccipital. The basituberal lamina, the ventrally arched medial floor of the basioccipital, and the narrow anteriorly oriented crista ventrolateralis together define a shallow anteroventral fossa on the anterior surface of the sphenio-occipital tubercle (visible in figs. 36A, B, 39).

SUPRAOCCIPITAL: The supraoccipital is well preserved and visible in IGM 3/905 (figs. 6B, 33D, 35B, 36B) and ZPAL MgR III/65 (figs. 11C). The HRXCT scans of IGM 3/55 reveal the presence of a complete supraoccipital, but offer only a few additional details (figs. 30, 37).

The supraoccipital possesses a distinct bony process (figs. 30, 33C, 35B, 36A, B) with a facet for an ascending process of the tectum synoticum, which augmented the connection between the parietal and braincase (fig. 37). A midline ridge is present on this process. It is

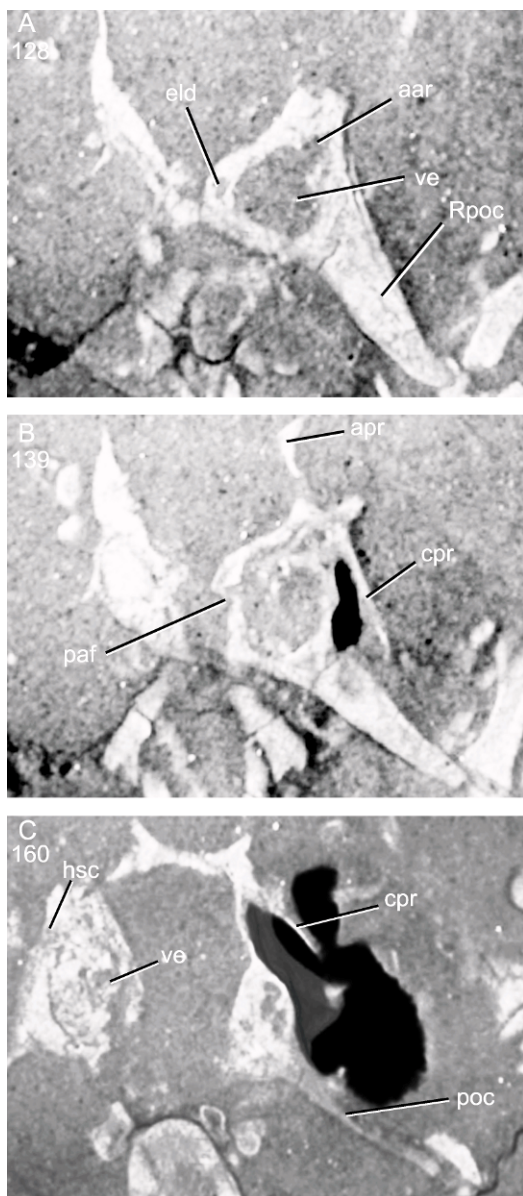


Fig. 38. Frontal HRXCT sections through the braincase of *Gobiderma pulchrum* (IGM 3/55), highlighting inner ear morphology. **A.** Section 128, near the dorsal end of the vestibule and the endolymphatic duct. **B.** Section 139, near the dorsal terminus of the crista proötica. **C.** Section 160, through a level near the ventral margin of the paroccipital processes.

most pronounced anterodorsally and becomes progressively weaker posteroventrally and is nearly nonexistent at the foramen magnum (figs. 30, 33D). The supraoccipital contacts the proötics and otooccipitals, and forms the dorsal midline of the braincase and foramen magnum. A parasagittal process extends anterolateral to the ascending midline process (visible in figs. 33D, 36A, B). This seems similar to the proötic process of some taxa (e.g., *Shinisaurus crocodilurus*; Conrad, 2004), but it does not directly overlie the proötic in *Gobiderma pulchrum*. The supraoccipital-proötic suture extends posterolaterally toward the paroccipital processes of the proötic, where it reaches its broadest point and invades the proötic-otooccipital contact dorsally. From this point, it extends posteromedially to form almost the entire dorsal margin of the foramen magnum.

PROÖTIC: Both proötics are well preserved and exposed in IGM 3/905 (figs. 33B, C, 36B), ZPAL MgR III/64 (fig. 3A), and ZPAL MgR III/65 (fig. 11B, C). Proötics are also visible in the HRXCT scans of IGM 3/55 (figs. 27, 37, 38). Each proötic contacts the epipterygoid, parabasisphenoid, supraoccipital, otooccipital, and the basioccipital. The shape of the proötic-basioccipital contact is unclear because many sutures are fused in the available braincases. The proötic houses the anterior part of the membranous labyrinth (figs. 37, 38).

The proötic alar process is very strongly developed (figs. 27, 28C, 33C, 36A, B) and extends anterolaterally toward the parietal, which it contacts via the decensus parietalis. This alar process extends well anterior to the anterior semicircular bulla (cupola anterior of de Beer, 1937; nonhomologous to any of the bullae present in mammals) and the anterior ampullar recess as in most other scleroglossans (e.g., *Phelsuma*, *Proscelotes*, *Xenosaurus*). The dorsal margin of the proötic arcs ventromedially toward the supraoccipital contact, then dorsolaterally as the dorsal margin of the paroccipital process. The paroccipital process of the proötic covers the anterior margin of the oto-occipital paroccipital process in a flat lap joint. The proötic paroccipital process narrowly contacts the supratemporal distally (visible in IGM 3/905; fig. 33C).

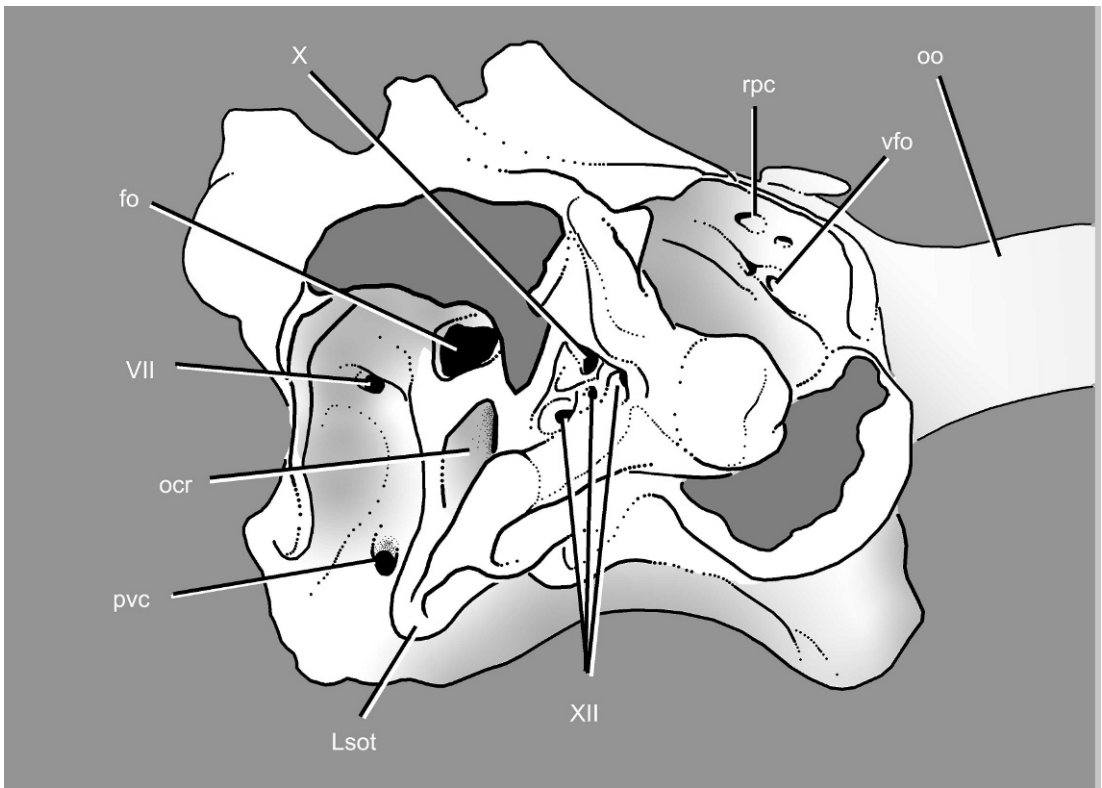


Fig. 39. Line drawing of reconstruction of the occipital recess of *Gobiderma pulchrum* (IGM 3/905) left posterolateral view. Broken surfaces in dark gray.

The anterior bulla for the anterior semi-circular canal is only very weakly visible externally. The trigeminal notch (= incisura proöticum of Jollie, 1960; and Bever et al., 2005a) is deeply developed (fig. 36A, B). It is dorsally bounded mostly by the alar process and also by the anterior bulla; it is ventrally bounded by the inferior process of the proötic. The anteroventrally directed inferior process is laterally concave, forming a shallow fossa (figs. 28, 33C). This fossa may have been filled by the *M. protractor pterygoideus* and the mandibular division of the trigeminal nerve based on comparisons with *Ctenosaura pectinata* as described by Oelrich (1956). A supratrigeminal process is present, but is expressed only a small, pointed, tubercle medial to the dorsal margin of the trigeminal notch (visible in fig. 33C).

The proötic-supraoccipital suture extends anterolaterally along the dorsal surface of the braincase to the base of the proötic parocci-

pital process (fig. 36A, B). Posterolateral to this point, the proötics paroccipital process anteriorly overlies the otooccipital paroccipital process posteriorly nearly to the level of the contact between the otooccipital, quadrate, and supraoccipital. The suture between the ventral side of the proötic paroccipital process and the otooccipital is visible posteriorly, but it is obliterated more anteriorly by bone intergrowth in IGM 3/905 (figs. 35A, 36B), ZPAL MgR III/64, ZPAL MgR III/65 (visible in the specimens; fig. 11C), and IGM 3/55 (HRXCT). There is no clear proötic-otooccipital suture in close proximity either to the fenestra ovalis or anterior to that point. It is impossible, therefore, to determine whether the proötic contributes to the posterior opening of the Vidian canal (figs. 33A, B, 35, 36A, B).

The crista proötica (proötic crest of some authors) is well developed and possesses both lateral and ventral projections for most of its

length (figs. 28C, 33A, B, 35A, 36A, B, 38B, C). It originates between the inferior process of the proötic and the basiptyergoid process of the parabasisphenoid and extends posteriorly to the proötic. Anteriorly, the ventral face fails to overlap the level of the posterior opening of the Vidian canal and, thus, does not hide it in lateral view (fig. 36A, B). The crista proötica is very weakly developed near the base of the proötic paroccipital process, in the region of the fenestra ovalis. This reduced area of the crista proötica may have allowed lateral extension of the stapes.

The crista proötica completely overlies the single facial foramen, the latter occurring near the medial edge of the crest just posteroventral to the ventralmost extension of the external auditory bulla. A narrow groove extends posteriorly from the facial region.

OTOOCCIPITAL: The fused exoccipital-opisthotic unit is here referred to as the *otooccipital*, following recent usage (Maisano, 2001c; Conrad, 2004; Bever et al., 2005a). The otooccipitals are well preserved in IGM 3/55 (figs. 4C, 5D, 34, 38), IGM 3/905 (figs. 26, 33B–D, 35, 36B), ZPAL MgR III/64 (fig. 3), and ZPAL MgR III/65 (fig. 11). The dorsal part of the left paroccipital process is visible in IGM 3/59 (fig. 22). Although the otooccipitals generally coossify with surrounding elements in *Gobiderma*, we have been able to identify the sutures with the supraoccipital and basioccipital using comparisons of HRXCT scans of IGM 3/55 (fig. 37) and the exquisitely prepared and preserved braincase of IGM 3/905 (figs. 33B–D, 35, 36B). Each otooccipital contacts the proötic, basioccipital, supraoccipital, parietal, supratemporal, and quadrate. It forms the dorsal, ventral, and posterior margins of the fenestra ovalis, the dorsal and posterior margins of the occipital recess, and the lateral margins of the foramen magnum (figs. 36A, B, 37A, 39). It also houses the exits for cranial nerves IX–XII (figs. 33D, 36A, B, 39).

Although some parts of the otooccipital–basioccipital suture are untraceable through the direct observation of any available specimen, the HRXCT scans demonstrate that the two elements form a broad contact in the area of the spheno-occipital tubercle (fig. 37). The otooccipital extends far down the dorsolateral surface of the basioccipital in

this region, thus forming most of the dorsolateral surface of the spheno-occipital tubercle and housing nearly all of the occipital recess. Some of the suture is visible in IGM 3/905 along the posterior surface of the crista tuberalis and approaching the occipital condyle. This suture is mostly linear and extends mediolaterally and very slightly ventrolaterally. However, the suture is obliterated by bone intergrowth medially and the contribution of the otooccipital to the occipital condyle cannot be determined.

The oblong occipital recess is very deep and relatively large as compared to the fenestra ovalis. It is subovate with a convex anterior border and a concave posterior one. It invades the base of the spheno-occipital tubercles (figs. 36A, B, 37A, 39). The undivided recessus scalae tympani is located in the center of the occipital recess in lateral view (fig. 37A). The crista interfenestralis (the bony flange dividing the occipital recess and the fenestra ovalis; see figs. 36A, B, 39) is flat, only expressed as a bladelike crest posteriorly near the contact with the crista tuberalis at the posterodorsal margin of the occipital recess. The crista interfenestralis is nearly as mediolaterally wide as deep, its medial margin being formed by the perilymphatic canal, thus joining the lagenar recess of the inner ear with the occipital recess (figs. 37, 38). By contrast, the crista tuberalis is anteroposteriorly very narrow and well defined. It is medially concave in posterior view, extending dorsomedially toward the foramen magnum from the dorsal base of the spheno-occipital tubercle before turning dorsally and dorsolaterally at the level of its contact with the crista interfenestralis.

The fenestra ovalis is relatively small, a feature often seen in relatively large anguimorphs like *Gobiderma pulchrum*, *Heloderma*, *Helodermoides tuberculatus* (see Conrad and Norell, 2008: fig. 5), and the larger species of *Varanus* (e.g., *Varanus komodoensis* and *Varanus exanthematicus*). It is subrectangular and wider than tall with its anterior end being slightly larger than its posterior end (fig. 36A, B). Rather than being oriented directly laterally, the fenestra ovalis is somewhat posterolaterally oriented. No stapes can be identified through direct observations or through the HRXCT scans.

A shallow and very poorly defined recess located adjacent to the occipital condyle and posteromedial to the crista tuberalis houses the vagus and hypoglossal foramina (figs. 33D, 36A, 39); this is similar to the condition in most anguimorphs and very like the condition described and illustrated for *Shinisaurus crocodilurus* (Conrad, 2004; Bever et al., 2005a, 2005b). This fossa is open laterally and ventrally, and is defined mostly by a gentle dorsal swelling or crest and the posterolateral swelling of the occipital condyle. The vagus foramen is dorsal to the three hypoglossal foramina and occurs nearest the dorsal crest. The hypoglossal foramina are separate from the vagus foramen and lie in an anteroposteriorly directed line. Whereas the posteriormost hypoglossal foramen is the largest and is similar in size to the vagus foramen, the other two hypoglossal foramina are equally sized and are somewhat less than half that diameter.

Robust, elongate, paroccipital processes lie lateral to the foramen magnum and dorso-lateral to the vagus and hypoglossal foramina (figs. 33B, D, 34, 35, 36A, 38, 39). The paroccipital process is not posteriorly deflected, but instead is mediolaterally oriented. The posterodorsal surface of the paroccipital process bears well developed surfaces that, based on comparisons with *Heloderma* (see Herrel and De Vree, 1999), received the insertions for the occipito-vertebral group of muscles. Lateral to these insertion surfaces, the paroccipital process flares dorsally near its lateral terminus where it contacts the parietal, supraoccipital, and quadrate (figs. 33D, 35B).

INNER EAR: The inner ear cavities are visible in the HRXCT scans of IGM 3/55 (figs. 37, 38). Although some details are not clear because of slight dorsoventral and lateral diagenetic deformation of the braincase, much of the morphology is visible.

The proötic shows virtually no external anterior auditory bulla (see fig. 36A, B) contrasting the condition in many anguimorphs (e.g., *Elgaria coerulea*, *Shinisaurus crocodilurus*, *Varanus acanthurus*; but see *Heloderma* and *Xenosaurus*; see Rieppel, 1980a; Conrad, 2004; Bonine, 2005a, 2005b; the Deep Scaly Project, 2007) and the HRXCT scans show a correspondingly small anterior ampullar re-

cess (fig. 38A). The delimitation between the anterior ampullar recess and the anterior semicircular canal is indistinct, without notable constriction between the two chambers, but the anterior semicircular canal does seem to originate more dorsally than in *Shinisaurus crocodilurus* (see Bever et al., 2005a, 2005b). The anterior semicircular canal extends almost directly dorsally and is very narrow (fig. 37B). Its posterior portion near the recessus crus communis is not visible. Only a small part of the latter structure is visible and only on the left side of the specimen (not figured here). A small part of the posterior semicircular canal is visible extending posteriorly from the recessus crus communis.

The horizontal semicircular canal originates very near the anteroventral part of the anterior semicircular canal (fig. 38C). The anterior one-half of the course of the horizontal semicircular canal runs along the posteromedial margin of the proötic paroccipital process, near its contact with the otooccipital and exits into the otooccipital at the level of the approximate midpoint of the fenestra ovalis. This resembles the condition in *Shinisaurus crocodilurus* (Bever et al., 2005a, 2005b). The posteromedial part of the horizontal semicircular canal's arch is only very thinly separated from the vestibule. The horizontal semicircular canal joins the vestibule at its posterior apex of the sub-spherical vestibule (fig. 38C).

The vestibule is large and forms a robust medial tympanic bulla (sensu Oelrich, 1956). The dorsoventrally oriented endolymphatic canal and the endolymphatic foramen are located on the wall of the medial apex of the vestibule (fig. 38A).

The lagenar recess is subovate, it is broader anteroposteriorly and dorsoventrally than mediolaterally. The perilymphatic duct connects the lateral side of the posteroventral margin of the lagenar recess with the occipital recess (fig. 38B). The shape and extent of the posterior lagenar recess is difficult to identify.

DENTARY: Most of the right dentary is preserved in IGM 3/905 (figs. 6D, E, 40A–C), a partial right dentary is preserved in ZPAL MgR III/66 (fig. 19D, E), and both dentaries are preserved in IGM 3/55 (figs. 4A, C, 5A,D, B, 41) and in ZPAL MgR III/64 (fig. 3A, C–E). The HRXCT

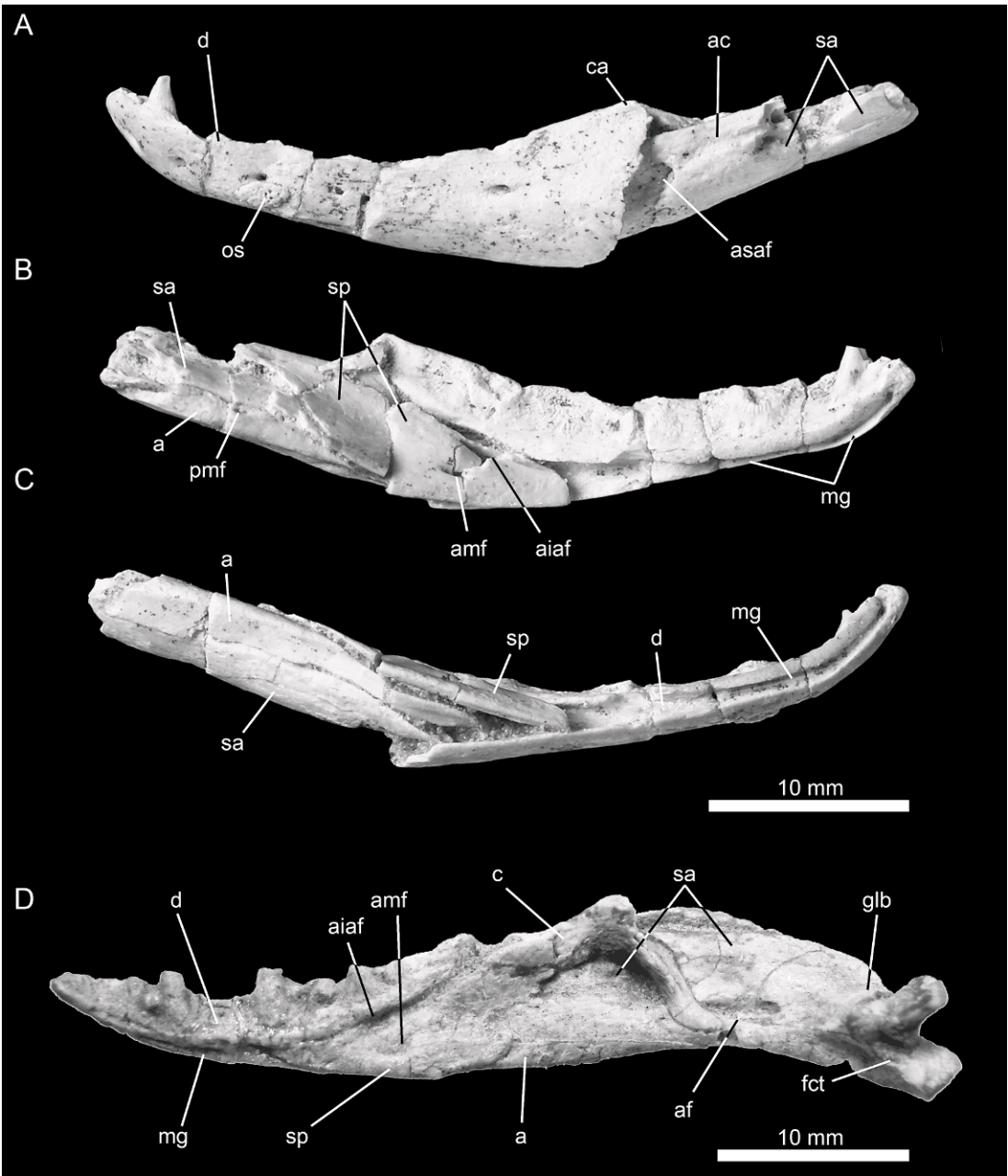


Fig. 40. The mandible of *Gobiderma pulchrum*. Incomplete left mandible of IGM 3/905 in **A**, lateral, **B**, medial, and **C**, ventral views. **D**. Right mandible of ZPAL MgR III/64 in medial view.

scans and isolation of the mandible of the latter allows views hidden by articulation and the remaining matrix. Each ventrally convex dentary contacts the splenial, surangular, coronoid, angular, and the other dentary in a narrow schizarthrotic symphysis. Six labial

foramina are present in the left dentary of IGM 3/905 and the right dentary of IGM 3/55, and five are present on the left dentary of IGM 3/55. Slight damage to all of the ZPAL MgR III dentaries prevents a certain count of labial foramina. There is no subdental shelf

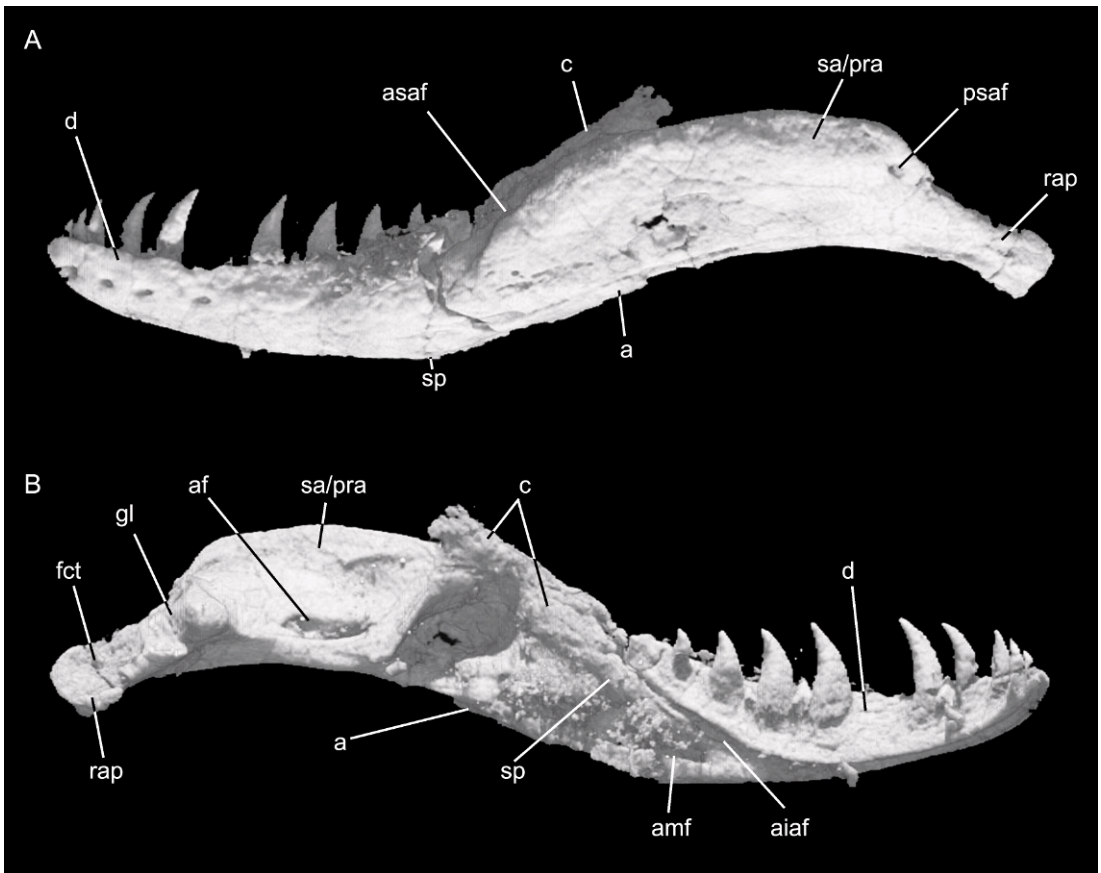


Fig. 41. The left mandible of *Gobiderma pulchrum* (HRXCT reconstruction of IGM 3/55) in **A**, lateral and **B**, medial views.

(figs. 13, 42). The dental ridge is broadest near the midpoint of the tooth row. The dentary contributes the dorsal border to the anterior inferior alveolar foramen, but only where it overlaps the splenial. Based on comparisons of various specimens, including impressions on the postdentary bones and HXRCT data (figs. 4C, 5D, 16, 41), we are able to confidently reconstruct the bifurcated posterolateral dentary margin (fig. 7A). The lateral surface of the posterodorsal end of the dentary bears a shallow and poorly defined facet that receives the anterior coronoid process on the lateral surface. The ventral process of the posterior end of the dentary extends ventral to the lateral exposure of the surangular and laterally overlies the ventrolateral surface of the angular (visible in fig. 4C).

Meckel's canal ventrally emarginates the dentary symphysis, giving it the characteristic kidney shape present in most nonophidian squamates (figs. 6E, 7D, 40, 41). Meckel's canal extends posteroventrally from the dentary symphysis on the ventromedial surface of the dentary and then expands to open more medially again where covered by the splenial.

The well-developed intramandibular septum lies at approximately the level of the last dentary tooth (fig. 42). Its posteroventral margin is free; thus, the alveolar and Meckel's canals remain confluent ventrally to a point just anterior to the last dentary tooth even though the posterodorsal extension of the intramandibular septum extends posterior to the level of the posterior margin of the last dentary tooth. Posterodorsally, the in-

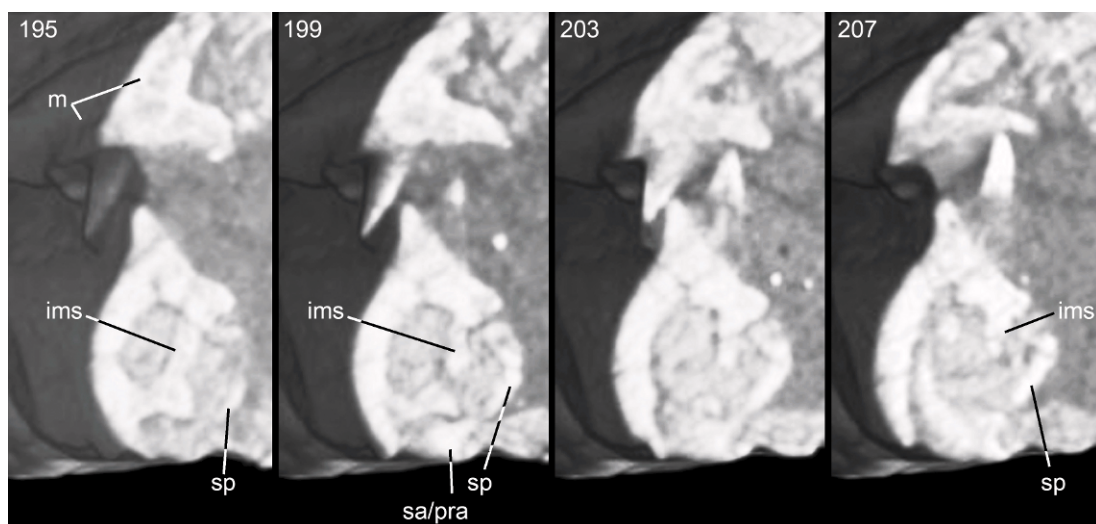


Fig. 42. Selected transverse HRXCT slices through the right mandible of IGM 3/55 illustrating the morphology of the intramandibular septum.

tramandibular septum is confluent with the narrowest part of the dental ridge.

SPLENIAL: Both splenials are preserved in IGM 3/55 (figs. 41, 42) and ZPAL MgR III/64 (fig. 3), part of the left splenial is preserved in IGM 3/59 and in IGM 3/905 (fig. 40B, C), and most of the right splenial is preserved in ZPAL MgR III/66 (fig. 19). The HRXCT scan of the right splenial in IGM 3/55 reveals much of the morphology of the bone in *Gobiderma pulchrum*. Both IGM 3/905 and IGM 3/59 preserve much of the middle portion. The posterodorsal part of the splenial is visible in IGM 3/59 (fig. 22).

The linguolabially thin splenial of *Gobiderma pulchrum* resembles the same element in *Heloderma*. Overall, it is triangular, with an acute anteroventral process medially walling Meckel's canal, an obtuse posteroventral flange contacting the angular, and an acute posterodorsal angle whose dorsal margin overlies the coronoid and whose posteroventral margin is overlain by the angular (figs. 7D, 40D, 41A). The anterior inferior alveolar foramen and the anterior mylohyoid foramen are housed within the splenial (figs. 40B, D, 41B). The tapering anterior end of the splenial approaches, but does not extend to, the midpoint of the dentary tooth row. The posterodorsal tip of the splenial does not reach the level of the coronoid apex

and the posteroventral tip extends little, if at all, beyond the anterior tip of the angular.

The splenial-angular contact is a narrow overlapping joint without a well-developed hinge joint like that seen in mosasaurs and *Lanthanotus borneensis*, or like that seen in snakes. The splenial-angular contact occurs on the ventral surface of the mandible and extends to the level of the last tooth (figs. 3E, 7D, 40B, D).

CORONOID: Most of the left coronoid is preserved and exposed in IGM 3/59, and both coronoids are visible in the HRXCT scans of IGM 3/55 (e.g., fig. 22). The left coronoid is complete and the right is slightly damaged along the coronoid eminence in ZPAL MgR III/64 (fig. 3A, C, E). Small fragments of the right coronoids are preserved with ZPAL MgR III/65 (fig. 11D) and ZPAL MgR III/66 (fig. 19E).

The coronoid is a complex bone. Its overall shape in medial or ventromedial view is a dorsal arch composed of descending anterior and posterior processes and a low dorsal eminence (figs. 3E, 7D, 32B, 40D, 41, 43, 44G–I). The anterior process is narrowly forked ventrally to clasp the posterodorsal margin of the dentary. Little of the coronoid is exposed in lateral view because of the dorsomedial extension of the coronoid eminence (see below) and the strong dorsolateral

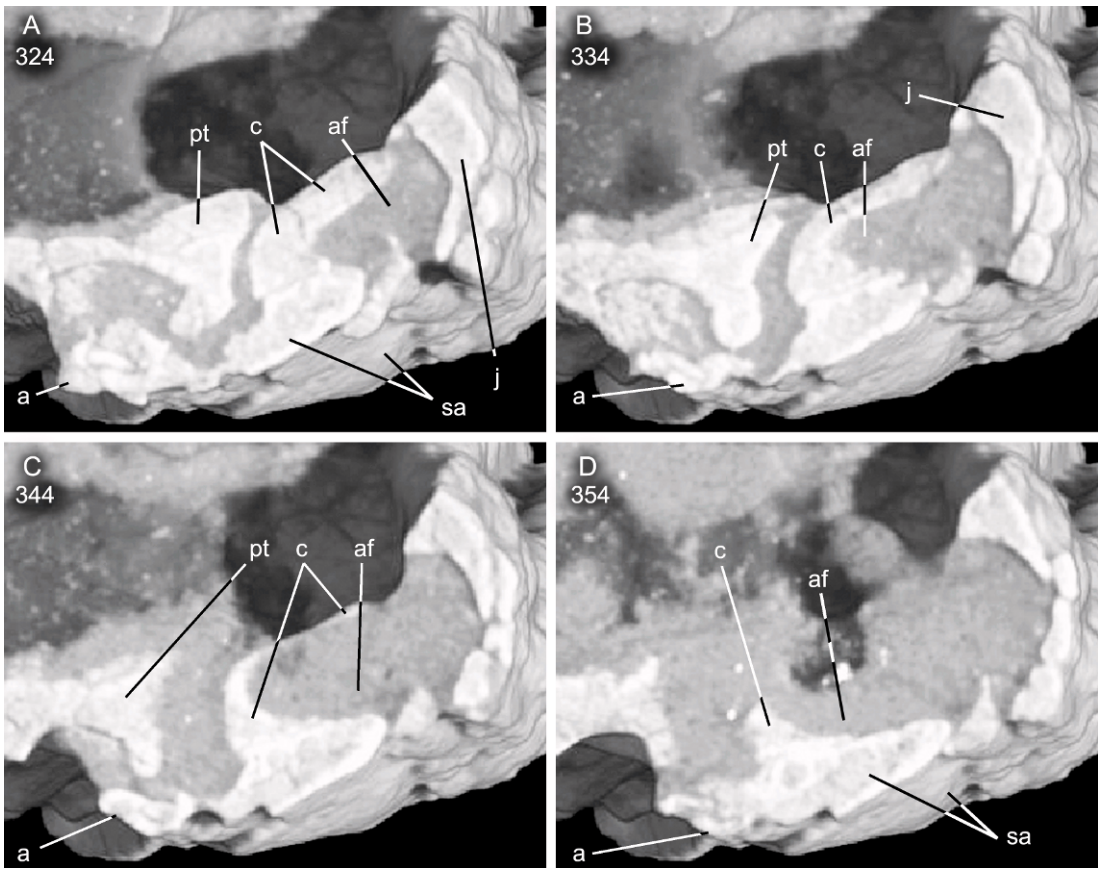


Fig. 43. Selected transverse HRXCT slices through the right mandible of IGM 3/55 illustrating the morphology of adductor fossa near the level of the coronoid. **A.** Section 324, illustrating the anterior part of the adductor fossa (af) occurring lateral to the coronoid eminence and laterally bounded narrowly by the surangular. The jugal, with it a pronounced ventral flange lies dorsolateral to the coronoid. **B.** A slightly more posterior section (334) with greater development of the adductor fossa, more deeply invading the coronoid and with a greater surangular contribution to its lateral margin. **C.** Section 344, illustrating the mediolateral shape of the adductor fossa near the posterior terminus of the coronoid eminence. **D.** Section 354, just behind the level of the coronoid eminence, where the adductor fossa occurs primarily on the medial mandibular surface.

projection of the surangular (figs. 32B, 40A, C, 41, 43A–C, 44I, J). The coronoid contacts the dentary, splenial, surangular, and prearticular. It extends from near the level of the posteriormost dentary tooth to a point near the middle of the mandibular adductor fossa. As with many other squamates, the tapered anterior end of the coronoid invades the dentary-splenial contact, but the coronoid does not reach the level of the anterior inferior alveolar foramen (figs. 7D, 40D). The anterior inferior alveolar foramen is located posterior to the level of the dentary

tooth row in *Heloderma* and the coronoid contributes the posterior border to the foramen (fig. 8D). This differs somewhat from the condition seen in some other squamates wherein a narrow anterior extension of the coronoid extends anteriorly to the level of the anterior inferior alveolar foramen (e.g., some iguanids, some chamaeleonids, and *Pseudopus apodus*).

The coronoid eminence is medially bowed near its ventral margin. Thus, rather than lying directly dorsal to the main axis of the mandibular ramus, the coronoid eminence

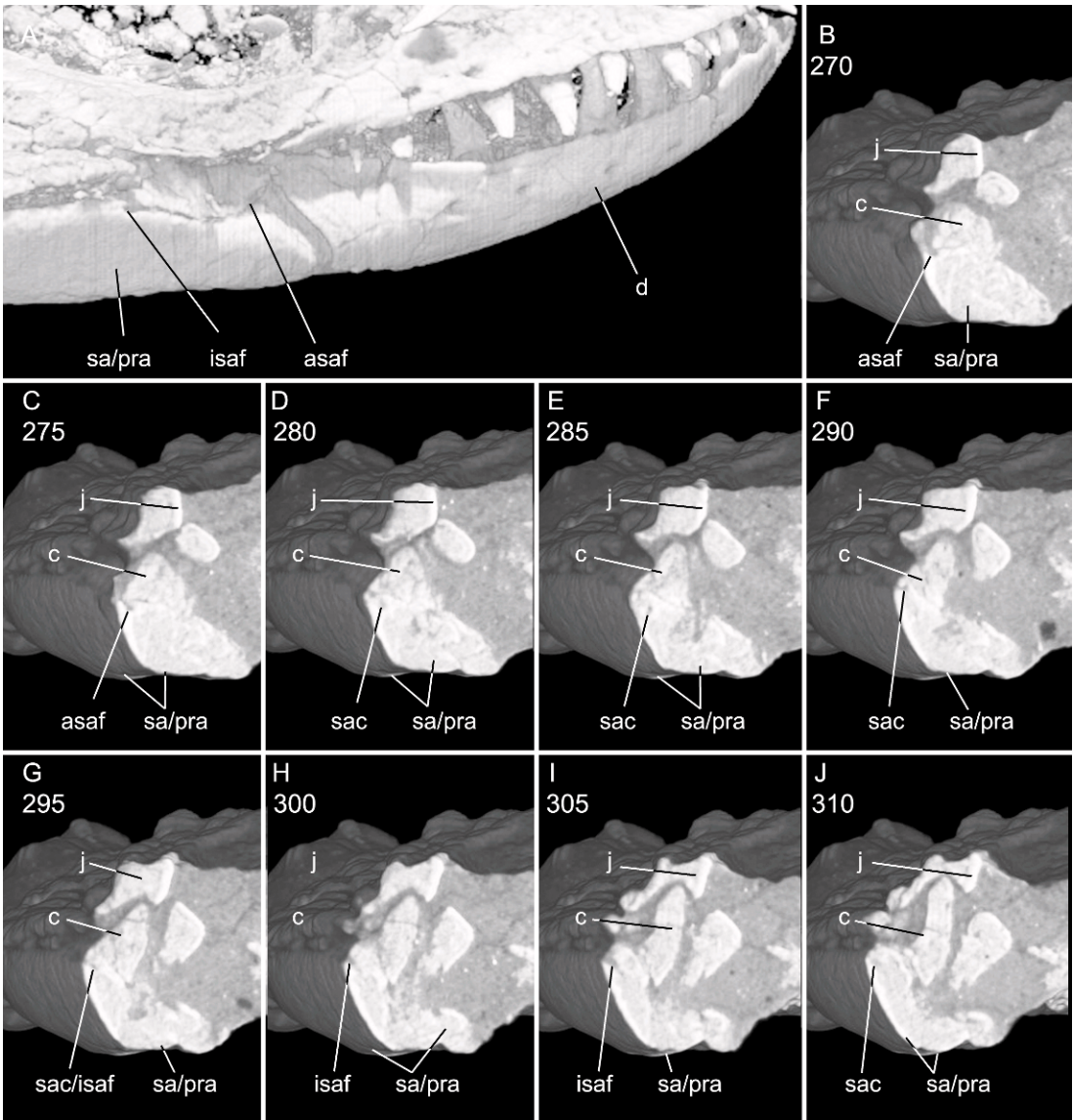


Fig. 44. The mandible of IGM 3/55, highlighting the morphology of surangular canal. **A.** HRXCT reconstruction of the right mandible in lateral view. **B–J.** Anterior and intermediate surangular foramina, surangular canal and nearby structures.

extends dorsomedially (figs. 32B, 40, 41, 43A–C). The coronoid eminence is posterodorsally inflected and somewhat tapered dorsally, but with a squared posterodorsal margin. The anterior margin of the coronoid eminence is very robust, with a weakly developed labial flange. Posteriorly, the coronoid eminence becomes a thin blade. This blade is continuous with a crest that extends

posteromedially on the lingual surface of the posterior descending process, just anterior to the adductor fossa (figs. 40D, 41B). The descending process descends to a level ventral to the adductor fossa and tapers posteroventrally to a point contributing to the anteromedial margin of the adductor fossa.

ANGULAR: Both angulars are preserved and exposed in ZPAL MgR III/64 (figs.

3C–E, 40D) and IGM 3/55 (figs. 4C, 5D). A small part of the right angular is preserved in ZPAL MgR III/66 (fig. 19C). A nearly complete left angular is preserved in IGM 3/905 wherein movement of the individual mandibular elements allows a view of the interrelationships of the bones (fig. 40B, C). All the preserved angulars are damaged. However, comparisons among these specimens allow understanding of the overall morphology of the angular. Also, the posteroventral processes of the dentary are broken on both sides of IGM 3/55, showing most of the anterior end of the left angular (figs. 4C, 5D).

The angular forms the anteroventral portion of the postdentary part of the mandible. It does not extend far up the lateral surface of the dentary and is consistently narrow for its entire length, except for its tapered ends. The angular contacts the dentary, splenial, surangular, and prearticular. Its anterior end tapers to a point that is ventrolaterally overlapped by the dentary and ventromedially overlapped by the splenial for more than one-half its length (fig. 40C, D). Thus, the angular contributes somewhat to the ventral margin of Meckel's canal along the middle of the jaw. The angular facet tapers posteriorly as in modern *Heloderma*.

The posterior mylohyoid foramen is clearly preserved only in the holotype and IGM 3/55. It is located within the anterior one-third of the angular, near the contact of the dentary, angular, and surangular (figs. 7D, 40B) anterior to the coronoid eminence.

SURANGULAR: The surangular is exposed in all of the examined specimens except IGM 3/57 (figs. 3D, E, 4A, C, 5A, B, D, 6D, E, 11D, 19D, E). Only the left is known from IGM 3/905, IGM 3/59, and ZPAL MgR III/65; both are directly observable and visible in the HRXCT scans of IGM 3/55 (figs. 32B, 40, 41–44).

The surangular is the largest element in the postdentary part of the mandible and is widely exposed in both medial and lateral views (see figure references above and the reconstruction in fig. 7A, D). Although the surangular tapers somewhat anteriorly, it comes to a blunt tip near the level of the last dentary tooth. The surangular contacts the dentary, splenial, coronoid, angular, and the prearticular-articular unit. It forms the pos-

terior part of Meckel's canal and the lateral margin of the adductor fossa. The postero-dorsal part is expanded dorsomedially into a robust buttress anterior to the articular glenoid fossa (figs. 33B, C, 40D, 41B). A similar buttress is seen to varying degrees in many squamates and its orientation in those taxa varies from being nearly vertical to facing mostly medially as in *Gobiderma pulchrum*.

The lateral exposure of the surangular tapers anteriorly between the subcoronoid and subsurangular processes of the dentary, and possesses broad dentary facets that medially underlie those processes of the dentary (visible in figs. 40A, 41A, 44A). An articular surface for the coronoid extends from the dorsal surface of the surangular and is divided into two less pronounced articular surfaces on its medial surface. The anterior part of the dorsolateral portion of the coronoid facet is undifferentiated from the contacting dentary facet. The medial surface of the surangular is visible between the two descending coronoid rami when the mandible is articulated (figs. 40D, 41B). Posterodorsally, the surangular possesses an anterior concavity that receives the glenoid portion of the articular. Posteroventral to that point, the surangular partly underlies the articular glenoid fossa. From the contact with the articular, the surangular extends anteromedially, forming the ventral margin of the adductor fossa (figs. 32B, 40D, 41B). An angular facet is present on the ventral surface of the surangular, extending from the level of the posterior tip of the coronoid eminence to near the posterior tip of the dentary tooth row. Posterior to the angular facet, the ventral surface of the surangular bears a well-defined prearticular facet.

The mandible of IGM 3/55 possesses surangular foramina anteriorly within the surangular (figs. 40A, 41A, 44A–C), which we term the *anterior surangular foramen* and the *intermediate surangular foramen*. These both communicate with the surangular canal located dorsolaterally within the surangular. Contrasting this condition is IGM 3/905, which apparently has only a single anterior alveolar foramen (fig. 40A). Comparisons with existing descriptions suggest that this canal housed the mandibular nerve (branch

3 of the trigeminal nerve) and that the intermediate and anterior surangular foramina accommodated transmission of superficial fibers innervating the lips and the skin around the craniomandibular joint (Oelrich, 1956; Schumacher, 1973; Kley et al., 2010).

Extant *Heloderma* are also variable in the presence of two (Bonine, 2005b; the Deep Scaly Project, 2007), or only a single anterior surangular foramen (Bonine, 2005a; fig. 8A). The anterior surangular foramen is present on the anterodorsal surface of the surangular (fig. 38A; visible in fig. 7A). The external border of the anterior surangular foramen is shared between the coronoid dorsally and the surangular ventrally (figs. 7A, 40A, 41A, 44A–C). Posteriorly, near the level of the anteromedial extent of the articular glenoid fossa, the posterior surangular foramen passes posteromedially through the dorsal part of the surangular (figs. 4C, 5D).

The adductor fossa is not well developed posteroventrally to the coronoid eminence as it is in some squamates (e.g., some lacertoids; J.L.C., personal obs.). However, the adductor fossa extends anteriorly onto the dorsal surface of the mandible (figs. 32B, 43). The dorsomedial arching of the coronoid at the level of the coronoid eminence forms the ventral margin of this anterior extension of the adductor fossa. The lateral margin of this extension is formed by a dorsolateral crest of the surangular that overlaps the level of the coronoid eminence and extends posterior from that level. Based on comparisons with descriptions of extant taxa, this part of the mandible likely gave rise to the M. adductor mandibulae externus superficialis (Oelrich, 1956; Rieppel, 1980a; Abdala and Moro, 2003).

PREARTICULAR AND ARTICULAR: The prearticular and articular are represented in all the specimens except IGM 3/57 (figs. 3D, E, 4C, 5A, B, D, 6D, E, 11D, 19D). However, only a small part of the anterior (prearticular) process may be identified in ZPAL MgR III/66 (fig. 19D). An articular portion lacking a retroarticular process is preserved in ZPAL III/65 (fig. 11D).

It is common for Meckel's cartilage to ossify posteriorly to form the articular bone in reptiles (de Beer, 1937; Romer, 1949, 1956) and it often becomes fused to the prearticular

such that no remnant of a suture remains. As with many squamates (but not mosasaurids) the articular forms the cotylar surface of the articular glenoid fossa (hereafter, the glenoid fossa) and its further extent cannot be discerned.

The glenoid fossa is dorsomedially oriented (figs. 3E, 7D, 38D). It lacks a strong division of medial and lateral surfaces, but possesses strong anterior and posterior buttresses. The prearticular is relatively small and thin and extends along the posteroventral part of the surangular, beneath the glenoid fossa, and forms the retroarticular process. The retroarticular process is somewhat twisted such that the broadest surfaces are oriented dorsomedially and ventrolaterally (figs. 7D, 40D). Torsion of the retroarticular process is similar to that of most other platynotans, but not so great as in anguids or the Eocene varanoid *Eosaniwa koehni* (Rieppel et al., 2007). The dorsal process (or dorsolateral surface, given the torsion) of the retroarticular process is gently concave. Posteriorly, the retroarticular process is somewhat expanded with a small anteromedially oriented hook of bone visible on both sides of IGM 3/55 (figs. 4C, 5D) and on the right retroarticular process of IGM 3/59.

A single foramen chorda tympani is visible in the HRXCT scans of the left prearticular of IGM 3/55. It is located on the descending surface of the posterior (prearticular) buttress of the glenoid fossa (fig. 5B).

OSTEODERMS: All the specimens for which skull material is known are preserved with small, irregularly shaped, nonoverlapping osteoderms (visible in figs. 3–6, 11–13, 16–20, 22–27, 33D, 35). These osteoderms are partially coossified to the nasals, maxillae, prefrontals, frontals, parietals, and jugals. The osteoderms are somewhat thickened and show the pitted morphology typical of most known monstersaurs (sensu Conrad, 2008; see Hoffstetter, 1957; Estes, 1964, 1983; Pregill et al., 1986; Cifelli and Nydam, 1995; Nydam, 2000), but osteoderms are unknown in *Estesia mongoliensis* (Norell et al., 1992; Norell and Gao, 1997). This type of osteoderm is also found in most glyptosaurines (see Conrad et al., 2011, for a discussion of this character given different anguimorph topologies).

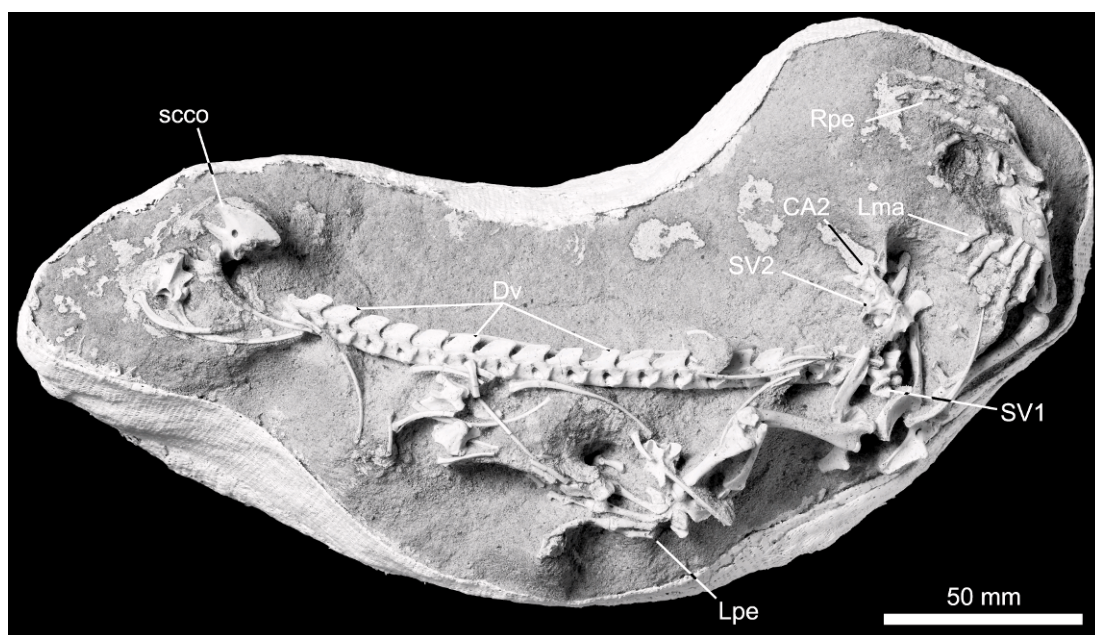


Fig. 45. Incomplete postcranial skeleton of *Gobiderma pulchrum* (IGM 3/905), mostly in left lateral view. This partly articulated specimen includes most of a skull (see figs. 6, 12, 23, 24, 26, 33B–D, 35, 36B, 40A–C), 22 presacral vertebrae with some associated ribs, both sacra, and two proximal caudal vertebrae as well as a right scapulocoracoid, an incomplete left manus, a complete pelvis, and most of both hind limbs.

Smooth, smaller, nonoverlapping osteoderms are present on the underside of the head in IGM 3/55 in one large patch and a slightly smaller patch near the right side of the braincase (visible in fig. 4B). These osteoderms are similar to those seen in extant *Heloderma* (see Bonine, 2005a, 2005b; and the Deep Scaly Project, 2007), but their presence or absence is uncertain in other monstrosaurids.

AXIAL SKELETON

PRESACRAL VERTEBRAE: One specimen, IGM 3/905, is preserved with a superb, nearly complete, postcranial skeleton (figs. 45–51). Twenty-two presacral vertebrae are preserved with this specimen; 18 are preserved in articulation and exposed on a block in left lateral view (fig. 45). One presacral is located on the block anterior to the left scapulocoracoid. Two others are preserved lying ventral to the sixth vertebra in the series of the articulated series. One more disarticulated presacral is preserved between the 12th

vertebra in the articulated series and the left pes. These 22 presacral vertebrae are preserved such that all views are available. The procoelous vertebrae lack precondylar constriction and possess moderately oblique condylar-cotylar articulation. Dorsolaterally oriented zygosphenes are present (fig. 46A).

The first vertebra in the articulated series retains an elongate rib (fig. 45). The vertebra preserved out of articulation and lying anterior to the articulated series also has two associated, elongate ribs. Based on comparisons with other anguimorphs, the presence of elongate ribs in association with these vertebrae suggests that at least eight vertebrae were present anterior to the articulated series (Rieppel, 1980b; Conrad, 2006b). We interpret there to have been a minimum of 26 presacral vertebrae.

No preserved vertebrae in this specimen are demonstrably postaxial cervical, so the relative lengths of the cervical and dorsal vertebrae remain unknown. However, the atlas-axis complex is preserved in IGM 3/55 (figs. 4C, 5C, D). Comparisons with IGM

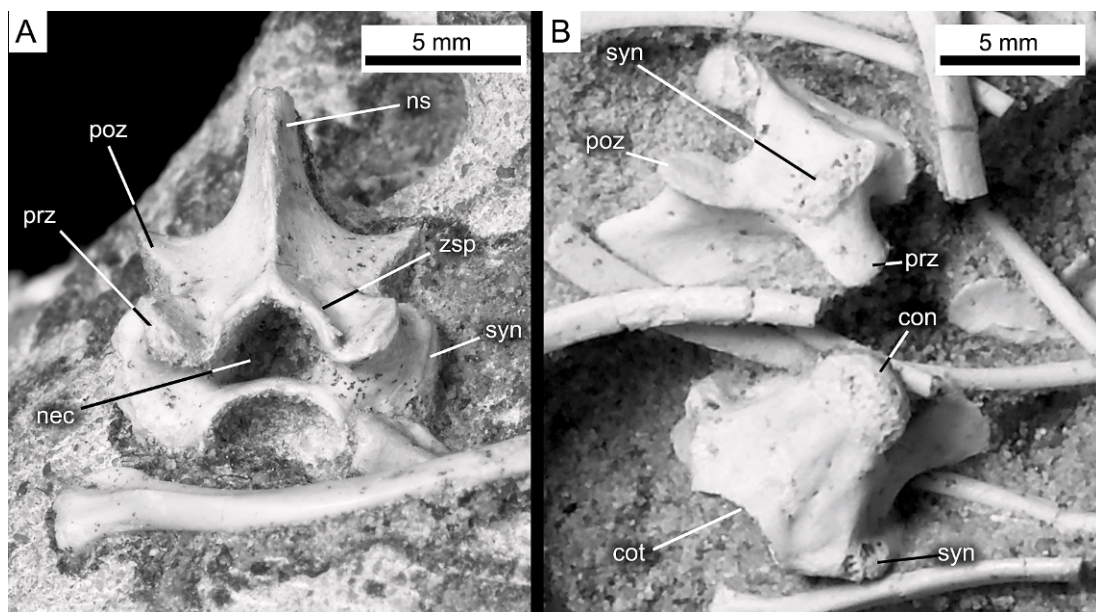


Fig. 46. Disarticulated presacral vertebrae from *Gobiderma pulchrum* (IGM 3/905). **A.** Vertebra near the preserved scapulocoracoid in anterior view. **B.** Two vertebrae located near the partial ribcage displaying left lateral and ventral views. Note the absence of a strong precondylar constriction in the vertebrae and the presence of zygosphenes-zygantra articular surfaces.

3/905 (figs. 45, 46) and IGM 3/59 (fig. 22) suggest the absence of cervical elongation like that typical of many varanines. All of the preserved presacral vertebrae possess relatively short neural spines that are anteroposteriorly broad. The synapophyses are located on the anterior one-third of the centrum. They are more dorsoventrally elongate than they are anteroposteriorly, and they are angled slightly posterodorsally, but they are laterally convex in both anterior and dorsoventral views (fig. 46).

Zygosphenes and zygantra are present, but they are not robust (fig. 46A). Situated relatively low on the neural arch, the zygosphenes are vertically oriented for the most part but with a slight dorsolateral angle. The zygosphenes are connected with the associated prezygapophysis via an arch of bone without an anterior emargination. The prezygapophyses are short and broadly rounded. Intervertebral articular surfaces are visible in most of the preserved vertebrae, demonstrating a relatively consistent condition of oblique articulations. Although Conrad explained this character by addressing the obliqueness of the vertebral

condyles and cotyles because it is more difficult to score in articulated specimens (Conrad, 2008: 62), preparation of IGM 3/905 allows for the identification of oblique condyle-cotyle contacts throughout the articulated series and in the isolated vertebrae (figs. 45–48).

The last two presacral vertebrae in extant *Heloderma* lack movable ribs (see Bonine, 2005c) and should be considered lumbar vertebrae. The penultimate presacral vertebra is exposed in the articulated series in IGM 3/905 and demonstrates the absence of a movable rib. Thus, *Gobiderma pulchrum* also possesses two lumbar vertebrae. However, the vertebra just anterior to this one is obscured by matrix and overlying elements and the presence or absence of an articular synapophysis cannot be reliably identified.

SACRAL VERTEBRAE: Both sacral vertebrae are preserved, but the sacrum itself is disarticulated (figs. 45, 47, 48). The first sacral remains in articulation with the presacral vertebrae and the second remains in articulation with the anterior section of the caudal vertebrae (figs. 45, 47). Thus, the condyle is visible in the first sacral and the cotyle is



Fig. 47. Pelvic girdle and associated structures in *Gobiderma pulchrum* (IGM 3/905).

visible in the second. The sacral vertebrae are disarticulated from the ilia, making the morphology of the sacral ribs visible.

The two sacral vertebrae are unfused as evinced by the separation of the sacral vertebrae without breakage, but we believe these to be adult specimens (see Discussion, below). Both neural spines are similar in size and shape to those of the presacral vertebrae immediately anterior to the sacrum. The condyle on the first sacral and the cotyle on the second are both somewhat mediolaterally expanded, making an ovoid rather than a round contact between the two elements (fig. 47). Both sacral ribs are anteroposteriorly expanded. As with many limbed squamates, the first sacral rib appears to be folded

over on itself distally so that the contact is increased and C-shaped in lateral view, with the open end facing posteriorly (fig. 47). The dorsal margin is posterodorsally inclined and the ventral margin is nearly horizontal. The first sacral rib is mediolaterally oriented and the second is slightly ventrolaterally inclined. Unlike the first sacral rib, the second is not folded distally, but instead is dorsoventrally narrow and thinner anteriorly. Distal contact between the two sacral ribs cannot be confirmed.

CAUDAL VERTEBRAE: IGM 3/905 preserves the first two caudals (fig. 48). Both are exposed primarily in ventral view, but are partly visible in left lateral view.

The neural spines and the zygapophyses of the caudals are similar in morphology

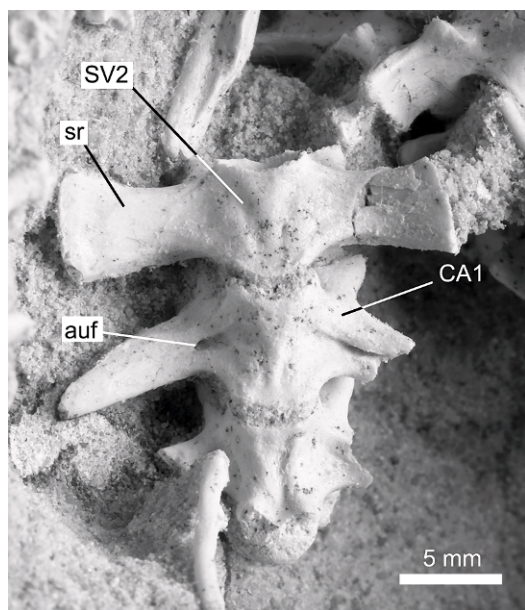


Fig. 48. Second sacral vertebra and the first two caudal vertebrae in *Gobiderma pulchrum* (IGM 3/905) in ventral view.

to those of the sacral vertebrae, with no indication of any of the aquatic adaptations visible even in the anterior most caudals of some aquatic taxa such as mosasaurs.

A chevron is preserved in association with the second caudal vertebra. That vertebra also preserves two small bulges and facets just anterior to the vertebral condyle that supported the chevron when articulated (fig. 48). The bulges are continuous with low, round, parasagittal ridges that extend from near the posteroventral margin of the centrum (anterior to the vertebral condyle) anteriorly. These low ridges define a narrow ventral sulcus. No chevron is preserved associated with the first caudal vertebra and that vertebra possesses no articular facets for a chevron. Thus, the first caudal vertebra was likely a pygal (but see the description of the anterior caudals in *Shinisaurus crocodilurus* by Conrad, 2006b). Rather than possessing the low parasagittal ridges and the concomitant medial sulcus, the first caudal possesses a very slight ventral bulge that is triangular, with a posterior point (fig. 48) this morphology is similar to that of the sacral and posterior dorsal vertebrae.

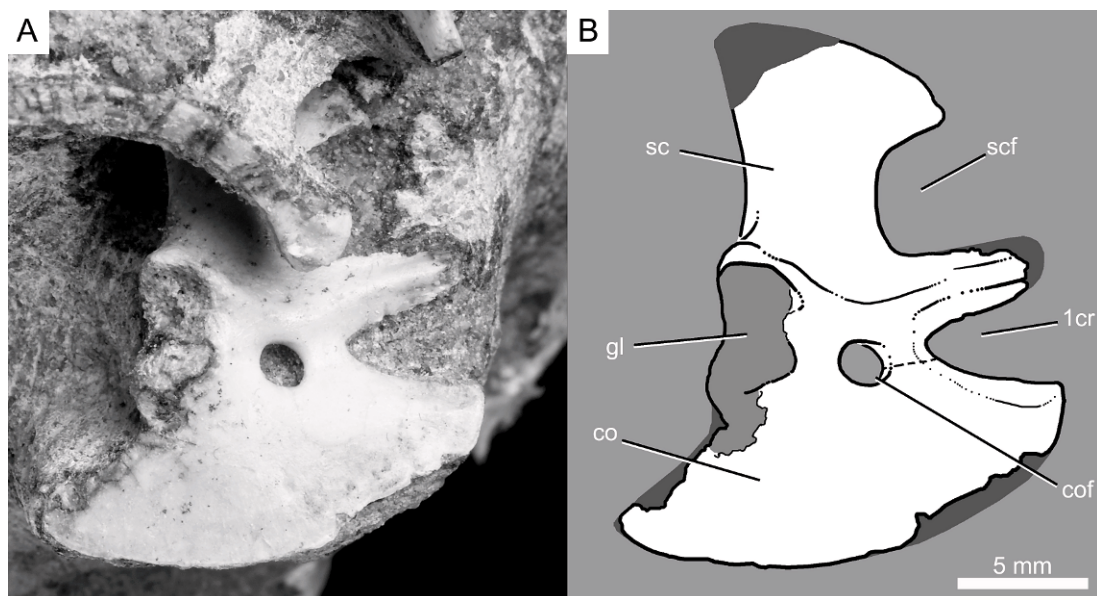


Fig. 49. A. Photograph and B. drawing of the right scapulocoracoid of *Gobiderma pulchrum* (IGM 3/905) in lateral view. Unknown/incomplete portions are represented by semiopaque, gray shadows in the drawing (B.).

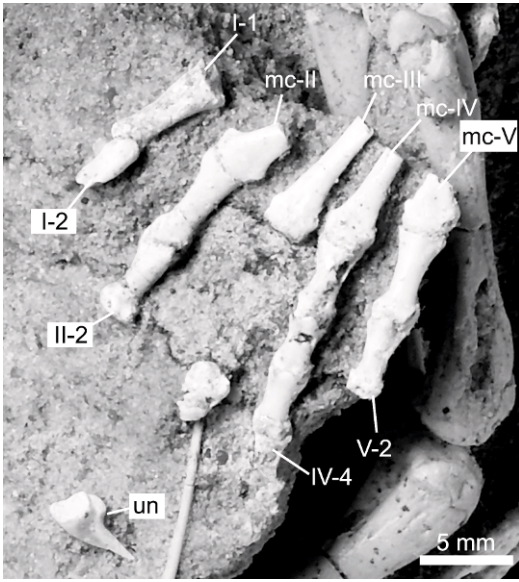


Fig. 50. Incomplete left manus of *Gobiderma pulchrum* (IGM 3/905) in dorsal view.

A complete transverse process is preserved on the right side of the first caudal vertebra and the bases of three additional transverse processes are present on the left side of the first caudal and the second caudal vertebra. Autotomy planes are absent from the first two caudal vertebrae, but often these are absent from the anteriormost vertebrae of squamates possessing autotomy planes within the tail. A so-called autotomy foramen (sensu Conrad, 2006b) is present on the base of each transverse process on the first caudal vertebra.

PECTORAL GIRDLE AND FORELIMB

The pectoral girdle and forelimb are incompletely known. Most of the right scapulocoracoid is preserved near the anterior end of the articulated presacral series (figs. 45, 49) in IGM 3/905. A partial left manus is preserved between sacral vertebra 2 and the trailing right hind limb (figs. 45, 50). The humerus, zeugopodium, and carpals are not preserved.



Fig. 51. Hind limbs of *Gobiderma pulchrum* (IGM 3/905). **A.** Left hind limb in posterior/posterodorsal view with femur remaining in articulation with the pelvis, but with slight postmortem movement of more distal elements. **B.** Right hind limb in posterodorsal view.

SCAPULOCORACOID: The ossified part of the left scapulocoracoid is complete, with very minor damage to the posteroventral rim of the humeral glenoid. It is laterally exposed, except for the posterodorsal (posterodistal) tip of the scapular blade (fig. 49). Although the epicoracoid, suprascapula, and other nonossified parts of the scapula and coracoid (see Shearman, 2005) typically are not preserved, the medially grooved surface remains intact.

The scapula and coracoid are fused into a single unit without a clear distinction between the two. However, a remnant of the suture between the coracoid proper and an element probably homologous with the procoracoid of more basal sarcopterygians (the precoracoid sensu Barrows and Smith, 1947; Costelli and Hecht, 1971; Rieppel, 1980b; Conrad, 2006b; see the recent discussion by Vickaryous and Hall, 2006) is present just anterior to the coracoid foramen (fig. 49B). The fused sutural remnant between the coracoid and procoracoid occurs in the same position in *Gobiderma pulchrum* as it does in juvenile/subadult *Shinisaurus crocodilurus*, extending from the coracoid foramen to the primary coracoid emargination. However, the delimitation between the coracoid and procoracoid is not evident posterior to the coracoid foramen. For simplicity, the coracoid-procoracoid component of the scapulocoracoid will herein be referred to as the *coracoid portion*.

The coracoid portion of the scapulocoracoid is an anteroposteriorly elongate plate. The medial margin of the coracoid is slightly eroded in some places, but the contact with the epicoracoid cartilage is still partly visible. The coracoid portion forms the medial, posterior, and lateral margins of the primary coracoid emargination, in contrast to the condition seen in modern *Heloderma* wherein there is no coracoid emargination.

Relative contributions to the glenoid from the coracoid portion and the scapula are unclear. The glenoid fossa is oriented posterolaterally as in most extant squamates. Both the dorsal and ventral buttresses are very robust. The dorsal buttress is narrowly contiguous with the procoracoid bar that separates the scapular emargination from the primary coracoid emargination.

The scapula is subtrapezoidal (fig. 49). Its posterior margin is straight and dorsoven-

trally oriented. The dorsal margin is dorsally convex, and extends anterior to a level anterior to the coracoid fenestra. Anteriorly, the scapular emargination is expressed as a posteriorly arching emargination with a smoothly rounded margin. The ventral end of the scapula is much narrower than the dorsal margin.

MANUS: Only the left manus of IGM 3/905 is preserved (figs. 45, 50). The carpals are not preserved. The distal parts of metacarpals II–V are preserved, including much of metacarpal III. Parts or impressions of nearly all the phalanges are preserved.

Five fully formed digits are present in *Gobiderma pulchrum*. Based on the preserved part of the hand, metacarpal III was the longest, II and IV are subequal in length, and I and V may be similar in length. The phalangeal formula is 2-3-4-5-?. Digit V possessed no fewer than three phalanges, but exactly how many were originally present cannot be determined with certainty. An ungual missing only its tip is preserved on digit I, and a complete ungual is preserved for digit III. It demonstrates that the unguals are relatively elongate, narrow, and sharp. The flexor tubercle is proximally placed and robust. The articular surface is broadly square in proximal view, but did not encircle the condyle of the penultimate phalanx to a high degree. The penultimate phalanges are not elongate with respect to the other phalanges and there is no dorsal sulcus as there are in some scansorial forms.

PELVIC GIRDLE AND HIND LIMB

The hind limb is known from nearly complete remains, including the elements of the pelvis, long bones, and pes (figs. 45, 47, 51). Bones from each half of the pelvic girdle remain in articulation with one another and with their respective hind limbs, but the two halves of the pelvic girdle are not preserved in articulation. The left pelvic girdle and hind limb are preserved such that the lateral margin is exposed dorsally, and the right pelvic girdle is preserved such that its ventral side faces mostly dorsally. Between the two sides of the specimen, all of the pelvic girdle and nearly all of the hind limb is known (see reconstruction in fig. 52).

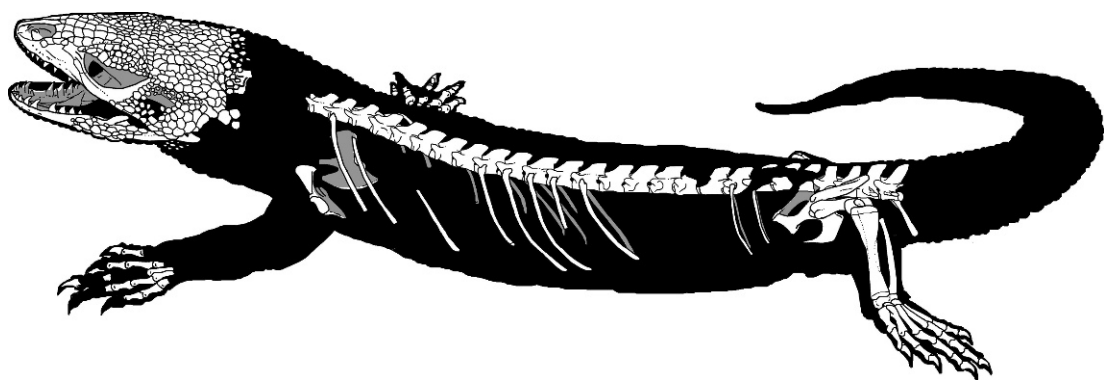


Fig. 52. Reconstructed skeleton of *Gobiderma pulchrum*. Skull and mandibles based primarily on ZPAL MgR III/64, IGM 3/55, and IGM 3/905. Postcranial skeleton based entirely upon IGM 3/905.

The bones of the pelvis are fused tightly together. The shape of the thyroid fenestra is unknown because the two halves of the pelvis have come out of articulation.

ILIUM: The elongate ilia are posterodorsally oriented and taper somewhat posteriorly and present squared posterodorsal tips (fig. 47). The head of the left femur is somewhat out of articulation, revealing the surface of the acetabulum. Both in the acetabulum and outside of it, the sutures between the pelvic bones have been obliterated by presumed intergrowth of the bones. The ilium contacts the sacral vertebrae, the femur, and the pubis and ischium.

A small anterior eminence is present on the ilium, near the anterodorsal margin of the acetabulum. This anterior eminence is not a distinctly offset process as it is in some squamates (e.g., lacertoids, varanines, most iguanians, and some gekkotans), but instead it is a gentle anterior swelling that likely provided the origin for the anterior head of the ilio-tibialis and, perhaps, some epaxial muscles based on comparisons of published data for other lepidosaurs (Romer, 1922, 1949, 1956). This anterior eminence is sub-ovate, being slightly longer dorsoventrally than mediolaterally. It tapers posterodorsally and is contiguous with the narrow, bladelike dorsal margin of the ilium. This bladelike dorsal margin tapers into the mediolaterally broad main shaft of the ilium near the level of the posterior one-fifth of the iliac blade.

The blade of the ilium is mediolaterally compressed anteriorly, but is subcylindrical

posteriorly. Ventrolateral to the main, subcylindrical, posterior, body of the ilium, the ilium possesses a narrow ventral keel (visible on both ilia in fig. 47). The medial view is unavailable so the extent of the sacral rib scars cannot be determined.

The acetabulum is subtriangular with rounded corners—a condition somewhat common among squamates (see Romer, 1942, 1956). A shallow and poorly defined fossa is present posterodorsal to the acetabulum proper and is mostly confluent with it. Based on comparisons with published descriptions (Romer, 1942), this fossa probably provided the origin for the ilio-femoral ligament. The edges of the acetabulum are slightly raised, although with only a gently convex rim like that of extant *Heloderma* and *Xenosaurus*.

PUBIS: Both pubes are preserved in articulation with the ilium and ischium (figs. 45, 47). The pubis is an elongate, posterodorsally oriented bone that is somewhat twisted along its long axis. Consequently, the pubis appears to be dorsoventrally flattened for most of its length and more mediolaterally flattened near the acetabulum and the obturator foramen. The pubis also describes a medial arc (see the right pubis in fig. 47: Rpu). Although the pubes are not preserved in articulation with one another, they preserve the medial articular facets, allowing reconstruction of their midline contact (fig. 52). The pubes also contact the other fused pelvic bones, but coossification of the pelvic bones makes it impossible to be sure of the shape of

these contacts. Depending on the contribution of the pubis and ischium to the acetabulum, those bones may also contact the femur.

Obliteration of the pelvic sutures prevents identifying the degree to which the pubis contributes to the acetabulum. However, the presumed proximal part of the pubis bears a strong posterolateral buttress of the acetabulum, most visible in dorsal or ventral view. From the level of this buttress, the pubis is constricted into a short neck at the level of the obturator foramen (fig. 47). The obturator foramen is somewhat elongate and slightly constricted at midlength. Distal to this level, the pubis is expanded again into the pubic tubercle. Ventrally, the pubic tubercle is contiguous with the ridge that flattens into the ventral margin of the pubis near the constriction of the obturator foramen. The anteromedial margin of the pubis is somewhat thickened, but the blade is relatively thin posterolateral to that margin.

ISCHIUM: Each ischium is subrectangular or hatchet shaped, with a narrow proximal, acetabular end and an expanded distal end (fig. 47). The anteroventral margin of the ischium, the surface contributing to the thyroid fenestra, arches anteriorly (figs. 47, 52). The anteromedial tip of the ischium forms a median, anterior point invading the thyroid fenestra posteriorly. From this anteromedial point, the elongate median contact of the ischium extends straight posteriorly before turning posterodorsally. The angle between the medioventral margin and the posterodorsally oriented part is relatively gently curved. However, the angle between the posterodorsally oriented margin and the posteroventrally oriented margin is sharper and more acute. A small ischial tubercle is present at this angle and is somewhat mediolaterally expanded. The posterodorsal margin is somewhat anteroventrally bowed, although not so much as the thyroid margin.

FEMUR: Both femora are completely preserved (figs. 45, 47, 51). The left femur is exposed in all views and articulated with the acetabulum and the tibia. The right femur remains in contact with the acetabulum, tibia, and fibula and is exposed in dorsal, anterior, and ventral views (figs. 45, 51A). The right femur remains articulated with the

hind limb zeugopodium, but not the pelvis (figs. 45, 51B).

The femur is elongate and robust, with a very slight curve. Its length is slightly less than the length of the five posteriormost presacral vertebrae (fig. 45), approximately 132% of the length of the tibia (fig. 51). The femur is most narrow just proximal to its midlength. The femoral head is distinctly offset and round. The internal trochanter is very large and robust (figs. 47, 51). It extends almost as far proximally as the femoral head and is more than one-half the breadth of the femoral head. An anteroposteriorly broad flange joins the head of the femur with the internal trochanter and forms a proximally concave margin. A shallow fossa is also present on the ventral surface of the femur between the internal trochanter and femoral head. The internal trochanter tapers into the main shaft of the femur near the proximal one-quarter of the femoral shaft. The ventral surface of the femur bears a narrow groove for more than one-third the length of its long axis.

Two distinct condyles are present on the distal end of the femur; the distal end of the femur expands to be more than half again the width of the femoral shaft at its narrowest diameter (fig. 51B). A narrow fibular articulation point is present on the lateral surface of the lateral condyle. The distal condyles extend for nearly 180° around the distal end of the femur. Posteriorly, these condyles form a narrow lip. The two distal condyles are only slightly separated by a shallow and broad sulcus.

Both femoral epiphyses are preserved in life position. Like the other preserved epiphyses, these remain clearly distinct even though they are strongly sutured to the diaphyses. The suture for the epiphysis of the femoral head runs around the limit of the articular surface of the femoral head posteriorly, ventrally, and for the visible part of the anterior surface. An expansion of the epiphysis is present extending to a point distal to the internal trochanter on the dorsal surface of the femur. A second element is present on the proximal tip of both internal trochanters (fig. 51B: ses). Although there appears to be no connection between this ossification and the epiphysis of the femoral head, this element may represent a remnant of the proximal

epiphysis. Otherwise, this element may be the mesial sesamoid, as evinced by comparisons with recent studies (Rewcastle, 1980; Maisano, 2002a, 2002b; Conrad, 2006b). The distal femoral epiphysis constitutes the articular surface and the major distal expansion of the femur. On its dorsal margin, the epiphysis has a slight proximal expansion around the level of the patella (fig. 51).

TIBIA: The tibia is robust and expanded proximally and distally (fig. 51). The tibia is approximately 76% of the length of the femur. It contacts the femur and the astragalocalcaneum.

The medial surface of the proximal end of the tibia is broad and flat (fig. 51B). There is no clear indication that the tibia and fibula contact proximally, and they were clearly separated distally based on the morphology of the astragalocalcaneum (fig. 51A). A shallow transverse articular surface receiving the femur is present on the proximal surface of the tibia. The cnemial crest is broad and rounded posterodorsally (fig. 51B). Although studies by Romer (1949) and Russell (1988) demonstrate that the tibialis anterior and peroneus muscles take their origin from the cnemial crest in squamates, there is no visible differentiation between the muscle origin scars in *Gobiderma pulchrum*. The cnemial crest extends along the dorsal one-third of the tibia.

The middle one-third of the tibial shaft is the narrowest part of the bone. Distal to this level, the posterior margin of the tibia possesses a short and dorsoventrally thin posterior process. This process extends for approximately one-quarter the length of the tibia and terminates just proximal to the distal tip, at the level of dorsolateral extent of the astragalar facet (visible in fig. 51A). Based on descriptions by Romer (1949), this crest probably provided insertion for the accessory head of the flexor digitorum longus. The distal articulation between the tibia and astragalus is gently arched, not distinctly notched as in many scleroglossans (Estes et al., 1988).

Both proximal and distal epiphyses are visible in the preserved tibiae. The proximal epiphysis includes a significant part of the dorsal tibia, contributing a portion whose proximodistal depth is nearly one-quarter its

dorsoventral length. The distal epiphysis constitutes only the articular surface.

FIBULA: Except for the proximal tip, the left fibula is complete (figs. 45, 51A). The right fibula is narrowly visible underlying the right tibia.

The preserved part of the fibula is extremely narrow proximally, but its distal end is more than three times as wide. The dorsal surface of the distal end is somewhat concave and the entire distal articular end is broader anteroposteriorly than it is deep dorsoventrally. The distal epiphysis remains in articulation with the astragalocalcaneum, separate from the distal end of the diaphysis of the fibula.

TARSALS: Three separate functional elements are present in the tarsus (figs. 45, 51A). The proximal tarsal, presumably, represents a coossification of the astragalus and calcaneum. This element, termed the *astragalocalcaneum*, is the largest element in the pes. There is no visible remnant of the suture between the astragalus and calcaneum in *Gobiderma pulchrum*.

A narrow, U-shaped, space invades the proximal surface of the astragalocalcaneum, helping to divide the astragalar and calcaneal parts. This vacuity separates the tibial and fibular facets. The medial, astragalar, part of the astragalocalcaneum possesses a narrow tibial buttress. Slight damage to the dorsal surface of the astragalus just distal to the tibial buttress precludes identification of the presence or absence of an astragalar foramen with certainty. The posterior margin of the calcaneal part is rounded with a slightly flattened proximal surface. This calcaneal flange extends posterior to the fibular facet for a length subequal to one-quarter the breadth of the fibular facet.

The distal margin of the astragalocalcaneum is sinuous, with the anterior (astragalar) margin extending further distally than the posterior (calcaneal) margin. The astragalar part of the astragalocalcaneum articulates with metacarpals I and II and with distal tarsal III. Astragalocalcaneal contacts with metatarsal I and distal tarsal 3 are subequal in size, and the contact with metacarpal II is about half that size. A facet for distal tarsal 4 is present on the calcaneal part of the astragalocalcaneum.

The mesial part of this facet extends farther anterodorsally than the posterior part.

Only distal tarsals 3 and 4 are present between the astragalocalcaneum and the metatarsals. Distal tarsals 3 and 4 are very similar in form to the same elements in *Shinisaurus crocodilurus* (see Conrad, 2006b). Distal tarsal 3 contacts the astragalocalcaneum, distal tarsal 4, metatarsal II, and metatarsal III. The exposed part of distal tarsal 3 is subtriangular with a nearly right posteroproximal angle. The long anterodistal surface of distal tarsal 3 forms an elongate contact with the proximal end of metatarsal II.

Distal tarsal 4 is approximately twice as large as distal tarsal 3. It contacts the astragalocalcaneum, distal carpal 3, and metacarpals III–V. Its proximal surface is narrowly grooved for its articulation with the astragalocalcaneum. Distal carpal 3 contacts the anterodistal surface of distal tarsal 4, metatarsal III contacts the distal surface, metatarsal IV contacts the posterodistal surface, and the hooked metatarsal V contacts the posterior surface.

Five complete digits are present (figs. 45, 51A). Metatarsal I is incomplete on the left side and is not preserved on the right side. The preserved portion suggests that this was the shortest metatarsal. Metatarsal III is the longest, metatarsals II and IV are subequal in length, and metatarsal V is only slightly shorter than II and IV (fig. 51A). However, because metatarsal V extends more proximally than the other metatarsals, its distal end does not approach the level of the distal end of metatarsals II–IV. Metatarsal V is robust. Ventrally, it bears a small lateral process and two relatively robust plantar tubercles. The lateral plantar tubercle is distally placed and approaches the distal condyle, a condition also seen in *Lanthanotus borneensis* (Rieppel, 1980b), shinisaurids (Conrad, 2006a, 2006b), some scincoids, some cordylids, and some diplodactylid geckos. By contrast, metatarsal V is dramatically shortened in *Heloderma*, rendering the relative positions of the medial and lateral plantar tubercles moot.

Through comparisons of the left and right pedes, the pedal digital formula can be reconstructed as 2-3-4-5-4 (figs. 45, 51A, 52). Each digit bears a dorsal sesamoid ossification

between the penultimate phalanges and the unguals. The pedal unguals are gently curved and sharp as in many other anguimorphs. As with the manual phalanges, the pes possesses relatively short penultimate phalanges.

JOINT SESAMOIDS: The dorsoventrally thin femoral patella is preserved in the right knee of IGM 3/905 (figs. 45, 51). It is subovoid in dorsal view; its proximodistal length is approximately 126% of its anterodorsal length. The femoral patella lies in a shallow, proximodistally oriented groove on the dorsal margin of the femur. A joint sesamoid distal to the femoral patella lies in the shallow femoral trochlea (fig. 51A). Based on its position, it is probably the mesial sesamoid (sensu Rewcastle, 1980). Other sesamoids may be present, but are hidden by the orientation of the preserved limb.

PHYLOGENETIC ANALYSES

RECENT PHYLOGENETIC STUDIES OF MONSTERSAURIA

Monstersauria is a name that was first applied to the *Heloderma* lineage by Norell and Gao (1997) who discovered the first complete skull of a *Heloderma* relative since *Gobiderma*. Subsequently, Gao and Norell (1998) presented a relatively comprehensive phylogenetic analysis of Anguimorpha with a topology for Monstersauria that would remain more or less stable across future analyses (fig. 53A).

Cifelli and Nydam (1995) and Nydam (2000) described significant fossil remains from North America that, importantly, push the minimum divergence time for Monstersauria back to the earliest Late Cretaceous. Although this early monstersaur, *Primaderma nessovi*, is relatively incomplete (fig. 9A), it has consistently resolved as a basal monstersaur in published analyses (Nydam, 2000; Conrad, 2008; Conrad et al., 2011) (figs. 53B, C, 54). The analysis of Nydam (2000), an expansion of the Gao and Norell (1998) analysis, offered somewhat more resolution and offered important new data regarding the evolutionary history of monstersaurs.

Conrad (2008) presented a morphological phylogenetic analysis of Squamata that

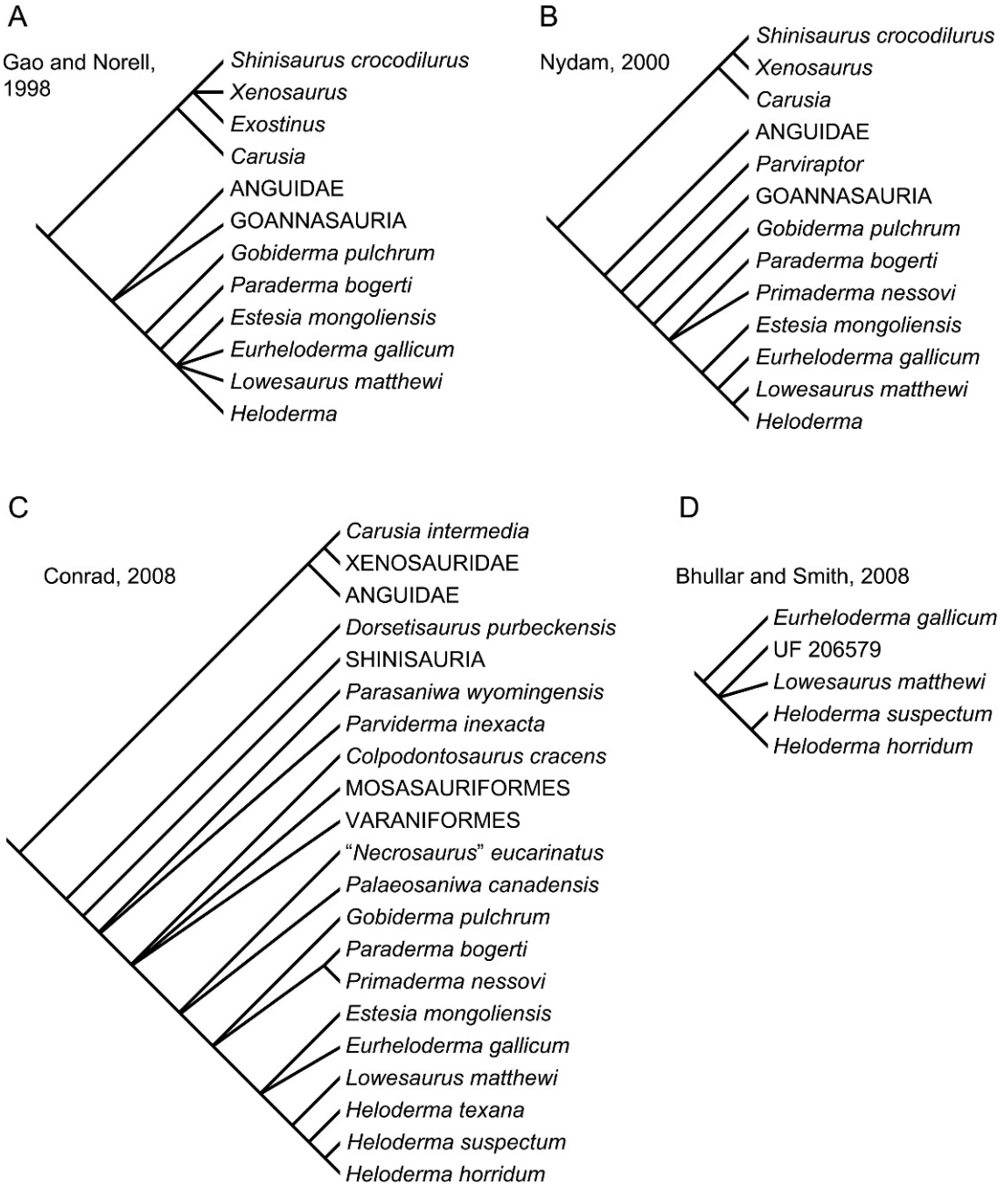


Fig. 53. Some recent morphology-based phylogenetic analyses that investigated monstersaurian interrelationships. Note that C represents only a subset of the 222 taxa included by Conrad (2008).

included a holophyletic Monstersauria, but with a slightly different topology and a somewhat more inclusive membership (fig. 53C). Conrad's analysis recovered a clade composed of *Paraderma bogerti* and

Primaderma nessovi, and found that this clade formed an unresolved trichotomy with *Gobiderma pulchrum* and higher monstersaurs (*Estesia mongoliensis*, *Eurheloderma gallicum*, *Heloderma*, and *Lowesaurus mat-*

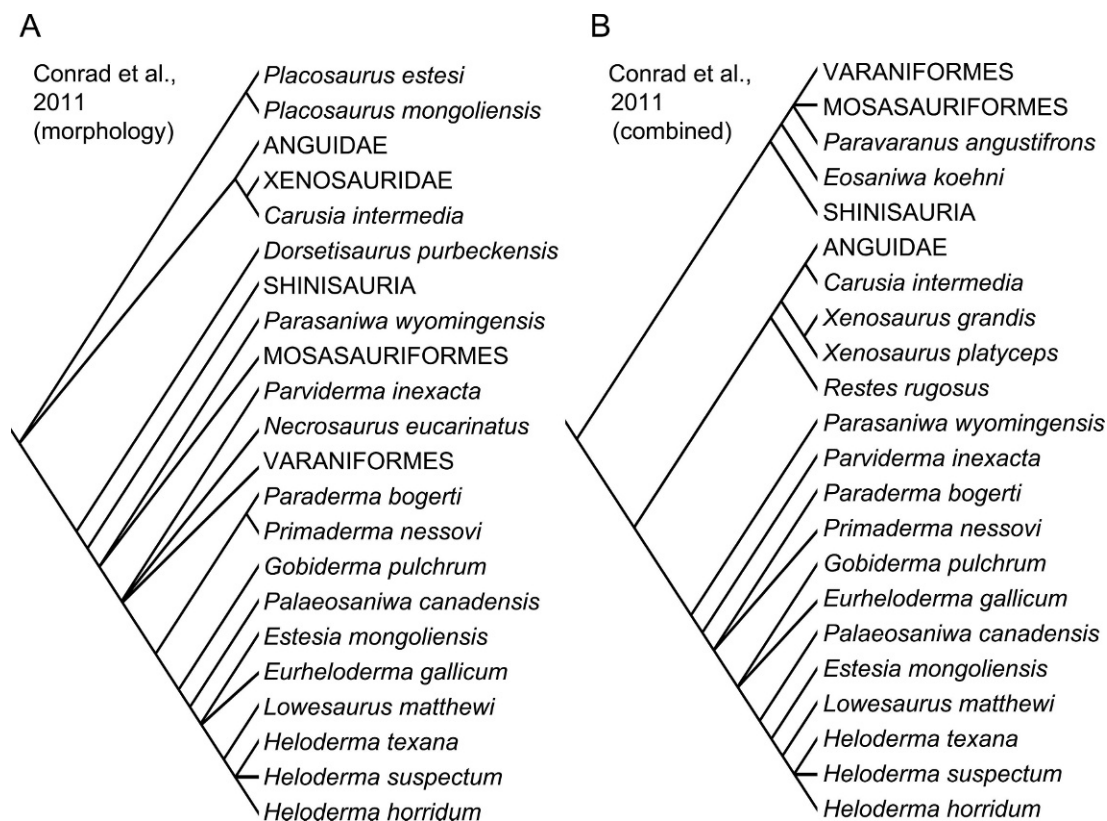


Fig. 54. A subset of the results from a recent publication investigating anguimorph interrelationships based on **A.** morphology and **B.** combined-evidence analyses (Conrad et al., 2011). Note that only species-level terminals were used in each analysis, but that some have been collapsed into their containing clades here for brevity, but highlighting monstersaurian species that were included.

thewi). Additionally, that analysis recovered “*Necrosaurus*” *eucarinatus* and *Palaeosaniwa canadensis* as basal monstersaurs in the Adams consensus (fig. 53C). *Palaeosaniwa canadensis* had also been recovered as a monstersaur in Balsai’s dissertation (Balsai, 2001).

Bhullar and Smith (2008) described a new fossil lizard known from a dentary with teeth from the Miocene of Florida. Their phylogenetic analysis included a subset of Helodermatidae (sensu Conrad, 2008) and found the specimen (UF 206579) to form an unresolved trichotomy with *Lowesaurus matthewi* and extant *Heloderma* (fig. 52D).

Recently, Conrad et al. (2011) performed a series of phylogenetic analyses of anguimorph interrelationships that included molecular, morphological (fig. 54A), and combined-evidence data matrices (fig. 54B). The morphological

analysis found the *Paraderma bogerti*–*Primaderma nessovi* clade to be basal amongst monstersaurs, with *Gobiderma pulchrum* and *Palaeosaniwa canadensis* forming successively more proximal outgroups to an unresolved trichotomy including *Estesia mongoliensis*, *Eurheloderma gallicum*, and higher helodermatids (*Lowesaurus matthewi* and *Heloderma*). The combined-evidence phylogenetic analysis recovered a slightly different topology wherein *Parasaniwa wyomingensis* and *Parviderma inexacta* are the basalmost monstersaurs; *Paraderma bogerti* and *Primaderma nessovi* form an unresolved trichotomy with higher monstersaurs, and *Gobiderma pulchrum* and *Eurheloderma gallicum* form an unresolved trichotomy with higher helodermatids. *Palaeosaniwa canadensis*, *Estesia mongoliensis*, and *Lowesaurus matthewi* were found to be successively more proximal out-

groups to an unresolved trichotomy of *Heloderma*.

PRESENT ANALYSIS

We modified the combined-evidence matrix of Conrad et al. (2011) for the present analysis. In its present form (appendix 2), the matrix includes all of the characters presented by Conrad et al. (2011), plus characters 3, 10, and 12 from Bhullar and Smith (2008). These characters, as included here, are thus formulated:

423. Dentary, posterodorsal bulge on lateral surface (Bhullar and Smith, 2008: char. 3): (0) absent, (1) present.

424. Dentary, medial face of the posterior end of the intramandibular septum (Bhullar and Smith, 2008: char. 10): (0) smooth; (1) eminence raised near the posteroventral corner; (2) eminence raised near the dorso-ventral midpoint.

425. Dentition, number of dentary teeth I (modified extensively from Bhullar and Smith, 2008: char. 12): (0) four; (1) five; (2) six; (3) seven; (4) eight; (5) nine; (6) 10; (7) 11; (8) 12; (9) 13.

426. Dentition, number of dentary teeth II (modified extensively from Bhullar and Smith, 2008: char. 12): (0) 14–16; (1) 16–18; (2) 18–20; (3) 20–22; (4) 22–24; (5) 24–26; (6) 26–28; (7) 28–30; (8) 30–32. This character uses an overlapping range of character states because perceived variation between specimens of species wherein more than a dozen teeth are commonly present.

For the purposes of the current analysis, we were unconcerned with the relationships within Mosasauridae and *Varanus*. Because each of these clades is consistently recovered as holophyletic, we included only limited sampling from within each. Additionally, we included the nonmosasaurid mosasauriforms and non-*Varanus* varaniforms included by Conrad et al. (2011). We excluded three anguoids from the Conrad et al. (2011) matrix because they were represented by a relative paucity of character data and because none have been considered potential members of Monstersauria. These taxa are: *Diploglossus bilobatus*, *Placosaurus estesi*, and *Placosaurus mongoliensis*. Thus, the current data matrix includes 98 taxa and 422 morphological characters, one biogeographic character,

and 5726 molecular characters. Note, however, that the biogeographic character was omitted for phylogeny reconstruction, just as it was in prior analyses of earlier versions of this matrix (Conrad, 2008; Conrad et al., 2011) and that character 236 and 242 have deactivated and replaced as described by Conrad et al. (2011). The morphology component of this analysis is presented in appendix 2. The molecular data are exactly those of Conrad et al. (2011) and available online as described in that paper.

We used NEXUS Data Editor (NDE) (Page, 2001) to assemble and manage the data matrix. Molecular base pairs were converted to Arabic numerals (1 = adenine, A; 2 = cortisol, C; 3 = guanine, G; 4 = tyrosine, T). We performed an analysis using the New Technology Search in the computer program T.N.T (Goloboff et al., 2003) (500 replicates) with “ratchet” and “drift” options employed. The shortest tree length recovered by the analysis had a length of 8888 steps, consistency index excluding uninformative characters of 0.3945, and a retention index of 0.5012. The analysis found 2214 trees of that length and none shorter.

A strict consensus of our analysis recovered very little resolution. Following some recent studies (Kearney and Clark, 2003; Norell et al., 2006; Turner et al., 2007a; Conrad, 2008; Conrad et al., 2011), we report the Adams consensus (figs. 55, 56) because it shows the relationships that are common to all trees and collapses volatile taxa to the level of their least inclusive node, following some other recent studies. The Adams consensus of our trees shows an unresolved basal tetrachotomy between a clade composed of *Eosaniwa koehni*, Mosasauriformes, and Varaniformes, a clade composed of Shinisauria, Anguioidea, and Monstersauria, and the labile terminals UF 206579 and *Necrosaurus eucarinatus*. Additionally, we also show the reduced strict consensus of the principal trees with those labile taxa pruned, with the same result as the Adams tree (figs. 55, 56). Placement of Shinisauria with monstersaurs and anguoids was unexpected because recent analyses have suggested them closer to varanids than to anguoids.

The topology recovered for Monstersauria in this is broadly similar to that of those

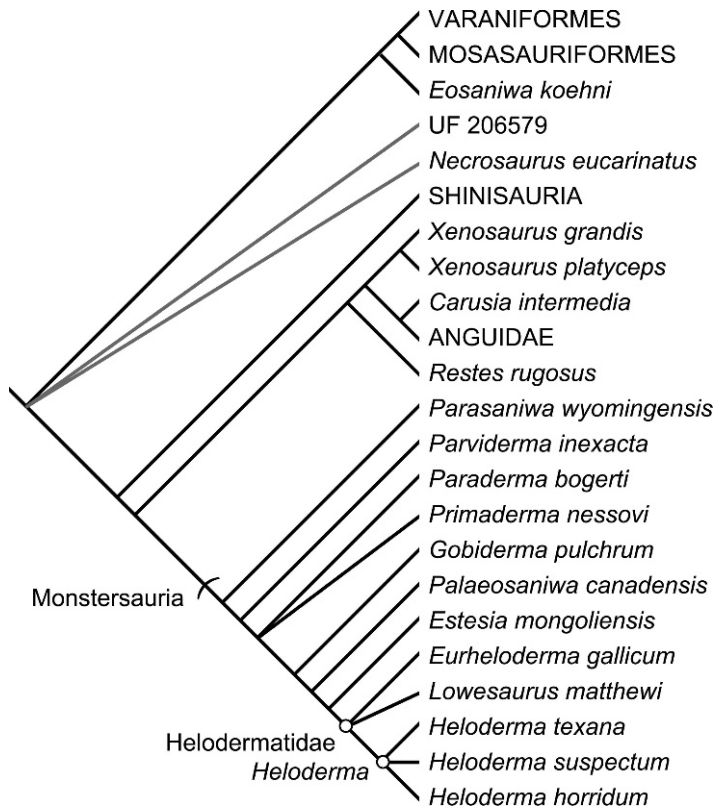


Fig. 55. Combined-evidence analysis as performed for the present study (2214 equally short trees recovered). Here we present both the Adams consensus and the reduced strict consensus. Note that the overall tree topology is the same in both cases and that only species-level terminals were used in each analysis, but that some have been collapsed into their containing clades here for brevity, but highlighting monstersaurian species that were included. Taxa pruned from the trees for the reduced strict consensus are joined to the tree by gray lines. Tree length for each principal tree = 8888 steps; consistency index excluding uninformative characters = 0.3945; retention index = 0.5012.

presented by Conrad et al. (2011), but with some important differences. Importantly, *Parasaniwa wyomingensis* and *Parviderma exacta* are the basalmost members of Monstersauria in this analysis. The relative positions of *Paraderma bogerti* and *Primaderma nessovi* were left unresolved with regard to one another and to more nested monstersaurs. *Gobiderma pulchrum* was recovered as the outgroup to *Palaeosaniwa canadensis*, *Estesia mongoliensis*, and Helodermatidae (sensu Conrad, 2008; and Conrad et al., 2011: *Eurheloderma gallicum*, *Heloderma horridum*, *Lowesaurus matthewi*, and all descendants of their last common ancestor). Monstersauria is supported by three unambiguous synapomorphies:

1. Presence of plicidentine (char. 218, state 1).
 2. Premaxillary teeth markedly smaller than the anterior maxillary teeth (char. 223, state 1).
 3. Presence of grooves separating the osteoderms on the maxilla (char. 309, state 1—this is reversed in *Gobiderma pulchrum*).
- Parviderma inexacta* is united with other monstersaurs to the exclusion of *Parasaniwa wyomingensis* based on three unambiguous synapomorphies:
1. Widely spaced marginal tooth bases (char. 211, state 1; see Conrad, 2008: 60).
 2. Marginal teeth with “modified pleurodont” tooth implantation (char. 214, state 2; Zaher and Rieppel, 1999; Rieppel and Zaher, 2000; Conrad, 2008).

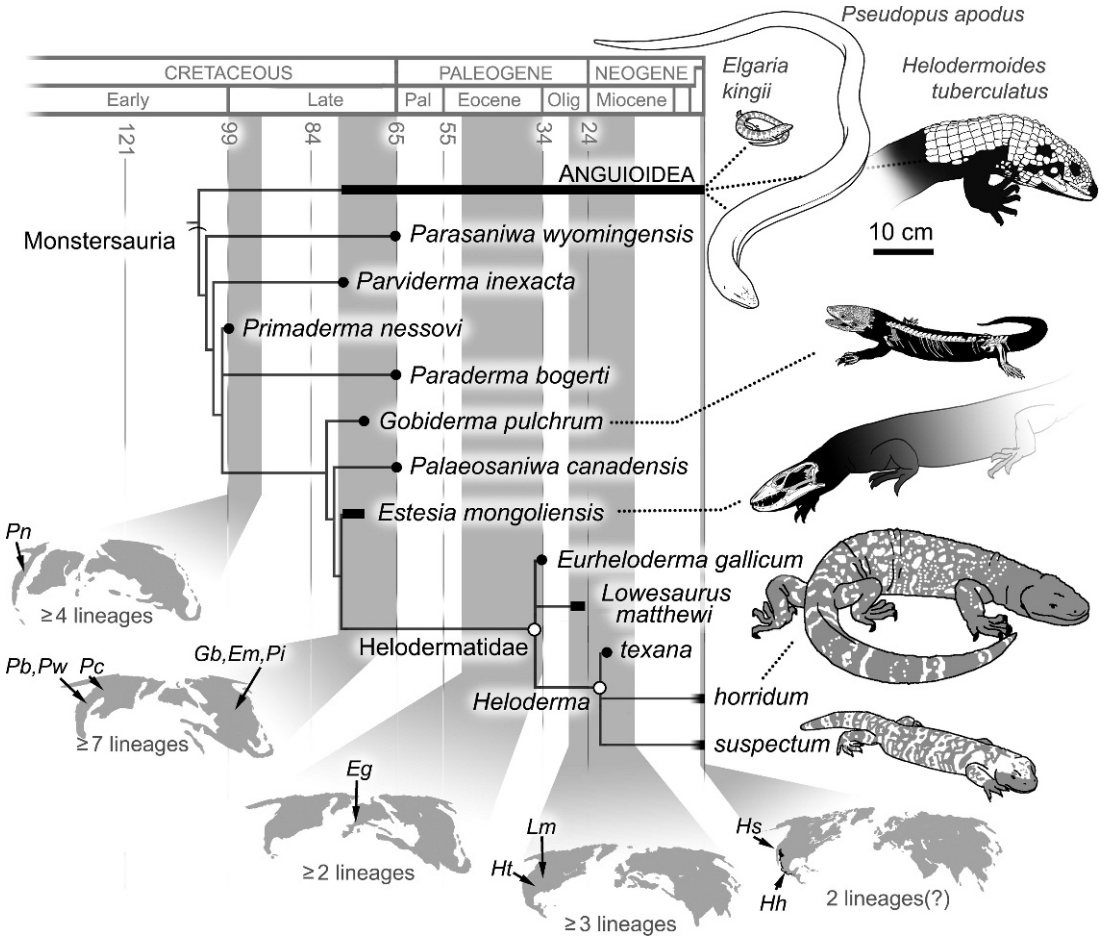


Fig. 56. Monstersauria interrelationships as presented in figure 55 presented as a temporally calibrated cladogram including biogeographic data and scaled thumbnail images of some of the relevant taxa. Gray vertical bars indicate time spans covered by the associated paleomaps. Note that the map for *Primaderma nessovi* represents a 94 Ma reconstruction; that for the remaining Cretaceous monstersauria (e.g., *Gobiderma pulchrum*) represents a 66 Ma reconstruction; the Eocene map is a 50.2 Ma reconstruction; the Oligocene-Miocene map is a 14 Ma reconstruction, and the Holocene map represents the presented continents in their current distribution. Maps based on Scotese (1991, 2003) and Scotese et al. (1988).

3. Presence of dorsoventrally thickened osteoderms expressed as polygonal mounds (char. 310, state 2).

The unresolved trichotomy composed of *Paraderma bogerti*, *Primaderma nessovi*, and higher monstersauria is supported by three unambiguous synapomorphies:

1. Presence of a blunt, rounded snout (char. 3, state 1—reversed in *Gobiderma pulchrum*).
2. Ventral origin of the jaw adductor muscles from the parietal (char. 86, state 1).
3. Presence of replacement teeth that form posterolaterally to the active tooth position and without a resorption pit (char. 221, state 2).

Gobiderma pulchrum, *Palaeosaniwa canadensis*, *Estesia mongoliensis*, and *Helodermatidae* are united to the exclusion of other anguimorphs based on three unambiguous synapomorphies:

1. Presence of snout elongation anteriorly such that a rostrum is present anterior to the level of the anterior margin of the septomaxilla (char. 2, state 1; Conrad, 2008; Conrad et al., 2011).
2. Dentary excluded from the margin of the anterior inferior alveolar foramen (char. 183, state 1).
3. Presence of zygosphenes with dorsolaterally oriented articular facets (char. 235, state 1).

Monstersaurs more closely related to Helodermatidae than to *Gobiderma pulchrum* form a clade as evinced by the presence of five unambiguous synapomorphies:

1. Frontals with a trapezoidal outline in dorsal view (char. 57, state 1).
2. Absence of a pineal foramen (char. 77, state 3).
3. Absence of a transverse, midline, posterior margin to the parietal table (char. 82, state 1; Conrad, 2008).
4. Chevrons that attach anterior to the postero-ventral margin of the centrum (char. 254, state 1).
5. Strongly sutured (rather than coossified or nonsutural) pelvic girdle elements (char. 284, state 1).

The principal trees of this analysis find various placements for UF 206579. It is variably recovered as the outgroup to *Heloderma*, as the sister group to *Heloderma texana*, as the sister group to *Estesia mongoliensis*, as part of a *Necrosaurus* clade (also including “*Saniwa*” *feisti*, *Necrosaurus cayluxi*, and, in some cases, “*Necrosaurus*” *eucarinatus*) within Varaniformes, as the sister group of *Saniwides mongoliensis* within Varaniformes, as a proximal varanid outgroup, or as the sister group to *Telmasaurus grangeri*. The tree topologies recovering UF 206579 as a varaniform require that grooved dentary teeth arose independently within Varaniformes and Monstersauria.

DISCUSSION

PHYLOGENETIC IMPLICATIONS

ANGUIMORPH INTERRELATIONSHIPS: A recent, combined-evidence, phylogenetic analysis of Anguimorpha revealed conflicting hypotheses of anguimorph interrelationships when results are compared between analyses of various data content and taxonomic sampling (Conrad et al., 2011). Importantly, monstersaurs were found to be closely related to goannasaurs (monitor lizards, mosasaurs, and other fossil relatives) in morphological phylogenetic analyses. In molecular-based phylogenetic analyses and in their combined, global, phylogenetic analysis of anguimorphs, Conrad et al. (2011) found monstersaurs to be the basal radiation of a clade also containing *Carusia intermedia*, *Restes rugosus*, *Xenosaurus*, and anguids. However, when they

deleted fossil taxa from their combined morphological/molecular data set, Conrad et al. (2011) found morphological and molecular data supporting a close relationship between monstersaurs and goannasaurs to the exclusion of other squamates.

Our phylogenetic analysis (figs. 55, 56) is in agreement with the results of the combined-evidence analysis presented by Conrad et al. (2011) in monstersaur membership and in suggesting that monstersaurs are closely related to anguoids. However, the present analysis differs in suggesting that shinisaurs also belong on that branch rather than with goannasaurs.

Fossils from Florida and Tennessee: Although the fossil dentary UF 206579 originally was suggested as a proximal outgroup to *Heloderma* and it possesses grooved teeth incipient to the *Heloderma* condition (Bhullar and Smith, 2008), still it is not recovered as an unambiguous helodermatid or even monstersaur in the current analysis (fig. 55). Indeed, it is one of the more labile taxa in the tree, along with “*Necrosaurus*” *eucarinatus*. Importantly, both of these taxa are known from very incomplete remains and this may contribute to the ambiguity regarding their phylogenetic placements in the current analysis.

The taxonomic sampling of the analysis provided by Bhullar and Smith (2008) constrained UF 206579 to be a nested helodermatid (sensu Conrad, 2008; Conrad et al., 2011). Certainly the presence of grooved dentary teeth, as well as some of the other characters described by Bhullar and Smith (2008) (and gestalt) would suggest that this is the proper placement of that taxon. However, the currently described remains simply cannot resolve the placement of UF 206579 with certainty (see above).

Similarly, fossil osteoderms recently described from Tennessee probably pertain to an unnamed helodermatid, but the remains are too incomplete to say much more than that (Mead et al., in press).

Estesia mongoliensis: Recently, Yi and Norell (2010) found *Estesia mongoliensis* to be a basal varaniform and reported on an analysis of 28 taxa coded for 389 characters that failed to recover a holophyletic Monstersauria. Instead, monstersaur monophyly was reportedly rejected, although the only support for this is a “polytomy between

three species of *Heloderma* (Miocene–Recent, North America), *Lowesaurus* (Oligocene–Miocene, North America), and *Eurheloderma* (Eocene/Oligocene of Europe), and varaniforms” (Yi and Norell, 2010: 191A) rather than a topology actually rejecting monstersaur holophyly. Indeed, given the results of the current analysis (figs. 55, 56) and recent, extensive combined-evidence analyses supporting monstersaur holophyly (Conrad et al., 2011; fig. 55), we feel that the result of Yi and Norell (2010) may have been caused by limited taxonomic sampling.

MONSTERAUR TOPOLOGY: The two extant monstersaur species are morphologically derived with numerous morphological specializations; they are transformed well beyond what might be considered plesiomorphic for either Anguioidea or Platynota (see data in Pregill et al., 1986; Nydam, 2000; Conrad, 2008; and Conrad et al., 2011). Monstersauria was distinct by the beginning of the Late Cretaceous as evinced by recovery of *Primaderma nessovi* as a basal monstersaur (Nydam, 2000; Conrad, 2008; Conrad et al., 2011) and we interpret the similarities between *Heloderma* and *Lanthanotus borneensis* as convergences rather than shared derivation, as has been suggested by some analyses (e.g., Caldwell, 1999).

Results from the present analysis and those from the comparative analyses of Conrad et al. (2011) further highlight the importance of *Gobiderma pulchrum*. *Gobiderma pulchrum* is a basal monstersaur, falling outside a clade that includes the Cenozoic helodermatids and the Cretaceous taxon *Estesia mongoliensis* (Norell and Gao, 1997; Gao and Norell, 1998; Conrad, 2008). As such, *Gobiderma pulchrum* is an important transitional form between helodermatids and the basal non-helodermatid members of Monstersauria. Indeed, given the paucity of relatively completely known basal monstersaurs, the data represented by the new *Gobiderma pulchrum* specimens are invaluable.

MATURITY OF DESCRIBED SPECIMENS

The known *Gobiderma pulchrum* specimens are similar in overall size. The holotype skull has a craniobasal length of approximately 52 mm as preserved, that of IGM 3/55 is approximately 61 mm, and that of the

partially disarticulated IGM 3/905 skull (lacking the snout tip) may be reconstructed as being between 56 and 60 mm long. The sacrum is disarticulated in the only specimen with preserved sacral vertebrae (IGM 3/905) (figs. 45, 47, 48). This suggests the possibility that this relatively large specimen is a juvenile. However, the pelvis is completely fused in IGM 3/905. Moreover, the holotype represents a relatively small individual, but in that specimen (and all other available specimens), the braincase elements show some obliteration of the sutures and the supratemporal arch remains in nearly complete natural articulation. This suggests to us these are adult or late subadult specimens. Vertebrae preserved with IGM 3/59 (fig. 22) and IGM 3/905 (figs. 45, 46) possess fused neural arches (indicating closure of the vertebral growth zones), further bolstering the hypothesis that these are adult individuals.

BASAL MONSTERSAURIAN MORPHOLOGY

Extant *Heloderma* have long been acknowledged for their morphological distinctiveness, including specializations associated with the presence of a specialized venom-delivery system (see, for example, Wiegmann, 1829; McDowell and Bogert, 1954; Rieppel, 1980a; and Pregill et al., 1986). They are the only extant lizards with an advanced venom-delivery system. Absence of a complete supratemporal arch and expansion of the jaw adductor musculature has led to comparisons with the enigmatic and derived varanid *Lanthanotus borneensis* (e.g., McDowell and Bogert, 1954), but this taxon has been demonstrated to be closer to *Varanus* than to *Heloderma* by numerous recent analyses (Estes et al., 1988; Norell et al., 1992; Wu et al., 1996; Norell and Gao, 1997; Evans and Barbadillo, 1998; Gao and Norell, 1998; Lee, 1998; Caldwell, 1999; Evans and Barbadillo, 1999; Lee, 2000; Lee and Caldwell, 2000; Evans et al., 2005; Conrad, 2008; Norell et al., 2008; Conrad et al., 2011). Lesser-acknowledged peculiarities of the *Heloderma* skeleton include the absence of coracoid and scapular fenestrations and the relatively short pes.

Gobiderma pulchrum differs from *Heloderma* in having a tapering snout (compare

figs. 3B, C, 4B, C, 5C, D, 7B, with 8B), a complete supratemporal arch (figs. 3C, 5C, 7A, B versus 8A, B), large patches of pterygoid teeth (figs. 4C, 5D, 7C, 17B, 43B, C versus 8C), a lack of grooved dentary teeth, and possession of an anterior coracoid fenestra and a relatively elongate pes. *Estesia mongoliensis* (fig. 9B) represents a fine morphological intermediate between *Gobiderma pulchrum* and *Heloderma*. *Estesia mongoliensis* retains the plesiomorphic features of a complete supratemporal arch and pterygoid tooth patches, but is similar to *Heloderma* in the shape of its skull and in the possession of grooved dentary teeth. Broader comparisons with nonmonstersaur anguimorphs, including the Cretaceous varaniform *Telmasaurus grangeri*, demonstrate that *Gobiderma pulchrum* exhibits the plesiomorphic condition with respect to *Heloderma* in all these characteristics.

Comparisons of *Gobiderma pulchrum* with extant *Heloderma*, shinisaurs, fossil varaniforms, and mosasaurs (such as *Telmasaurus grangeri* and *Adriosaurus suessi*), and with anguroids (including *Xenosaurus*, *Peltosaurus granulosus*, and *Gerrhonotus*), as well as the phylogenetic analysis suggest that basal monstersaurian apomorphies occurred in the skull while the postcranium remained relatively plesiomorphic. The monstersaurian apomorphies present in *Gobiderma pulchrum* (e.g., presence of a palatine flange of the maxilla and a pterygoid lappet of the quadrate) occur in the skull and lower jaw. The presence of an anterior coracoid emargination and absence of pedal foreshortening in *Gobiderma pulchrum* are plesiomorphic features.

One of the most conspicuous characteristics of modern *Heloderma* (as compared to other extant squamates) is its encrustation of mounded osteoderms, a condition distinct from all other extant squamates. Similar osteoderms are present in and often fuse to the skull bones of *Gobiderma pulchrum* as described above. However, the distribution of this characteristic indicates that it is not a monstersaur apomorphy, but that it characterizes a more inclusive node (see discussions in McDowell and Bogert, 1954; Sullivan, 1979; Conrad, 2008; and Conrad et al., 2011).

A REVISED DIAGNOSIS OF *GOBIDERMA PULCHRUM*

Borsuk-Białynicka (1984) offered separate generic and specific diagnoses for *Gobiderma pulchrum*. Her generic diagnosis (Borsuk-Białynicka, 1984: 39) reads as follows:

Medium-sized platynotan lizards about 5 cm of skull length. Sharp dentition with basal fluting. Lower teeth bigger than upper ones. External nares slightly retracted but not separating maxilla and nasal. Nasals paired. Subolfactory processes developed but weak. Postorbital joined to postfrontal from ventrolateral entering into the orbit. Parietal extended both laterally and posteriorly. Adductor musculature originating ventral on the parietal. Large alar process extending anteriorly. Small-plate osteodermal skull covering very strong, variable in ontogenesis with a tendency to eventually fuse into continuous although superficially sculptured layer. Rounded, perforated osteoderms of *Heloderma* type completely covering cheek region, supratemporal fossa and dorsal surfa of the orbit.

The specific diagnosis offered by Borsuk-Białynicka (1984: 41) is:

Skull subpentagonal in outline, its larger part posterior. Frontal paired but sometimes fusing with individual age. Posterolateral extensions of parietal close an angle of about 130°. An angle between paroccipital processes is only slightly less than this. Number of tooth positions is 11 on maxilla, 4 on premaxilla, 10 on dentary. Osteodermal skull covering of small-plate type or variable (anterior to the orbit).

Although many of the individual characteristics listed by Borsuk-Białynicka are shared by other taxa, the combination of character states described above diagnose *Gobiderma pulchrum*. Here, we emend this diagnosis by adding the following character states to the list: premaxillary nasal process is narrowest mediolaterally (figs. 3B, 4B, 5C, 6B, 7B), contrasting the condition in *Heloderma* and *Estesia mongoliensis* and most other non-*Varanus* anguimorphs); postfrontal and postorbital remain distinct (are unfused; figs. 6B, 7B, 19, 25), contrasting the condition in *Estesia mongoliensis*; *Heloderma* lacks a postorbital; postorbital extends posteriorly for almost the entire length of the supratemporal fenestra and approaches the

supratemporal (figs. 3B, 7B, 25A, 26; the only other monstersaur with a known post-orbital, *Estesia mongoliensis*, has a relatively much shorter postorbital); posterior opening of the Vidian canal enclosed by the parabasisphenoid (figs. 28C, 36A, B; *Heloderma* and *Estesia mongoliensis* possess a posterior opening of the Vidian canal occurring at the parabasisphenoid-proötic suture); presence of an anterior coracoid emargination (fig. 49; absent in *Heloderma* and unknown in other monstersaurs); obliteration of the pelvic sutures through bone intergrowth (the sutures remain visible and distinct in *Heloderma* and *Palaeosaniwa canadensis* [Balsai, 2001]); and distal placement of lateral plantar tubercle on metatarsal V (*Heloderma* possesses medial and lateral plantar tubercles on metatarsal V that possess an overlapping level; among anguimorphs, *Lanthanotus* and shinisaurs possess the condition seen in *Gobiderma pulchrum*).

A DIVERSITY OF CARNIVOROUS CRETACEOUS GOBI LIZARDS

Cretaceous Gobi lizard diversity has been reviewed by several authors over the last three decades revealing a vast systematic and morphological array (Borsuk-Białynicka, 1983, 1984, 1985, 1988, 1990, 1996; Borsuk-Białynicka and Moody, 1984; Borsuk-Białynicka and Alifanov, 1991; Norell et al., 1992; Alifanov, 1993, 1996, 2000; Gao and Hou, 1996; Norell and Gao, 1997; Gao and Norell, 2000; Conrad and Norell, 2006b, 2007; Norell et al., 2008). Indeed, the Cretaceous Gobi, particularly Djadokhta and similar deposits, is represented by a great number of species, including the three major dinosaurian clades (Ornithischia, Sauropodomorpha, and Theropoda; see, e.g., Makovicky and Norell, 2006; Ksepka and Norell, 2006, 2010; Turner et al., 2007a, 2007b; Miles and Miles, 2009) as well as a diversity of mammals (see, e.g., Rougier et al., 2001; Wible et al., 2001; Wible et al., 2004), among other taxa (see Loope et al., 1998; Gao and Norell, 2000). Together, these fossils indicate the presence of thriving ecological communities with a broad taxonomic diversity despite xeric conditions.

Importantly, the Djadokhta Formation includes a variety of lizards that, given their similarities with extant forms and based on their dental morphology, are presumed to be capable of taking vertebrate prey. These include the relatively diminutive gobiguanians (Conrad and Norell, 2007) as well as several anguimorphs such as some goannasaurs (Gilmore, 1943; Borsuk-Białynicka, 1984; Gao and Norell, 2000; Conrad, 2008; Norell et al., 2008), *Gobiderma pulchrum* (Borsuk-Białynicka, 1984; Gao and Norell, 2000), and *Estesia mongoliensis* (Norell et al., 1992; Norell and Gao, 1997). Relatively small anguimorph taxa such as *Aiolosaurus oriens* and *Ovoogurvel* might also have been capable of taking vertebrate prey; these taxa are larger than the tiny, extant monitors *Varanus brevicauda* and *Varanus eremius*, which are known to consume other lizards (Pianka and Vitt, 2003). *Shinisaurus crocodilurus* is known to take larval amphibians and fishes in addition to invertebrate prey (Ahl, 1930; Shen and Li, 1982; Sprackland, 1989).

Gobiguania is a clade composed of six species (*Anchaurosaurus gilmorei*, *Ctenomastax parva*, *Saichangurvel davidsonae*, *Temujinia ellisoni*, and *Zapsosaurus sceliphros*) of relatively small-bodied lizards. Because of their convergent similarities to modern crotaphytids (e.g., dentition, habitat choice, general proportions; Gao and Hou, 1995; Gao and Norell, 2000; Conrad and Norell, 2007), it is speculated they were capable of taking vertebrate prey (including mammals, in addition to other lizards), as are modern crotaphytids (McAllister and Trauth, 1982; Pianka and Vitt, 2003).

Telmasaurus grangeri is the largest varaniform known from diagnostic remains in the Djadokhta localities, with a femur length of approximately 48.5 mm (AMNH FR 6643) and a total parietal length of approximately 23.5 mm (AMNH FR 6645) (suggesting a skull length of perhaps 55–70 mm based on general comparisons with complete anguimorph skulls, especially varaniforms). This is slightly larger than the smaller of the two known Djadokhta monstersaurs, *Gobiderma pulchrum*. *Gobiderma pulchrum* (IGM 3/905) has a femur length of 38.3 mm and a skull length of approximately 60 mm (see above).

Estesia mongoliensis possesses a skull length of approximately 122.5 mm.

The lizard fauna of the Djadokhta is unusually rich, and the presence of several large-bodied forms is especially striking. However, a similarly xeric environment to the Cretaceous Gobi is present in the desert of modern Australia where there are at least six cooccurring species of *Varanus* (Farlow and Pianka, 2000; Pianka and Vitt, 2003). Even the smallest of these species, (*Varanus brevicauda*; the smallest known varanid) is known to take relatively large prey items, including other lizards (Pianka and Vitt, 2003). Additionally, the two extant species of *Heloderma* share a narrow distributional overlap in northwestern Mexico. Perhaps something similar occurred in the Late Cretaceous of the Gobi, with the various types of lizards preying upon one another with theropod dinosaurs representing the apex predators.

Two features considered to be characteristic of modern *Heloderma* (grooved teeth associated with venom delivery and mounded osteoderms) uniformly cooccur in all known Helodermatidae, but have a dissociated distribution within the Djadokhta monstersaurs. *Estesia mongoliensis* possesses grooved teeth and apparently lacks osteodermal encrustation. By contrast, *Gobiderma pulchrum* possesses domed osteoderms, but lacks grooved teeth. Domed osteoderms may be plesiomorphic for a clade that is more inclusive than Monstersauria (Conrad, 2008; Conrad et al., 2011); thus, their presence in *Gobiderma pulchrum* and many helodermatids may be a retention of a plesiomorphic character state rather than a monstersaur innovation. *Estesia mongoliensis* is the earliest monstersaur known to have grooved dentary teeth. The plesiomorphic condition for the *Estesia mongoliensis*–*Helodermatidae* clade is to possess osteoderms and grooved teeth, with the loss of osteoderms a derived state in *Estesia mongoliensis*.

The selective pressures that would have led to the loss of osteoderms in *Estesia mongoliensis* are unknown. Given the hypothesis that *Estesia mongoliensis* was a predator of reptile nests (Norell et al., 1992) like modern *Heloderma* and many *Varanus* (Bogert and Del Campo, 1956; Pianka and Vitt, 2003), one might expect osteoderms to be important defensive structures (although no *Varanus*

possesses monstersaur-style dermal armor). Development of a venom-delivery system might have been a defensive innovation rendering passive defensive structures less critical; that is, in this case, the best defense may have been a good offense. Despite the presence of much larger reptiles with impressive offensive weaponry (e.g., dromaeosaurid theropods with enlarged pedal unguals and serrated teeth), it may be that *Estesia mongoliensis* had no serious predators. Lacking the ability to threaten animals with an advanced venom-delivery system, coeval *Gobiderma pulchrum* relied on plesiomorphic defensive structures and strategies. Additional data might shed light on this evolutionary story; certainly, the currently available evidence appears inadequate to provide a definitive understanding of the ecological complexities in this ecosystem.

CONCLUSIONS

Fossil material from the Gobi Desert continues to offer new information about the origin and evolution of various squamate groups as well as increasing their known diversity (Gao and Norell, 2000; Conrad and Norell, 2006a, 2006b; Norell et al., 2008). The basal monstersaur *Gobiderma pulchrum* is pivotal for understanding the early evolution of monstersaurs and the derived extant squamate group *Heloderma*. The new material described above and reexamination of the fossils originally described by Borsuk-Białynicka (1984) allow rediagnosis of *Gobiderma pulchrum* and a more complete reconstruction of the animal as a whole (fig. 56). Among Cretaceous varaniforms and monstersaurs, only *Gobiderma pulchrum*, *Palaeosaniwa canadensis*, and *Telmasaurus grangeri* are known from relatively complete skulls and associated postcrania. The postcranial remains of *Palaeosaniwa canadensis* are, apparently, less complete than those of *Gobiderma pulchrum* and still await formal description (but see Balsai, 2001), making the documentation of the *Gobiderma pulchrum* postcranium all the more influential for understanding character polarities within Anguimorpha.

Gobiderma pulchrum and *Palaeosaniwa canadensis* are the most proximal helodermatid outgroups (figs. 55, 56) and lack grooved

dentition. That *Gobiderma pulchrum* co-occurred with a larger and more helodermatid-like monstersaur is significant because it offers an opportunity to further investigate the Djadokhta fauna. As with modern communities wherein lizards are a conspicuous part of the fauna, it is likely that some prey partitioning existed. *Gobiderma pulchrum*, the relatively smaller monstersaur, may have been taking small prey items while the broad-snouted, larger-bodied, and perhaps venomous *Estesia mongoliensis* might have had a broader range of potential prey items.

In conclusion, *Gobiderma pulchrum* represents an important transitional form linking basal monstersaurs with the more derived Helodermatidae and its proximal outgroups. Further discovery of *Gobiderma pulchrum* and other Gobi lizards may offer greater understanding of their diversity, the Djadokhta communities, and offer opportunities to the understand mosaic evolution.

ACKNOWLEDGMENTS

For collecting the specimens, we thank members of the AMNH–Mongolian expeditions to the Gobi Desert. For specimen preparation, we thank A. Davidson. Digital scans of IGM 3/55 were performed at the University of Texas, Austin, HRXCT laboratory with the aid of J. Maisano and M. Colbert. We thank H. Voris and A. Resetar (FMNH, Herpetology), W. Simpson (FMNH, Geology), J. Rosado (MCZ, Herpetology), M. Carrano and M. Brett-Surman (NMNH, Paleobiology), P.M. Barrett (NHM, Palaeontology), C.M. Mehling (AMNH, Paleontology), M. Borsuk-Białynicka (ZPAL), and D. Kizirian and D. Frost (AMNH, Herpetology) for access to specimens. We thank A.M. Balcarcel, T.B. Conrad, M.M. Conrad, S. Eliya, C.F. Kammerer, T.E. Macrini, C.M. Mehling, R.M. Shearman, and A.H. Turner for helpful discussions and support. A.M. Balcarcel and C.M. Mehling assisted with specimen maintenance and figure construction.

REFERENCES

- Abdala, V., and S.A. Moro. 2003. A cladistic analysis of ten lizard families (Reptilia: Squamata) based on cranial musculature. *Russian Journal of Herpetology* 10: 53–78.
- Ahl, E. 1930. Beitrage zur Lurch und Kriechtier-fauna Kwangsi: Section 5, Eidechsen. Sitzungs-berichte der Gesellschaft der naturforschenden Freunde zu Berlin 1930: 326–331.
- Alifanov, V.R. 1993. New lizards of the family Macrocephalosauridae (Sauria) from the Upper Cretaceous of Mongolia, critical remarks on the systematics of the Teiidae (sensu Estes, 1983). *Paleontological Journal* 27: 70–90.
- Alifanov, V.R. 1996. Lizard families Priscagami-dae and Hoplocercidae (Sauria, Iguania): phylogenetic position and new representatives from the Late Cretaceous of Mongolia. *Paleontological Journal* 1996: 100–118.
- Alifanov, V.R. 2000. The fossil record of Cretaceous lizards from Mongolia. In M.J. Benton, M.A. Shishkin, D.M. Unwin, and E.N. Kurochkin (editors), *The age of dinosaurs in Russia and Mongolia*, 368–389. Cambridge: Cambridge University Press.
- Ast, J.C. 2002. Evolution in Squamata (Reptilia). Ph.D. dissertation, University of Michigan, Ann Arbor. 276 pp.
- Balsai, M.J. 2001. The phylogenetic position of *Palaeosaniwa* and the early evolution of platynotan (varanoid) anguimorphs. Ph.D. dissertation, University of Pennsylvania, Philadelphia. 253 pp.
- Barrows, S., and H.M. Smith. 1947. The skeleton of the lizard *Xenosaurus grandis* (Gray). *University of Kansas Science Bulletin* 31: 227–281.
- Bever, G.S., C.J. Bell, and J.A. Maisano. 2005a. The ossified braincase and cephalic osteoderms of *Shinisaurus crocodilurus* (Squamata, Shinisauridae). *Palaeontologia Electronica* 8: 1–36.
- Bever, G.S., C.J. Bell, and J.A. Maisano. 2005b. *Shinisaurus crocodilurus*. Internet resource (http://digimorph.org/specimens/Shinisaurus_crocodilurus/adult/), accessed 2006.
- Bhullar, B.-A.S., and K.T. Smith. 2008. Helodermatid lizard from the Miocene of Florida, the evolution of the dentary in Helodermatidae, and comments on dentary morphology in Varanoidea. *Journal of Herpetology* 42: 286–302.
- Bogert, C.M., and R.M. Del Campo. 1956. The gila monster and its allies: the relationships, habits, and behavior of the lizards of the family Helodermatidae. *Bulletin of the American Museum of Natural History* 109 (1): 1–238.
- Bonine, K. 2005a. *Heloderma suspectum*. Internet resource (http://digimorph.org/specimens/Heloderma_suspectum/adult/), accessed 2006.
- Bonine, K. 2005b. *Heloderma suspectum* [juvenile, head]. Internet resource (http://www.digimorph.org/specimens/Heloderma_suspectum/juvenile/head/), accessed 2006.

- Bonine, K. 2005c. *Heloderma suspectum* [juvenile, whole]. Internet resource (http://www.digimorph.org/specimens/Heloderma_suspectum/juvenile/whole/), accessed 2008.
- Borsuk-Białynicka, M. 1983. The early phylogeny of Anguimorpha as implicated by craniological data. *Acta Palaeontologica Polonica* 28: 5–105.
- Borsuk-Białynicka, M. 1984. Anguimorphans and related lizards from the Late Cretaceous of the Gobi Desert, Mongolia. *Palaeontologia Polonica* 46: 5–105.
- Borsuk-Białynicka, M. 1985. Carolinidae, a new family of xenosaurid-like lizards from the Upper Cretaceous of Mongolia. *Acta Palaeontologica Polonica* 30: 151–176.
- Borsuk-Białynicka, M. 1988. *Globaura venusta* gen. et sp. n. and *Eoxanta lacertifrons* gen. et sp. n.—non-teiid lacertoids from the Late Cretaceous of Mongolia. *Acta Palaeontologica Polonica* 33: 211–248.
- Borsuk-Białynicka, M. 1990. *Gobekko cretacicus* gen. et sp. n., a new gekkonid lizard from the Cretaceous of the Gobi Desert. *Acta Palaeontologica Polonica* 35: 67–76.
- Borsuk-Białynicka, M. 1996. The Late Cretaceous lizard *Pleurodontagama* and the origin of tooth permanency in Lepidosauria. *Acta Herpetologica Polonica* 41: 231–252.
- Borsuk-Białynicka, M., and S.M. Moody. 1984. Priscagaminae, a new subfamily of the Agamidae (Sauria) from the Late Cretaceous of the Gobi Desert. *Acta Palaeontologica Polonica* 29: 51–81.
- Borsuk-Białynicka, M., and V.R. Alifanov. 1991. First Asiatic ‘iguaniid’ lizards in the Late Cretaceous of Mongolia. *Acta Palaeontologica Polonica* 36: 325–342.
- Boulenger, A.G. 1891. On the osteology of *Heloderma horridum* and *H. suspectum*, with remarks on the systematic position of the Helodermatidae and on the vertebrae of Lacertilia. *Proceedings of the Zoological Society of London* 1891: 109–118.
- Caldwell, M.W. 1999. Squamate phylogeny and the relationships of snakes and mosasauroids. *Zoological Journal of the Linnean Society* 125: 115–147.
- Cifelli, R.L., and R.L. Nydam. 1995. Primitive, helodermatid-like platynotan from the Early Cretaceous of Utah. *Herpetologica* 51: 286–291.
- Conrad, J.L. 2004. Skull, mandible, and hyoid of *Shinisaurus crocodilurus* Ahl (Squamata, Anguimorpha). *Zoological Journal of the Linnean Society* 141: 399–434.
- Conrad, J.L. 2006a. An Eocene shinisaurid (Reptilia, Squamata) from Wyoming, U.S.A. *Journal of Vertebrate Paleontology* 26: 113–126.
- Conrad, J.L. 2006b. Postcranial skeleton of *Shinisaurus crocodilurus* (Squamata: Anguimorpha). *Journal of Morphology* 267: 759–775.
- Conrad, J.L. 2008. Phylogeny and systematics of Squamata (Reptilia) based on morphology. *Bulletin of the American Museum of Natural History* 310: 1–182.
- Conrad, J.L., and M. Norell. 2006a. A complete Cretaceous iguanian (Squamata) from the Gobi. *Journal of Vertebrate Paleontology* 26 (suppl. 3): 51A–52A.
- Conrad, J.L., and M.A. Norell. 2006b. High-resolution X-ray computed tomography of an Early Cretaceous gekkonomorph (Squamata) from Öösh (Övörkhanga; Mongolia). *Historical Biology* 18: 405–431.
- Conrad, J.L., and M.A. Norell. 2007. A complete Late Cretaceous iguanian (Squamata: Reptilia) from the Cretaceous of the Gobi and identification of a new clade of Iguania. *American Museum Novitates* 3584: 1–47.
- Conrad, J.L., and M.A. Norell. 2008. The braincases of two glyptosaurines (Anguinae, Squamata) and anguid phylogeny. *American Museum Novitates* 3613: 1–24.
- Conrad, J.L., J.C. Ast, S. Montanari, and M.A. Norell. 2011. A combined evidence phylogenetic analysis of Anguimorpha (Reptilia: Squamata). *Cladistics* 27: 230–277.
- Costelli, J., Jr., and M.K. Hecht. 1971. The postcranial osteology of the lizard *Shinisaurus*: the appendicular skeleton. *Herpetologica* 27: 87–98.
- Criley, B.B. 1968. The cranial osteology of gerrhonotiform lizards. *American Midland Naturalist* 80: 199–219.
- de Beer, G. 1937. *The development of the vertebrate skull*. Oxford: Oxford University Press, 554 pp.
- Deep Scaly Project, *Heloderma horridum*, beaded lizard. Internet resource (http://digimorph.org/specimens/Heloderma_horridum/), accessed 2011.
- Estes, R. 1964. Fossil vertebrates from the Late Cretaceous Lance Formation eastern Wyoming. *University of California Publications in Geological Sciences* 49: 1–180.
- Estes, R. 1983. *Sauria terrestria*, Amphisbaenia. New York: Gustav Fischer Verlag, 249 pp.
- Estes, R., K. de Queiroz, and J. Gauthier. 1988. Phylogenetic relationships within Squamata. In R. Estes and G. Pregill (editors), *Phylogenetic relationships of the lizard families*, 119–281. Stanford, CA: Stanford University Press.
- Evans, S.E. 2008. The skull of lizards and tuatara. In C. Gans, A.S. Gaunt, and K. Adler (editors), *Biology of the Reptilia*, vol. 20: Morphology H, the skull of Lepidosauria, 1–344. Ithaca, NY:

- Society for the Study of Amphibians and Reptiles.
- Evans, S.E., and L.J. Barbadillo. 1997. Early Cretaceous lizards from Las Hoyas, Spain. *Zoological Journal of the Linnean Society* 119: 23–49.
- Evans, S.E., and L.J. Barbadillo. 1998. An unusual lizard (Reptilia: Squamata) from the Early Cretaceous of Las Hoyas, Spain. *Zoological Journal of the Linnean Society* 124: 235–265.
- Evans, S.E., and L.J. Barbadillo. 1999. A short-limbed lizard from the Lower Cretaceous of Spain. *Special Papers in Palaeontology Series* 60: 73–85.
- Evans, S.E., and Y. Wang. 2005. Early Cretaceous lizard *Dalinghosaurus* from China. *Acta Palaeontologica Polonica* 50: 725–742.
- Evans, S.E., Y. Wang, and C. Li. 2005. The early Cretaceous lizard genus *Yabeinosaurus* from China: resolving an enigma. *Journal of Systematic Palaeontology* 4: 319–335.
- Farlow, J.O., and E.R. Pianka. 2000. Body form and trackway pattern in Australian desert monitors (Squamata: Varanidae): comparing zoological and ichnological diversity. *Palaios* 15: 235–247.
- Fry, B.G. 2005. From genome to “venome”: molecular origin and evolution of the snake venom protome inferred from phylogenetic analysis of toxin sequences and related body proteins. *Genome Research* 15: 403–420.
- Fry, B.G., et al. (2009). A central role for venom in predation by *Varanus komodoensis* (Komodo Dragon) and the extinct giant *Varanus (Megalania) priscus*. *Proceedings of the National Academy of Sciences of the United States of America* 106: 8969–8974.
- Fürbringer, M. 1900. Beitrag zur Systematik und Genealogie der Reptilien. *Jenaischen Zeitschrift für Naturwissenschaften* 34: 596–682.
- Gao, K.-Q., and L. Hou. 1995. Iguanians from the Upper Cretaceous Djadochta Formation, Gobi Desert, China. *Journal of Vertebrate Paleontology* 15: 57–78.
- Gao, K.-Q., and L. Hou. 1996. Systematics and taxonomic diversity of squamates from the Upper Cretaceous Djadochta Formation, Bayan Manahu, Gobi Desert, People's Republic of China. *Canadian Journal of Earth Sciences* 33: 578–598.
- Gao, K.-Q., and M.A. Norell. 1998. Taxonomic revision of *Carusia* (Reptilia: Squamata) from the Late Cretaceous of the Gobi Desert and phylogenetic relationships of anguimorph lizards. *American Museum Novitates* 3230: 1–51.
- Gao, K.-Q., and M.A. Norell. 2000. Taxonomic composition and systematics of Late Cretaceous lizard assemblages from Ukhaa Tolgod and adjacent localities, Mongolian Gobi Desert. *Bulletin of the American Museum of Natural History* 249: 1–118.
- Gilmore, C.W. 1943. Fossil lizards of Mongolia. *Bulletin of the American Museum of Natural History* 81 (4): 361–384.
- Goloboff, P.A., J.S. Farris, and K.C. Nixon. 2003. T.N.T.: Tree analysis using new technology. Goloboff, Farris, and Nixon. Internet resource (www.zmuc.dk/public/phylogeny).
- Herrel, A., and F. De Vree. 1999. The cervical musculature in helodermatid lizards. *Belgian Journal of Zoology* 129: 175–186.
- Hoffstetter, R. 1957. Un saurien helodermatidé (*Eurheloderma gallicum* nov. gen. et sp.) dans la faune fossile des Phosphorites du Quercy. *Bulletin de la Société Géologique de France* (6) 7: 775–786.
- Jollie, M.T. 1960. The head skeleton of the lizard. *Acta Zoologica* 41: 1–64.
- Kearney, M., and J.M. Clark. 2003. Problems due to missing data in phylogenetic analyses including fossils: a critical review. *Journal of Vertebrate Paleontology* 23: 263–274.
- Klembara, J. 1979. Neue Funde der Gattungen *Ophisaurus* und *Anguis* (Squamata, Reptilia) aus dem Untermiozän Westböhmens (CSSR) / New finds of the genera *Ophisaurus* and *Anguis* (Squamata, Reptilia) in the Lower Miocene of western Bohemia (CSSR). *Vestník Ústředního Ústavu Geologického* 54: 163–169.
- Klembara, J. 1981. Beitrag zur Kenntnis der Subfamilie Anguinae (Reptilia, Anguinae). *Acta Universitatis Carolinae Geologica* 2: 121–168.
- Klembara, J. 1986. New finds of the genus *Ophisaurus* (Reptilia, Anguinae) from the Miocene of western Slovakia (Czechoslovakia). *Acta Universitatis Carolinae Geologica* 2: 187–203.
- Kley, N.J., et al. (2010). Craniofacial morphology of *Simosuchus clarki* (Crocodyliformes: Notosuchia) from the Late Cretaceous of Madagascar. *Journal of Vertebrate Paleontology* 30 (s1): 13–98.
- Ksepka, D.T., and M.A. Norell. 2006. *Erketu ellisoni*, a long-necked sauropod from Bor Guvé (Dornogov Aimag, Mongolia). *American Museum Novitates* 3508: 1–16.
- Ksepka, D.T., and M.A. Norell. 2010. The illusory evidence for Asian Brachiosauridae: new material of *Erketu ellisoni* and a phylogenetic reappraisal of basal titanosauriformes. *American Museum Novitates* 3700: 1–27.
- Lee, M.S.Y. 1997. The phylogeny of varanoid lizards and the affinities of snakes. *Philosophical Transactions of the Royal Society of London B Biological Sciences* 352: 53–91.
- Lee, M.S.Y. 1998. Convergent evolution and character correlation in burrowing reptiles: towards a resolution of squamate relationships.

- Biological Journal of the Linnean Society 65: 369–453.
- Lee, M.S.Y. 2000. Soft anatomy, diffuse homoplasy, and the relationships of lizards and snakes. *Zoologica Scripta* 29: 101–130.
- Lee, M.S.Y., and M.W. Caldwell. 2000. *Adriosaurus* and the affinities of mosasaurs, dolichosaurs, and snakes. *Journal of Paleontology* 74: 915–937.
- Loope, D.B., L. Dingus, and C.C. Swisher, III. 1998. Life and death in a Late Cretaceous dune field, Nemegt Basin, Mongolia. *Geology* 26: 27–30.
- Maisano, J.A. 2001a. *Heloderma texana*. Internet resource (http://digimorph.org/specimens/Heloderma_texana/), accessed 2006.
- Maisano, J.A. 2001b. *Lanthanotus borneensis*. Internet resource (http://digimorph.org/specimens/Lanthanotus_borneensis/), accessed 2006.
- Maisano, J.A. 2001c. A survey of state of ossification in neonatal squamates. *Herpetological Monographs* 15: 135–157.
- Maisano, J.A. 2001d. *Varanus gouldii*. Internet resource (http://digimorph.org/specimens/Varanus_gouldii/), accessed 2007.
- Maisano, J.A. 2002a. Postnatal skeletal ontogeny in *Callisaurus draconoides* and *Uta stansburiana* (Iguania: Phrynosomatidae). *Journal of Morphology* 251: 114–139.
- Maisano, J.A. 2002b. Postnatal skeletal ontogeny in five xantusiids (Squamata: Scleroglossa). *Journal of Morphology* 254: 1–38.
- Maisano, J.A., C.J. Bell, J. Gauthier, and T. Rowe. 2002. The osteoderms and palpebral in *Lanthanotus borneensis* (Squamata: Anguimorpha). *Journal of Herpetology* 36: 678–682.
- Makovicky, P.J., and M.A. Norell. 2006. *Yamaceratops dorn gobiensis*, a new primitive ceratopsian (Dinosauria: Ornithischia) from the Cretaceous of Mongolia. *American Museum Novitates* 3530: 1–42.
- McAllister, C.T., and S.E. Trauth. 1982. An instance of the eastern collared lizard, *Crotaphytus collaris collaris* (Sauria: Iguanidae) feeding on *Sigmodon hispidus* (Rodentia: Cricetidae). *Southwestern Naturalist* 27: 358–359.
- McDowell, S.B., Jr. and C.M. Bogert. 1954. The systematic position of *Lanthanotus* and the affinities of the anguimorph lizard. *Bulletin of the American Museum of Natural History* 105 (1): 1–142.
- Mead, J.I., B.W. Schubert, S.C. Wallace, and S.L. Swift. In press. Helodermatid lizard from the Mio-Pliocene oak-hickory forest of Tennessee, eastern USA, and a review of Monstersauria osteoderm. *Acta Palaeontologica Polonica*, 1–35, [doi:10.4202/app.2010.0083]
- Mertens, R. 1942. Die Familie der Varane (Varanidae). Zweiter Teil: der Schädel. *Abhandlungen der Senckenbergischen Naturforschenden Gesellschaft* 465: 117–234.
- Miles, C.A., and C.J. Miles. 2009. Skull of *Minotaurasaurus ramachandrani*, a new Cretaceous ankylosaur from the Gobi Desert. *Current Science* 96: 65–70.
- Montero, R., and C. Gans. 1999. The head skeleton of *Amphisbaena alba* Linnaeus. *Annals of Carnegie Museum* 68: 15–79.
- Norell, M.A., and K.-Q. Gao. 1997. Braincase and phylogenetic relationships of *Estesia mongoliensis* from the Late Cretaceous of the Gobi Desert and the recognition of a new clade of lizards. *American Museum Novitates* 3211: 1–25.
- Norell, M.A., M.C. McKenna, and M.J. Novacek. 1992. *Estesia mongoliensis*, a new fossil varanoid from the Late Cretaceous Barun Goyot Formation of Mongolia. *American Museum Novitates* 3045: 1–24.
- Norell, M.A., et al. (2006). A new dromaeosaurid theropod from Ukhaa Tolgod (Ömnögovi, Mongolia). *American Museum Novitates* 3545: 1–51.
- Norell, M.A., K.-Q. Gao, and J.L. Conrad. 2008. A new platynotan lizard (Diapsida: Squamata) from the Late Cretaceous Gobi Desert (Ömnögovi), Mongolia. *American Museum Novitates* 3605: 1–25.
- Nydam, R.L. 2000. A new taxon of helodermatid-like lizard from the Albian-Cenomanian of Utah. *Journal of Vertebrate Paleontology* 20: 285–294.
- Oelrich, T.M. 1956. The anatomy of the head of *Ctenosaura pectinata* (Iguanidae). *Miscellaneous Publications Museum of Zoology University of Michigan* 94: 1–122.
- Oppel, M. 1811. Die Ordnungen, Familien, und Gattungen der Reptilien als Prodom einer Naturgeschichte derselben. München: Joseph Lindauer, 86 pp.
- Page, R.D.M. 2001. NDE: Nexus Data Editor for Windows. Glasgow: R.D.M. Page.
- Pianka, E.R., and L.J. Vitt. 2003. Lizards: windows to the evolution of diversity. Berkeley: University of California Press, 346 pp.
- Pregill, G.K., J.A. Gauthier, and H.W. Greene. 1986. The evolution of helodermatid squamates, with description of a new taxon and an overview of Varanoidea. *Transactions of the San Diego Society of Natural History* 21: 167–202.
- Rewcastle, S.C. 1980. Form and function in lacertilian knee and mesotarsal joints; a contribution to the analysis of sprawling locomotion. *Journal of Zoology (London)* 191: 147–170.
- Rieppel, O. 1980a. The phylogeny of anguimorph lizards. Basel: Naturforschenden Gesellschaft, 86 pp.
- Rieppel, O. 1980b. The postcranial skeleton of *Lanthanotus borneensis* (Reptilia, Lacertilia). *Amphibia-Reptilia* 1: 95–112.

- Rieppel, O. 1983. A comparison of the skull of *Lanthanotus borensis* (Reptilia: Varanoidea) with the skull of primitive snakes. *Zeitschrift für zoologische Systematik und Evolutionsforschung* 21: 142–153.
- Rieppel, O., and H. Zaher. 2000. The intramandibular joint in squamates, and the phylogenetic relationships of the fossil snake *Pachyrhachis problematicus* Haas. *Fieldiana (Geology)*, new series 43: 1–69.
- Rieppel, O., J.L. Conrad, and J.A. Maisano. 2007. New morphological data for *Eosaniwa koehni* Haudbold 1977 and a revised phylogenetic analysis. *Journal of Paleontology* 81: 760–769.
- Romer, A.S. 1922. The locomotor apparatus of certain primitive and mammal-like reptiles. *Bulletin of the American Museum of Natural History* 46 (10): 517–606.
- Romer, A.S. 1942. The development of tetrapod limb musculature—the thigh of *Lacerta*. *Journal of Morphology* 71: 251–298.
- Romer, A.S. 1949. The vertebrate body. Philadelphia: W.B. Saunders, 643 pp.
- Romer, A.S. 1956. Osteology of the reptiles. Chicago: University of Chicago Press, 772 pp.
- Rougier, M.J., M.J. Novacek, M.C. McKenna, and J.R. Wible. 2001. Gobiconodonts from the Early Cretaceous of Oshih (Ashile), Mongolia. *American Museum Novitates* 3348: 1–30.
- Russell, A.P. 1988. Limb muscles in relation to lizard systematics: a reappraisal. In R. Estes and G. Pregill (editors), *Phylogenetic relationships of the lizard families*, 493–568. Stanford, CA: Stanford University Press.
- Schumacher, G.H. 1973. The head muscles and hyolaryngeal skeleton of turtles and crocodilians. In C. Gans and T.S. Parsons (editors), *Biology of the Reptilia*, vol. 4: Morphology D, 101–199. London: Academic Press.
- Scotese, C.R. 1991. Jurassic and Cretaceous plate tectonic reconstructions. *Palaeogeography, Palaeoclimatology, Palaeoecology* 87: 493–501.
- Scotese, C.R. 2003. PALEOMAP. Internet resource (www.scotese.com), accessed 2011.
- Scotese, C.R., L.M. Gahagan, and R.L. Larson. 1988. Plate tectonic reconstructions of the Cretaceous and Cenozoic ocean basins. *Tectonophysics* 155: 27–48.
- Shearman, R.M. 2005. Growth of the pectoral girdle of the leopard frog, *Rana pipiens* (Anura: Ranidae). *Journal of Morphology* 264: 94–104.
- Shen, L.-t., and H.-h. Li. 1982. Notes on the distribution and habits of the lizard *Shinisaurus crocodilurus* Ahl. *Acta Herpetologica Sinica* 1: 4–5.
- Sprackland, R.G. 1989. An enigmatic dragon brought to light, the Chinese crocodile lizard in captivity, *Shinisaurus crocodilurus*. *Vivarium, Lakeside* 2: 12–14.
- Sullivan, R.M. 1979. Revision of the Paleogene genus *Glyptosaurus* (Reptilia, Anguillidae). *Bulletin of the American Museum of Natural History* 163 (1): 1–72.
- Townsend, T.M., A. Larson, E. Louis, and J.R. Macey. 2004. Molecular phylogenetics of Squamata: the position of snakes, amphisbaenians, and dibamids, and the root of the squamate tree. *Systematic Biology* 53: 735–757.
- Turner, A.H., S.H. Hwang, and M.A. Norell. 2007a. A small derived theropod from Öösh, Early Cretaceous, Baykhangor Mongolia. *American Museum Novitates* 3557: 1–27.
- Turner, A.H., D. Pol, J.A. Clarke, G.M. Erickson, and M.A. Norell. 2007b. A basal dromaeosaurid and size evolution preceding avian flight. *Science* 317: 1378–1381.
- Vickaryous, M.K., and B.K. Hall. 2006. Homology of the reptilian coracoid and a reappraisal of the evolution and development of the amniote pectoral apparatus. *Journal of Anatomy* 208: 263–285.
- Vidal, N., and S.B. Hedges. 2005. The phylogeny of squamate reptiles (lizards, snakes, and amphisbaenians) inferred from nine nuclear protein-coding genes. *Comptes rendus Biologies* 328: 1000–1008.
- Wible, J.R., M.J. Novacek, and G.W. Rougier. 2004. New data on the skull and dentition in the Mongolian Late Cretaceous eutherian mammal *Zalambdalestes*. *Bulletin of the American Museum of Natural History* 281: 144.
- Wible, J.R., G.W. Rougier, M.J. Novacek, and M.C. McKenna. 2001. Earliest eutherian ear region: a petrosal referred to *Prokennalestes* from the Early Cretaceous of Mongolia. *American Museum Novitates* 3322: 44.
- Wiegmann, A.F.A. 1829. Ueber das Acaltetepon oder Temacuicahuya des Hernandez, eine neue Gattung der Saurer, *Heloderma*. *Isis von Oken* 22: 624–629.
- Wu, X.-c., D.B. Brinkman, and A.P. Russell. 1996. *Sineoamphisbaena hexatabularis*, an amphisbaenian (Diapsida: Squamata) from the Upper Cretaceous redbeds at Bayan Mandahu (Inner Mongolia, People's Republic of China), and comments on the phylogenetic relationships of the Amphisbaenia. *Canadian Journal of Earth Sciences* 33: 541–577.
- Yi, H.-Y., and M.A. Norell. 2010. New materials of *Estesia mongoliensis* (Reptilia: Squamata) from the Late Cretaceous of Mongolia cast doubt on the monophyly of Monstersauria. 70th Anniversary Meeting of the Society of Vertebrate Paleontology: program and abstracts 191A.
- Zaher, H., and O. Rieppel. 1999. Tooth implantation and replacement in squamates, with special reference to mosasaur lizards and snakes. *American Museum Novitates* 3271: 1–19.

APPENDIX 1

Anatomical Abbreviations from Figures

a	angular	is	ischium
aar	anterior auditory recess	isaf	intermediate surangular foramen
ac	surface articulating with the coronoid	ist	ischial tubercle
aec	articular facet for the ectopterygoid	itr	internal trochanter
af	adductor fossa	j	jugal
aiaf	anterior inferior alveolar foramen	l	lacrimal
alc	alveolar canal	L	left
am	articular facet for the maxilla	lf	lacrimal foramen
amf	anterior mylohyoid foramen	lgr	lagenar recess
aoo	articular surface receiving the otoocci- pital	m	maxilla
apr	alar process of the prootic	ma	manus
apra	articular surface of the processus as- cendens	mb	mystery bone
asaf	anterior surangular foramen	mc-#	metacarpal identity
asc	anterior semicircular canal	mg	Meckel's groove
asca	astragalocalcaneum	Mppf	M. protractor pterygoideus fossa
auf	autotomy foramen	mt	maxillary teeth
avc	anterior opening of the Vidian canal	n	nasal
ax	axis	nec	neural canal
bo	basioccipital	ns	neural spine
bpt	basipterygoid process	o	orbit
c	coronoid	oam	origin point for the adductor muscula- ture
CA	caudal vertebra (with number, e.g., CA2)	ocr	occipital recess
cal	alar crest	of	obturator foramen
cc	subolfactory processes (crista cranii)	onf	orbitonasal fenestra
ccc	cranial carotid canal	oo	otooccipital
CDv	presacral vertebra(e)	os	osteoderms
cfo	carotid fossa	p	parietal
cnc	cnemial crest	pa	palatine
co	coracoid	paf	posterior auditory foramen
cof	coracoid foramen	pat	patella
con	condyle	pcr	posterior crest of the qua- drate
cot	cotyle	pd	perilymphatic duct
cpr	crista proötica	pe	pes
d	dentary	pf	postfrontal
dp	decensus parietalis	pfc	postfoveal crest
dt	dentary teeth	pfo	parietal fossa
Dv	dorsal vertebra(e)	pif	pineal foramen
e	epipterygoid	pm	premaxilla
ec	ectopterygoid	pmf	posterior mylohyoid foramen
ef	ethmoid foramen	po	postorbital
eld	endolymphatic duct	poc	paroccipital process
f	frontal	pof	postorbitofrontal
fct	foramen chorda tympani	popr	postorbital process
fe	femur	poz	postzygapophysis
fi	fibula	pra	prearticular
fo	fenestra ovalis	prf	prefrontal
ftb	frontal tab	pro	proötic
gl	glenoid	prz	prezygapophysis
glb	glenoid buttress	ps	parasphenoid/parasphenoid rostrum
hd	head	psaf	posterior surangular foramen
hsc	horizontal semicircular canal	pt	pterygoid
il	ilium	ptp	pterygoid tooth plate
ims	intramandibular septum	ptpr	pterygoid process
ioc	infraorbital canal	ptu	pubic tubercle
iof	infraorbital foramen	pu	pubis
ipr	inferior process of the proötics	pvc	posterior opening of the Vidian canal
		q	quadrate
		R	right
		rap	retroarticular process
		rpc	posterior cerebral vein
			recess
		rst	recessus scalae tympani
		sa	surangular

sac	surangular canal
sc	scapula (scapular part of the scapulo-coracoid)
scco	scapulocoracoid
scf	scapular fenestra/scapular emargination
ses	sesamoid
sm	septomaxilla
smc	semicircular canal/external bulla forming the margin of the semicircular canal
so	supraoccipital
sorf	supraorbital fenestra
sot	spheno-occipital tubercle
sp	splénial
sph	basisphenoid
sq	squamosal
sr	sacral rib
st	supratemporal
sut	supratrigeminal tubercle
SV	sacral vertebra(e)
syn	synapophysis
tcr	tympanic crest
ti	tibia
un	ungual
v	vomer
vc	Vidian canal
ve	vestibule
vfo	vagus foramen
V-n	trigeminal notch
vno	vomeronasal opening
zsp	zygosphen
lcr	primary coracoid fenestra/emargination
I–XII	cranial nerves (skull); digit identity (autopodia)
I-#	phalangeal identities

APPENDIX 2

Morphological Phylogenetic Data Matrix

Below is the character and character state matrix used in the present analysis in TNT format. At the end of the matrix are some codes that turn off certain characters and order others as described above and in Conrad et al. (2011). This matrix may be cut from the pdf of this paper and pasted into an appropriate text-editing program for use in TNT.

Xread
426 93
&[num]

Gephyrosaurus bridensis 100??01001 1102000000
001000-010 0100000000 1000000010 0010100000
0-0-000010 0011000-00 0100001-00 0010020000
???000000 0000000000 -100000?? 12?0????? ??0-
?10?0 0?0?????00 ?200?1000- -000???101 00300-01-- -
00000-000 ?00-000000 000[01]000000 000000???0
100-1?1002 0?00000?0 000000???0 100?00?000
????0000?? ????1011000 01???????? ????0000??
????????? ????0000?? ????0000?? ????0000??

???4?-2002 ?00?1?0?? -00-??-?0? ????00????- -0??0800-
0 0????????? ???-??
Sphenodon punctatus 000110-000 01020000000
101000-000 0000000000 3-00000010 0000000000
0-0-00001- 000?102000 0100000000 0010020000
0000000010 0000201200 -100000000 0200000--1
0010201000 0000000000 ?20001000- -0201--101
00-00-01-- -10000010? ?00-000000 0101100000
3030000000 100-002-02 0100010000 0200001000
1001001000 0001000002 0001210000 21000001-0
00000-00-- -0000?0000 00000----- 000?0000?0
0???0?0001 11[01]00-1-- 10-90-0002 1000?0?0?0 -
10-??-?00 ??0--??1?- -00-0000-0 008-500100 000-??
Aspidoscelis tigris 1000000001 11[01]0000000
1030111000 0001000010 1000001100 0101102100
100-000011 0110023000 0010000010 0211011000
0000100110 0010100210 1011000000 0000000001
0000011000 0000000010 200000001- -000010100
02020-0010 0120110000 0011000010 0400000000
0000001001 20012?2-1-- 0001010000 1000001001
1110011000 0100002000 0000200000 010100?211
00000-0--- 0000004020 0????????? ????0000??
????????? ????0000?? ????3000000 1000?0?0?0 000-??-
?-2 ?1--??1?0 -0010??1?0 005-61-202 1100??
Xantusia vigilis 1000000111 1200000000 002000-000
0110000000 2000001100 0001102100 100-010011
0102-20001 0001010100 0-210-0001 0000110110
0010100210 1001010000 0100101000 0001001000
10000?0011 200001000- -00101-101 22110-01-- -
110100100 1110000000 0000000000 0000000001
20010?2-11 0011000000 ?00000?001 1100001000
0000000000 0000201000 0101000201 00000-0-0
0001021020 00200????? ????01?22 1???1?????
????????? ????30-0-02 1000?0?0?0 -?0-??-?-? ????-??1?0
-0-?0?0-0 009-61-?11 000?9?
Eolacerta robusta 100?000111 110?000000
1130?00000 ?000?00?0 10?000000 0001000100
???1?011 011?-20000 00?0?1?00 0???0?1001
1????????? ????02?? ????0?0?? ?0?0????? ?10????000
0?00?0?1? ????0?000? ?000??000 0001100010
010010?10? ?010100000 0000000000 000000?0?1
2001222-?? 00?010000 0000000?01 110?00?010
00?00000- 1001100000 01?????20? ?0?1?0?00
0????????? ????0000?? ????0000?? ????0000??
???40?00? ?000?120?0 000-??-?-2 ????-???? ?0-0?0-
0 0?9-6????? ?0?-[78]
Yabeinosaurus tenuis ?000?00111 11?00?00? ????0-
000 01000000?? ????001000 000?002000 100-???011
0112000000 010001?10 00100?001 ????1?0???
???00?00?? ????0?0?? ????0000?? ????0000??
?000?0?00? ????0?0?? ????0?0?? ?1?010????
???0000121 00000000010 000000?0?1 200?1????
0???010?0? 0???00???? ?10?00???? ????00?000
000?0?000 00???0??? ????0-0--- 0????????? ????0000??
????????? ????0000?? ????0000?? ????0000??
?0???-?-1 ?000?0?0 -???0310-0 0?8-????? ?0?-[45]
Carusia intermedia 1000?00111 0101000000
01300?0000 0100000010 2000000001 0011102100
0-0-110001 011?-20?00 0100010110 0-11001000
????100011 1000100110 1000000000 0000002000
0010?11000 00100?0?11 ?000?10001 103000-100
0001100010 0120100?00 000-000101 2000000000
100001?0?1 2?0??????? 0?0??????? ????0000??
????0001? ????0000?? ????0000?? ????0000??
0????????? ????0000?? ????0000?? ????0000??

??80000?0 1?00?110?0 100-??-?02 ??100????0
-0100[45]00?? ?????????? ??0?-[67]
Xenosaurus grandis 1000000111 1101000000
1130000000 0100000010 1000000011 0011102100
0-0-010001 0110-10101 0011010010 0-11001000
1000100110 0010101210 0000010000 0000002001
0010001000 0010000011 2000010001 101001-100
0011100010 01[12]0100000 000-100101 0300000000
1000001101 2001122-00 0021010000 0200000000
1100001000 0001000000 0000201000 11000001-1
0000100000 1000032110 0101????? 0000?00001
010110000? 011??????? ??33000000 1000?110?0 000-
??-?11 ??0-0-??0 -01-0310-0 02-3600210 0000-[12]
Xenosaurus platyceps 1000000111 1101000000
1130000000 0100000010 1000000011 0011102100
0-0-010001 0110-10101 0010010010 0-11001000
1000100110 0010101210 0000010000 0000002001
0010011000 0010000011 2000010001 103001-100
0011100010 01[12]0100000 000-100101 0300000000
1000001101 2001122-10 0021010000 0200000000
1100001000 0101000000 0000201000 01000001-1
0000100000 10000321?? 0????????? ??????????
????????? ?????????? ??33000000 1000?110?0 000-??-
?11 ??0-0-??0 -01-0?20-0 02-3600?? ??00??
Restes rugosus ?????00111 ?????00???0 ??????0000
??000?00?0 10?00000001 011?1?210? 0-0-??0001
01??????? ???????1? 0????10?? ?????????? ??????????
????1???? ?????????? ?????????? ?????????? ??????????
????????? ?0????????? ?????????? ?????????? 0300000000
1??0?0??1 20010????? ?????????? ?????????? ??????????
????????? ???21???? ?????1-? ?????????00 0?????????
????????? ?????????? ?????????? ?????????? ??3?????
??0????? ?????-??0 ?????????? ?????????? ??????????
?????
Eosaniwa koehni 301?200111 ??0?00000 0?????1??
?1000?0?? 10?20000100 ?1??0?2100 0-0-??0?1
??????????? ?????????? ?????????? 1??2?01?00
11110?111? ????0?00?? 0????????? ??20??2?0?0
0?200????? ?000?1000? ?1--??-100 00?2??000?
0111?1?000 ??0-101?2 12000000000 2?0000??1
2102??2-?? 0?1101???? ?11??????? ??????????
????000?0? ?????????? ?????0?1-? ?1?10?2??0 01???????
????????? ?????????? ?????????? ?????????? ??40?????
??0?1?0?? ??0-??-?? ?1?00?2??0 -??-0?2?0?0 ??????????
??0??
Bahndwivici ammoskius 1011?00111 110?000000
0?10?20000 ??010?01?1 10?0000001 010110200? 0-
0-0?2011 011?010?00 010000011? 00100?100?
????1???? ?????????? ?????????? ??00????? ??????????
?????????11 ?100?2000? ??????0000 01??2?00?1
01?010?0?0 ?0?2000101 020000?000 1?000?2?1
2001022-?? 00?2010000 0000000?00 1??20?0?0
0??20000?? ?000101000 21??20??? 0?0?10?0??
01??????? ?????????? ?????????? ?????????? ??????????
????3????? ??00?110?0 -00-?1-?-? ?????????? -??0?2?0?
009-????? ??????
Shinisaurus crocodilurus 1011000111 1101000000
011000-000 01010001[01]1 100000000[01]
0101102000 0-0-010011 0111010000 0110000110
0011011001 1000100110 0010101101 -0010010000
00000021-1 [01]010011000 0010000011 2100000000
2000000000 01[01]1100011 0110100000 000-000101
0200001000 1010001101 20010[12]2-11 0011010000
0000000000 1100001010 0001000001 0000101000
21000021-1 0000100000 0100032110 0??20?????

00?0?00001 00?0100??? ?????????? ??80000000
10001110-0 -00-01-0-1 100000-1?0 -01-02[01]0-0
00[89]-600?? ??00??
Merkurosaurus ornatus 10????01?1 11?10000??
????0-00? ?10??????? ???0000001 01??102100 0-0-
?10011 0111010000 01000001?? ?????????? ??????????
??????11?? ?????????? ?????????? ?????????? ??????????
??????0?0? 1?????00? 00?1????? ?????????? ??????????
0200001000 ?0?000??? ?????????? ?????????? ??????????
????????? ?????????? ?????????? ???????1-? ???10?200
01??????? ?????????? ?????????? ?????????? ??????????
??4????? 1??0?2??0 ?00-????? ??300?2??0 ??-021??
????????? ??????
Dalinghosaurus longidigitus 101?200111 110?000000
0010?0-000 000100011? ???000001 01?1102100 0-0-
0100?1 011?010?00 0010000110 00100?1001
???10?2?? 0?100?10?? ?0?????000? 0000?21-?
??100?10?0 00?2?????10 ?100?0000? ?000?20000
0??1120010 011010?000 ?00-10?21? 020000?000
?00000??21 2001?22-?? 0??10100?? 0000001?21
010?00?010 0??2001000 0000100000 1?220?2??
0?0?0-0-- 01??????? ?????????? ?????????? ??????????
??????????? ??28?00000? ??00?110?0 ?00-??-??
??00?2??0 -??0210?0 00[89]-????? ??????
“*Saniwa*” *feisti* 10???0-0?0 11??00?0? ??????01?
??000?0?? 10?2001000 01?110200? ???1?2??1
011?0?0?00 0?0000011? ???????0?? 1?????????
????????? ?????????? ?????????? ?????????? ??????????
????000?? ?????01?0 ?????????? ?????????? ??0-000??
120?00?100 ??2000??1 2?1?122-?? ???010000
02?200??20 1??20?20? ????00?00? ?00?2??000
?1????1-1 001?1?1?0 01??????? ?????????? ??????????
????????? ?????????? ??4????? ?0?0????? ??-??-??
????????? ?????0????? ?????????? ??????
Necrosaurus cayluxi ???20-000 1?0?20?0? 0?30???01?
?0?????0?? ?????????? ???2102000 10?21?2001
0111110000 ?20000??? ??21????? 1?????????
???2??1?? ???0????? ?????????? ?????????? ??????????
??????0?? 1????10? 010??2000? ?????????? ??????????
1202001100 20?200??1 201?1????? 1?1?1?1?00
0211????? ?????????? ?????????? ?????????? ??????????
0?0?20?200 01??????? ?????????? ?????????? ??????????
????????? ??4????? ?????????? ?????????? ?????00?????
????0????? ?????????? ?????-1
“*Necrosaurus*” *eucarinatus* ???200?21 ??????????
??30??201? ?01??????? ?????????? ???20?200? 100-
??2001 ?110010000 ?20000??? ?????????? ??????????
????????? ?????????? ?????????? ?????????? ??????????
??????0?21 1????200? 01?22-?0?0 ?????????? ??????????
1202001100 ?????00?? ?????????? ?????1????? ??????????
????????? ?????????? ?????????? ?????????? ???????1-? 0?1?1?2??0
01??????? ?????????? ?????????? ?????????? ??????????
??4????? ?????????? ?????????? ?????????? ?????0?????
????????? ??????
Proplatynotia longirostrata 1100?10011 1101001000
0030011110 0100000000 1000001101 010?002000 0-
0-11?011 011001000? 000000?210 00100?2???
?000?00110 1100100011 0010010?? ????2??0??
?????0010?? ?????????? ??????00000 ??????20100
0112120001 0?11?1???? ?00-????? 1200001000
201000??? ?????????? ?????????? ?????????? ??????????
????????? ?????????? ?????????? ?????????? ??????????
????????? ?????????? ?????????? ?????????? ??????????
????????? ?????????? ?????????? ?????????? ?????8?0?0?
??001110?0 101001?0?? ?0?2????? ?01-0310??
????????? ???-[01]

11101?1211 00?200001? 000?021-? 001???000
0?00?0?1? ????????? ????????? ?????????
???????? 12020011?1 2???0???? ?????????
???????? ????????? ????????? ?????????
0?0?1???12 0???????? ????????? ?????????
???????? ?????30?0?0 ?0?0?10?0 ?1???-?? ?-??
????0???? ????????? ?0???
Lowesaurus matthewi ?1?1?1?1? ???????? ?1?????
?1????? ??????00? ?0?001000 11?01?00? ?10-
13?? ?????1??? ????????? ?????????
???10???? ????????? ????????? ?????????
2?????0? 01????? ????????? 120?1101
2???00??? ????????? ????????? ?????????
???????? ????????? ?????????1-? ??????12 0?????
???????? ????????? ????????? ????????? ?3????
???????? ?????????-? ????????? ?0?0???? ??????
???1??
Gobiderma pulchrum 1100?01111 1201000000
0030010010 0010000010 1000000001 0101002000
100-000011 0110-10000 1000010110 0010021001
?000101110 1110101011 0001010010 0000002000
0010001011 00100?-10 ?000010001 ????00-000
01120-0001 0111110001 000-100101 1202001100
201000???1 210112-? ????10000 ?00000???
?10?00??? ????0?0? ?000101000 21????1-1
?????0002 0???????? ????????? ?????????
???????? ?3?0000000 1?011100?0 001001-0-1
?000000100 -01-0110-? 0???????? ?00?
Telmasaurus grangeri ?0?0?-000 ????????? ??????
?100?0?0 10100?1100 01?1[01]?211? 10?10001
0110010000 01?0000110 002[01]001001 ??????
1100001011 000100?000 000?02001 ?1?11000
00100?011 ?100???? ??????0? ?????????
????????? 1?02?1?00 2???0???1 2?121?2-?
????010?0 ????00??? ????0???? ????0?00?
???1100000 21????? ????????? ?????????
???????? ????????? ????????? ?80???? ?0????
????-?? ????0???? -???????? 0???????? ????
Parviderma inexacta ?0?0?[01]?11 ?0?0???000
?30?0??? ????0?00?0 ?0?0???? ????10210? 0-0-
0?001 ?10?0?0? ?0?0?1? 00100?00? 1?????
0?000?0011 000?0000? ????????? ?????????
?????0?0? ????0?0?0? 01020-00?1 001111?001
00?0?0??? 1202?11?0 1???0?0??? ????0?0???
???????? ????????? ????????? ?????????
?????1-? ?????0?02 0???????? ?????????
???????? ????????? ?80???? ?0???? ????-??
????0???? ????0???? ????????? ????
Paraderma bogerti ?01?0111? 1?100000 ?????01?
???????? ????????? ????????? ?12-1000?
????1???? ????????? ????????? ?1????
???????? ????????? ????????? ?1 2?????000
010?0-?00? ????0?0??? ????0?0??? 1?02001100
201000???1 210?02-? ????0?0??? ?0?0?0?
???????? ????????? ????????? ?1-? ?????12
0???????? ????????? ????????? ?????????
????3???? ?0?0?0?0? ????????? ?????0?0?
???????? ????
Primaderma nessovi ?1?01?0? ?????1?0? ?????0?
0????0? ?0?0?0000 ????????? ?????????
????10?0? ????????? ????????? ?????????
???????? ????????? ????????? ?1 ?????00
010?0?00? ????0?0??? ????0?0??? 120?0?1100
?1000?0?1 2?0?0?0? ?1????? ?????????
???????? ????????? ?????????1-? ??????12 0?????

???????? ????????? ????????? ????????? ?3?0?0?
????????? ?????????? ?????????? ????0?0?0? ?????????
?????
Abronia deppii 1010000?0 1110000000 1130?0000
1100000010 1000000000 0001102000 0-0-[01]11001
0110-10?00 1000010110 0010001001 1000100111
0010100211 0000000000 0000002000 0010011000
00100?0011 20000[01]0001 2010000000 0011100010
0110100?00 100-101102 0000000000 1000011001
2001122-10 0021010000 200100?000 11000?1010
000?000000 ?000201000 ?1?000?211 0011101000
0100032110 01?10?0??? ????0?0?0? ????1?0?0?
???????? ?33000? ?00?0?0? ????-?-? ?-?-??0
-0?0?0-0 00?0?0?0 ?0?0?
Abronia oaxacae 1000000001 1110000000
1030010000 1100000010 1000000000 0001102000
0-0-011001 0110010000 1000010110 0010011001
1000100111 0010100211 0010000000 0000002000
0010011000 00100?0?11 ?00001000? ?010000100
0011100010 010010000? ?00-101102 0200000000
100000???1 20?0?0?00 ????1?0?0? ????0?0?
???????? ????????? ????????? ??????2? ?????????
???????? ????????? ????????? ????????? ?????????
???30000?0 100?0?0?0? 0?0-??-?-? ?-?-??0 -0?0?0?0?
?0?0?00?? ?0?0?
Anguis fragilis 101000-000 1100001000 0010000000
1100000000 1000001000 0001001000 100-010001 0-
1?-10000 00?1010110 0010011001 1000100110
0010101[12][01]1 0000000000 00000021-1
0010011000 00100?0011 2100000001 20011-0000
0021110000 0100100100 000-101102 1200000000
1010001101 2001122-01 0021011000 200200?000
000-1?2000 010?4----- --2201--1 --0-0?211 00101-
1-00 0000032110 01?10?0??? 0?0?00002 0000100???
???????? ????4000?? ?000?110?0 ?00-??-?-?1
?000?0?0 -01?0110-- 00?1-210 000?5-
Anniella pulchra 100000-000 1100000000
0110010000 1100-01000 1000001000 1001001000
110-010001 011?0-0?00 -0--100110 0110001111
1000100110 0111101211 0010010000 02100-2-1
0020111000 0010000021 2100000001 20001-0110
0020110000 0100100?0 000-101102 1200000000
101000?101 2001122-02 0?2101100? ?00200?000
1---1--1-- 2---4----- --2201--1 --0-0?211 11100-0--
--000?2110 11?10?0??? 0--0?00000 0000100???
???????? ?33000?? ?000?110?0 ?????-?-? ?1--??0
-0?0110-- 00?1-210 00004-
Anniella geronemensis [only molecular data includ-
ed] ????????? ????????? ????????? ?????????
???????? ????????? ????????? ????????? ?????????
???????? ????????? ????????? ????????? ?????????
???????? ????????? ????????? ????????? ?????????
???????? ????????? ????????? ????????? ?????????
???????? ????????? ????????? ????????? ?????????
???????? ????????? ????????? ????????? ?????????
???????? ????????? ????????? ????????? ?????????
???????? ????????? ????????? ????????? ?????????
Apodosauriscus minimus ????0000? ????1?0?
?????000? ?10?0?0?0? ????????? ????0?2?0 ?10-
???01 ????0?0?0 ????0?0?0? ????????? ?????????
???????? ????????? ????????? ????????? ?????????
?????0?0?1 2???0?0?0 002011001? ????0?0?0?
???????? 0000?00010 1???1??? ????????? ?????????
???????? ????????? ????????? ????????? ?????0?21?
001?1?1?0 00?0?0?0? ????????? ????????? ?????????

- 100-010001 0110-101?? 1000010?10 0?2001100?
??00000110 00100?001? ?10000000 0000?0?000
00[12]0311000 10000?2?1? ?0?000000? ?011000100
0011100011 0100100000 100-101102 0600000000
101000?2?1 2?01112-?? ????200?2? 2001?22??
????220?10 ????00000? ????222?0 ?1?22?1-1
0?11101002 21?2222?? ????2222?? ????2222??
????2222?? ?2300?2?? ?0?2210? ?2222-2?? ?200?2220 -
0?20?20?0 ?0?2222?? ?20??
- Melanosaurus maximus* ?200?01111 11?2000?20
????2222?? ?100?20?2? ????2000010 0101101000 100-
?2001 0110-101?0 ?222010110 0?10001001 ????2222??
????20?20?2? ????22220000 000?00?001 ?01031?000
00000?2?11 ?000?20?2? ????2222100 002111001?
010010?200 ?00-2222?? 06000000010 101001?2?1
2?011?2-?? ????22221000 2?012222?? ????2222??
????200?0?2? ????222200? ????222222?? 22220?2222??
????2222?? ????2222?? ????2222?? ????2222?? ?230?2222??
?20?2210? ????2222-? ?200?22220 -?20?20?0 ?0?2222??
?????
- Odaxosaurus piger* ?0?222200?1 11?200?2?? ?230000000
?10?220?2?? ?222200?220 ?2222002000 100-21?001 0110-
10000 100001?21? 0?2222?? ????2222?? ????222201?
????2222?? ????2222?? ????2222?? ????2222?? ?230?2222??
22222222100 002?1?001? 01?212222?? ?00-2222??
06000000010 101001?2?1 20?11?2-?? ????2222??
????2222?? ????2222?? ????2222?? ????2222?? ?221?
001?1010?0 00?2222?? ????2222?? ????2222?? ????2222??
????2222?? ?232222?? ????2222?? ?20-2222?? ?200?2222??
??-0?20? ????2222?? ?222??
- Paraglyptosaurus yatkolai* ?21?2222?? 11?1000?2??
????2222?? ????2222?? ????20?222?? ?222101000 0-0-
?222001 0?10-101? ?222001?220 ????2222?? ????2222??
????2222?? ????2222?? ????2222?? ????2222?? ????2222??
????2222000? ?2222000000 00111000?0 010010?000? ?00-
101102 0500?00010 10?2000?2?? ????2222?? ????2222??
????2222?? ????2222?? ?22220?200? ????2222?? ?222221-?
?0?2122?02 22222222?? ????2222?? ????2222?? ????2222??
????2222?? ?222222?? ?20?2222?? ????2222?? ????2222??
????20?20? ????2222?? ?222??
- Placosaursaurus rugosus* ?22221?211 ????2222?? ?210?2222??
?2220000?20 ?22222222?? ?222?101000 100-01?2001
01?2222?? ????2222?? ????2222?? ????2222?? ????2222??
????2222?? ????2222?? ????2222?? ????2222?? ????2222??
????2222?? ????2222?? ????2222?? ????2222?? ????2222??
????2222?? ????2222?? ?22222222-? ?2221?222 22222222??
????2222?? ????2222?? ????2222?? ????2222?? ?224?2222??
?20?2222?? ?222222?? ????2222?? ????2222?? ????2222??
?????
- Paraplocosauriops quercyi* ?2222?11? ????2222??
????222200? ?1?2222?? ????2222?? ????2222?? ????2222??
????2222?? ????2222?? ????2222?? ????2222?? ????2222??
????2222?? ????2222?? ????2222?? ????2222?? ????2222??
1?2222?000 00211?0?2? ????2222?? ????2222??
0600000010 1?2001?2?? ?22222222?? ?22222222??
????2222?? ????2222?? ????2222?? ????2222?? ?22222222??
?2221?2220 22222222?? ????2222?? ????2222?? ????2222??
????2222?? ?224?2222?? ?20?2222?? ????2222?? ????2222??
????2222?? ????2222?? ?222??
- Peltosaurus granulatus* 1000?01111 1100000000
0130010000 11000000010 10000000000 010110200?
10?2110001 011?1-10000 1101010010 0-11021001
10?0100110 10?01100111 0010010000 0000002000
0020011000 00000?2?11 ?100010000 1030?2-000
- 0011100010 011010?000 ?00-100102 06000000010
101001?2?1 2?010?22?? 0?222222?? ????2222??
11?2?1?010 0?222222?? ????2222?? ????200?201
0011101000 21?20?22?? ????2222?? ????2222??
????2222?? ????2222?? ?230?200?2? ?20?2210? ?2222-2-?
?200?2220 -?20?20? ?0?2222?? ?222??
- Proxestops jepseni* ?2222[01]1? ????2222?? ?230000?0?
?1?2220?2? ?22220?222? ?2222002000 1?2221?001 ?21?-
1?000 0000?1?2?? ????2222?? ????2222?? 0?100?221?
????2222?? ????2222?? ????2222?? ????2222?? ????2222??
?020?221?0 ?0?1100?2? ?100?0?00? ?00-2222??
0600000010 1?2001?2?1 2?01?22-?? ?22201?22?
????2222?? ????2222?? ????2222?? ????2222?? ????2222??
001?20?0?0 21?2222?? ????2222?? ????2222?? ????2222??
????2222?? ?232222?? ????2222?? ????2222?? ????2222??
????2222?? ????2222?? ?222??
- Xestops vagans* ?22221?21 ?1?2222?? ?222222?0?
????2222?? ????2222?? ?2220?1000 0-0-2222?? 0?1?2222??
????2222?? ?2222210? ????2222?? ?22220?20? ?21?2222??
?20?2222?? ????2222?? ????2222?? ?22221?221 102?2222??
????2222?? ????2222?? ????2222?? ?22220010 1?2220?22?
????2222?? ????2222?? ????2222?? ????2222?? ????2222??
????2222?? ?2222221? ?21?21?2220 22222222?? ????2222??
????2222?? ????2222?? ????2222?? ?22222222?? ????2222??
????2222?? ?222200?2222?? ????2222?? ????2222?? ?222??
- Parasaniwa wyomingensis* ?2222[01]1?1 11?2000?2?
?22220?20? ????2222?? ????2222?? ?222212?200 10?2222??
0110010001 000000?2?? ?22222222?? ?22222222??
????2222?? ????2222?? ?22220?222? ????2222?? ????2222??
????2222?? ?1?2222000 01?20-001? ????2222?? ????2222??
0200001100 101000?2?? ?201?2222?? ?22222222??
????2222?? ????2222?? ????2222?? ????2222?? ?222221-?
????2222?? 0?2222?? ????2222?? ????2222?? ????2222??
????2222?? ?232222?? ?20?2222?? ?20?2222?? ?200?2222??
??-0?20? ????2222?? ?222-8-
- Dorsetisaurus purbeckensis* ?222?200011 1?0?20?000
0?20?00000 ?0000?00? ?1?0000?2?? ?2222002100 1?0-
?22011 0110000000 0?200000010 0?1?2222?? ????2222??
0?200?20?2? ????22220000 000?0?2000 001?211000
00100?22?? ?222?1000- 00001--00? 00?1100001
011011?200 ?00-1?2221 0012000000 ?222000?2??
?22222-?? ?2221?22? ????2222?? ????2222?? ?222220?2?
????2222?? ?2222221? ????2222?? ????2222?? ????2222??
????2222?? ????2222?? ????2222?? ?224000?2? ?20?2222??
????2222?? ?222200?2222?? ?22220?2222?? ?22222??
- Aphanizocnemus libanensis* ?220?2-?20 1?220?222?
????2222?? ????2222?? ?22220?2200 ?22210210? ????2222??
001?20?222 ?22220?220 0?210?10?1 ????2222?? ????2222??
????2222?? ?20?2222?? ????2222?? 0?222221? ?200?20?2?
????2222?? ?22222011 1?2222?? ?20?2222?? ?222222??
????2222?? 20?1222-?? 0321010001 0211000?00
010?20?2?? ?222200?20? ?002211100 ?0?2222??
????2222?? ????2222?? ????2222?? ????2222?? ????2222??
????2222?? ?224?2222?? ?20?2222?? ????2222?? ????2222??
- ?22222-0 0?2222?? ?222??
- Dolichosaurus longicollis* ?22222222?? ?22222222??
????2222?? ????2222?? ????2222?? ????2222?? ????2222??
????2222?? ????2222?? ????2222?? ????2222?? ????2222??
????2222?? ????2222?? ????2222?? ?210?2222??
?2222210? 1?22220?1 11?21?22? ?20?2222?? ?222222??
?222222221 2001222-?? 03?201?2?? 01?2000?2?
?000?221-- 0-1?2000?2? ?222222?? ?222222?? ?222222??
????2222?? ????2222?? ????2222?? ????2222?? ????2222??
?224?2222?? ?222222?? ?222222?? ?222222?? ?222222??
?0?-2222?? ?222??

Coniasaurus gracilodens ??????0?0 ???????? ????00-
11? ????0000?? ???? ?????? ????102100 100-?1??11
01?1????? ???? ?????? ???? ?????? ???? ??????
???? ?????? ???? ?????? ???? ?????? ???? ??????
???? ?????? ???? ?????? ???? ?????? 1312?00000
0?0000??1 20012?2-? ????1???? ???? ??????
?00?10???? ???? ?????? ???? ?????? ???? ??????
???? ?????? ???? ?????? ???? ?????? ???? ??????
??4????? ???? ?????? 1?0-?2-?? ???? ?????? ??-0??-?
???? ?????? ????
Adriosaurus suessi 110??1-000 1???????? 0030??110
??000?00?? ????0?0?? ????00010? ???? ??????
011?010000 000?00011? 001?????? ????1?????
???? ?????? ???? ?????? ???? ?????? ???? ??????
?????0?0? ???? ?????? ???? ?????? ???? ??????
???? ?????? ???? ?????? ????222-?? 03??1?0?11
0212000?? ?00?0?0?? ????0?00? 00012??100
?0????? ???? ?????? ???? ?????? ???? ??????
???? ?????? ???? ?????? ????40???? ?0?1?2?? 10??-??
???? ?????? ???? ?????? ???? ??????
Pontosaurus kornhuberi 200??1-000 121?000??
??0?11?10 ?0101001?0 ????0?1100 010110010?
??0?0?112 00110?0?00 0100000?10 001102?001
?0??0111? ???? ?????? ???? ?????? ?000?2?? ???? ??????
???? ?????? ???? ?????? ???? ?????? ???? ??????
??0?001100 120?000?00 ?000000??1 20??222-??
03011?001? 0212000?0? ????1?0000 0??102001
0001?1?110 -0??0?1?? 0?000-0--- 00?0?0???
???? ?????? ???? ?????? ???? ?????? ????40????
?0??-??0 100-??0?-1 ????????? 0??-0??0?0 ?0-89????
?????
Pontosaurus lesuerii 2100?1-000 120?000000
1130?11110 ?001?0110 ????001100 010110010?
??0?0?1?1 021?1?0?00 ????000?10 0?00?1001
???? ?????? ???? ?????? ???? ?????? ???? ??????
0?? ?????? ?011?0110? ?1--001000 0102--1011
111101?11 000-101?01 12010001000 ????000?11
2001?22-?? 0311110011 0211000?0? ?10?10?0??
????00200? ?00????? ???? ?????? ???? ??????
???? ?????? ???? ?????? ???? ?????? ????40?00?
?0?1?2?? 100-??0?-1 ??-???? 0?1-0??-0 ?0-9????
?????
Agialosaurus dalmaticus 2100?1?000 ?1?000??
??????110 ?0101?01?0 1??011100 01011?200?
??????111 0110010?00 000000?10 0011021001
???? ?????? ???? ?????? ???? ?????? ???? ??????
??????11 ?01010?10? ?1--0?1100 01?2--1011
1?1101?01 000-100101 1202001000 1?000?11
2001222-?? 0?11010?11 0201000?? ???? ??????
??0?00?00- 1001101000 ???? ?????? ???? ??????
???? ?????? ???? ?????? ???? ?????? ???? ??????
??4????? ?00????? ???? ?????? ???? ?????? -??0?0?0
0????? ????
Opetiosaurus bucchichi 1110?1?000 1???000??
1?????110 ?0101?0?0 1???001100 010110200?
??????011 0110010?0 001000?1? 0?10?1001
???? ?????? ???? ?????? ???? ?????? ???? ??????
??????11 01?0110? ?000?1100 01?2--1011
1?100?01 000-100101 1202001000 100000??1
2?01222-?? ????01?11 020100??? ?00?10???
??0?00000- 100??0000 ?0?0?0?? ???? ??????
???? ?????? ???? ?????? ???? ?????? ???? ??????
??4????? ?0?0???? ???? ?????? ???? ?????? -??0?0?0
0????? ????
Judeasaurus tchernovi 2?0?1-000 1??000???

?????0?10 ????????? ????0?010? 0?011?10?0 1?0-????
0011?0?0?0??0?011?002102?00?0??1????????????
???? ?????? ???? ?????? ???? ?????? ????10?0??
????100 ?22-?? ?1?1?1?? ???? ?????? 0000000000
??000??? ???? ?????? ???? ?????? ???? ??????
???? ?????? ???? ?????? ???? ?????? ???? ??????
???? ?????? ???? ?????? ???? ?????? ???? ??????
?0?0???? ???? ?????? ???? ?????? ???? ??????
Tethysaurus nopscai 3100?1-000 121?000?? ?????0110
??10000?0 10?010010 0101101010 0-0-000011
2211000000 0010000110 0?11021001 ?010?0???
??????1? ????0?0?0 0?0?0?0?? 1?0??0?100 ?1????11
?010?01?? ?1--?0100 01?2--1011 1001????? ?00-
101?01 1202001100 100000?0?1 20012?2-??
0?1?01??1 0201????? ?10?10??? ????1?10??
??2101110 ???? ?????? ???? ?????? ????0?0?? ???? ??????
???? ?????? ???? ?????? ????4??00? ?00????0
?10-??-? ?0?0?0?0 -?1-0100?? 0?????? ?0?0??
Russellosaurus coheni 21??1-000 11?2000?? ?0?0?0-
110 ?0?0100?? ????000010 ?1102000 0-0-000011
0111010100 0000000110 0011010001 ????1????
0?001?011? ????0?0000 000?0200? 0010?01100
01100??11 ?010?00101 2031001100 01?2--10?1
101101?011 000-100101 1202001000 000000???
???? ?????? ???? ?????? ???? ?????? ???? ??????
???? ?????? ???? ?????? ???? ?????? ???? ??????
???? ?????? ???? ?????? ???? ?????? ???? ??????
???? ?????? ???? ?????? ????30000? 0?0?0?0?0 -
10-??0?1 ?0?01????0 -01?0?0?-? ???? ?????? ????
Halisaurus arambourgi 310?1-000 10?0000??
??????1? ????100?? ????011?0? 0??1?1010 0-0-
?00111 011?0?0?0 010000011? ????0?1? ???? ??????
??????11? ????000? 0?0?0?0?? ?000?1?0 1??????1
?012?01?? ?000?0100 0102--1011 1011010011
0000100101 1202001?10 ?00000?1 20010?2-??
0?11011011 0201????? ????1010??
??2??101? ???? ?????? ???? ?????? ???? ??????
???? ?????? ???? ?????? ???? ?????? ????6?0? ?00??1??
??????1?? ?0101???? 0??0100?0 2???????? ????
Varanus niloticus 21[01]0010001 1200001001
1130010110 1010000100 111100110- 11-1002000
110-000011 0211010000 0100000110 0011021001
100-101110 1100101211 0001010100 00000021-1
1010001010 1010000011 2000000001 1010000000
01120-0011 0110110001 000-100101 1512001100
2010001101 2012022-01 1211010000 0211001000
1110012000 000200000- 1001100000 000000?1-1
0000?0?00? 0000?0?? ???? ?????? ???? ??????
???? ?????? ???? ?????? ????5000010 ?20101?1[02]0
20?12-1-1 11?-10110 -01-0?0000 00?700300 110?9-
Varanus varius 3110010001 1200001001 0130011110
1010000100 11110011? 12-1002100 110-000011
0111010000 0000000110 0011021001 100-101111
1100101211 0001010000 00000021-1 10000?1010
1010000011 2100000001 1010000000 01120-0001
0110110001 000-100001 1202001100 201000?0??
???? ?????? ???? ?????? ???? ?????? ????00000-
100??0000 ?1?00?1-1 0000?0?? ?00?0?0??
0???????? ???? ?????? ???? ?????? ????90????
?00?01?100 101100-0-1 ?12--02110 -01-0?0?0
00?700?? ?0?9-
ccode+0 24 31 58 82 89 92 95 110 113 123 135 136 161
163 180 188 219 279 284 312 316 322 329 366 385
388 417 *] 235 241 363;
proc/;